



universität
wien

MASTERARBEIT / MASTER'S THESIS

Titel der Masterarbeit / Title of the Master's Thesis

„Regulatory Role of HDAC1 in Human Keratinocytes“

verfasst von / submitted by

Eva Zorec, BSc

angestrebter akademischer Grad / in partial fulfilment of the requirements for the degree of
Master of Science (MSc)

Wien, 2019 / Vienna 2019

Studienkennzahl lt. Studienblatt /
degree programme code as it appears on
the student record sheet:

A 066 834

Studienrichtung lt. Studienblatt /
degree programme as it appears on
the student record sheet:

Molekulare Biologie

Betreut von / Supervisor:

Ao. Univ.-Prof. Dr. Christian Seiser

Meinen Eltern gewidmet

Acknowledgments

An dieser Stelle möchte ich mich bei meinem Betreuer Christian Seiser bedanken, dass er mir ermöglicht hat, die Masterarbeit in seiner Arbeitsgruppe zu machen und dass er sich immer die Zeit genommen hat, um Experimente und Schwierigkeiten zu besprechen. Seine große Kompetenz, seine stetige gute Laune, die Lockerheit und Witzigkeit haben mir meinen Laboralltag sehr erleichtert. Danke für all diese schönen und lernreichen Erfahrungen.

Weiterhin möchte ich mich auch bei Heinz Fischer bedanken, der mir die Methoden und Techniken im Labor beigebracht hat und immer ein offenes Ohr für mich hatte. Danke für deine Geduld, Warmherzigkeit und für die aufmerksame Führung.

Ganz herzlichen Dank an Corinne Drexler, die zwei Monate meiner Masterarbeit mit mir verbracht hat und mir dabei eine große und Hilfe war. Dank ihrer Gelassenheit und Freundlichkeit war das Arbeiten mit ihr ein Vergnügen.

Ein großer Dank geht auch an Verena Moos, für die hilfreichen Tipps und für die Vorarbeit mit den Plasmiden, und an Brigitte Gundacker für ihre Hilfe bei den Western Blots und ihr schnelles Agieren, was die Bestellungen und die Lab-Organisation betrifft.

Zusätzlich möchte ich mich bedanken bei Lena Hess für ihre „Cookie-Spenden“ und Kollegialität, bei Gülnihal Kavaklioglu und Terezia Včelková für die ausgelassenen täglichen Unterhaltungen, bei Petra Lapšanská und Tamara Groffics für die tägliche Dosis Arbeitsmotivation und bei Lisa Grabner für die angenehme Gesellschaft in der Zellkultur. Danke auch an Magdalena Gamperl – ihre amüsante Stimmung hat allezeit die Arbeitsatmosphäre aufgelockert und an Aleksej Drino für die wertvollen und pfiffigen Methoden-Tipps, und zu guter Letzt an Marta Solano Mateos für den Spanisch-Schnellkurs.
:P

Mein besonderer Dank gilt meiner Familie, insbesondere meinen Eltern, die mich während meines Studiums allseitig unterstützt haben. Ohne ihren Rückhalt wäre dieses Studium für mich nur ein idealistischer Traum. Ebenso gilt mein Dank Aleksandar, der mich speziell beim Schreiben der Abschlussarbeit immer wieder ermutigt und motiviert hat.

Abstract

Class I HDACs such as HDAC1 and HDAC2 play a major role in the regulation of the cell cycle, proliferation and differentiation in the mammalian organism. Knockout studies in mice have demonstrated the importance of HDAC1 and HDAC2 for proliferation and differentiation in different cell types and organs. The mammalian skin is a multifunctional organ consisting of three layers. The uppermost, multi-layered part, epidermis, serves as the interface between the body's inner and outer environment. The epidermis represents a suitable system for the observation of genetic manipulations due to immediate visual manifestation of the phenotype and is an excellent model for the well-orchestrated regulation of proliferation, differentiation and cell death.

The aim of this master project was the set-up of a model system based on the newly created human keratinocyte cell line NHEK/SVTERT3-5 to characterize the regulatory function of class I histone deacetylases. To this end, we investigated the expression of class I HDACs during proliferation and differentiation of NHEK/SVTERT3-5 cells. HDAC1, HDAC2 and HDAC3 expression was found to be downregulated during differentiation, whereas HDAC8 levels increased in differentiated keratinocytes. In parallel, acetylation levels of H3K56 increased, while H4K8 acetylation decreased during differentiation. The class I-specific HDAC inhibitor MS-275 led to upregulation of the CDK inhibitors p21 and reduced proliferation of pre-confluent keratinocytes NHEK/SVTERT3-5 cells. Differentiated keratinocytes showed higher sensibility towards MS-275 resulting in increased cell death. One important goal of this project was the generation of a novel genetically engineered model system that mimics the effect of an HDAC1-specific inhibitor via CRISPR/Cas9 gene editing. By screening several hundred single clones we managed to create cell lines expressing catalytically inactive HDAC1 or wild-type HDAC1. Furthermore, we abolished the expression of endogenous HDAC1 in different NHEK/SVTERT3-5 cell lines by shRNA-mediated knock-down.

These novel keratinocyte cell systems will allow the comparison of effects of the class I-specific HDAC inhibitors with individual inhibition of HDAC1 in the presence and absence of endogenous HDAC1 in growing and differentiated human keratinocytes. The data from these experiments with human cells will complement and extend results from previous mice studies and might provide a rationale for the development of isoform-specific HDAC inhibitors.

Zusammenfassung

Klasse I Histondeazetylasen (HDACs), wie HDAC1 und HDAC2, spielen eine bedeutsame Rolle in der Regulation des Zell-Zyklus, der Proliferation und der Differenzierung von Säugetierzellen. Knock-out Studien in der Maus haben die Bedeutung von HDAC1 und HDAC2 für die Proliferation und Differenzierung von unterschiedlichen Zelltypen und Organen dargelegt. Die Haut der Säugetiere stellt ein multifunktionelles Organ dar, und besteht aus drei Kompartimenten. Die äußerste, mehrschichtige Epidermis dient als Grenzfläche zwischen dem Körperinneren und der Außenwelt. Die Epidermis stellt ein sehr gut geeignetes System für genetische Manipulationen dar, da sich diese sichtbar darstellen und leicht zu beobachten sind. Aus dem Grund wird die Haut oft als Modell für die Untersuchung der Proliferation, Differenzierung und Zelltod angewandt.

Das Hauptziel dieses Masterprojektes war die Schaffung eines auf der kürzlich generierten menschlichen primären Keratinozyten-Zelllinie NHEK/SVTERT3-5 basierenden Modellsystems zur Charakterisierung der regulatorischen Funktion von Klasse I HDACs. Zu diesem Zweck untersuchten wir zuerst die Expression dieser Enzyme während der Proliferation und Differenzierung der Keratinozyten-Zelllinie. Die Expression von HDAC1, HDAC2 und HDAC3 wurde im Laufe der Differenzierung reduziert, während HDAC8 in differenzierten Keratinozyten raufreguliert wurde. Gleichzeitig waren die Azetylierungslevels von H3K56 in differenzierten Keratinozyten erhöht, während die H4K8-Azetylierung während der Differenzierung sank. Behandlung mit dem für Klasse I Deazetylasen spezifischen HDAC-Inhibitor MS-275 resultierte in erhöhter Expression des CDK-Inhibitors p21 und reduzierter Proliferation von präkonfluenten Keratinozyten. Differenzierte Keratinozyten zeigten ein dosisabhängiges Auftreten von Zelltod nach Behandlung mit MS-275.

Ein wichtiges Ziel war die Schaffung von transgenen NHEK/SVTERT3-5 Zelllinien, die aktives oder katalytisch inaktives HDAC1 Enzym exprimieren mittels der CRISPR/Cas9-Technologie. Nach Screenen von Hunderten Einzelklonen gelang es uns, NHEK/SVTERT3-5 Zelllinien, die FLAG-getaggttes aktives oder katalytisch inaktives HDAC1 Enzym exprimieren, zu etablieren. Zusätzlich konnten wir endogenes HDAC1 in verschiedenen NHEK/SVTERT3-5 Zelllinien mittels shRNA-Knockdowns ausschalten.

Diese neuartigen Zellsysteme werden uns erlauben, die Effekte der HDAC Inhibitor Behandlung mit denen der genetischen Inaktivierung von HDAC1 zu vergleichen. Diese Analysen werden die Erkenntnisse von vorangegangenen Maus-Studien erweitern und eine Grundlage für die zukünftige Entwicklung von Isoform-spezifischen HDAC Inhibitoren bilden.

Table of contents

1. Introduction	10
1.1. Epigenetics	10
1.1.1. From genetics to epigenetics	10
1.1.2. Epigenetics.....	11
1.1.3. Organization of genetic material	12
1.1.4. Epigenetic modifications.....	14
1.2. Histone deacetylases (HDACs).....	18
1.2.1. HDAC1 and HDAC2	20
1.3. Skin.....	21
1.3.1. Epidermis	22
1.3.2. Keratinocytes are expressing keratins and other proteins during differentiation ...	24
1.4. HDAC inhibitors (HDACis).....	25
1.4.1. HDACi mechanisms of action	27
1.4.2. Entinostat (MS-275, SNDX-275).....	28
1.5. Aim of the study	28
2. Materials and Methods	30
2.1. Work with human cells	30
2.1.1. Thawing of cells.....	30
2.1.2. Cell passaging.....	30
2.1.3. Cell counting	31
2.1.4. Cell freezing	31
2.1.5. Transfection of NHEK/SVTERT3-5 cells.....	31
2.2. Work with RNA.....	32
2.2.1. RNA isolation.....	32
2.2.2. Reverse transcription.....	33
2.2.3. Quantitative Real-Time PCR (qRT-PCR).....	34
2.3. Work with DNA.....	35

2.3.1. Isolation of genomic DNA from keratinocytes by phenol-chloroform extraction	35
2.3.2. Direct-PCR DNA isolation	35
2.3.3. Polymerase chain reaction (PCR)	36
2.3.4. Agarose gel electrophoresis	36
2.4. Work with proteins and histones	37
2.4.1. Harvesting cells for protein and histone extraction	37
2.4.2. Preparation of protein isolates (freeze/thaw method)	37
2.4.3. Histone acid extraction	37
2.4.4. Extraction of insoluble proteins from keratinocytes	38
2.4.5. Bradford assay	39
2.4.6. Sodium dodecyl sulfate-polyacrylamide gel electrophoresis (SDS-PAGE)	39
2.4.7. Coomassie blue staining	40
2.4.8. Wet blot transfer	41
2.4.9. Antibody incubation	42
2.4.10. Immuno-detection by enhanced chemiluminescence (ECL)	43
2.4.11. Activity assay of histone deacetylases	43
2.4.12. MTS proliferation assay	44
2.5. Generation of keratinocyte cell lines overexpressing HDAC1 wildtype and HDAC1 H141A using CRISPR/Cas9 technology	44
2.5.1. Electroporation of the NHEK/SVTERT3-5 cells	44
2.5.2. Clonal dilution and expansion of cell lines	45
2.5.3. Validation of knock-in and screening of cell clones (PCR, Western blot, IF)	46
2.5.4. Screening of cell clones by immunofluorescence labeling	46
2.5.5. Immunofluorescence labeling of cells grown on coverslips	47
2.6. Work with bacteria	47
2.6.1. Inoculation of overnight culture	47
2.6.2. Preparation of bacterial glycerol stocks	47
2.6.3. Midiprep plasmid purification	47
2.7. shRNA-mediated knockdown of HDAC1 in NHEK/SVTERT3-5 cells	48
3. Results	51

3.1. Characterization of the immortalized human epidermal keratinocyte cell line NHEK/SVTERT3-5.....	51
3.1.1. Expression of differentiation markers by NHEK/SVTERT3-5	51
3.1.2. p21-induced growth arrest in post-confluent keratinocytes	53
3.1.3. Keratin 5 is a marker of proliferating, pre-confluent keratinocytes.....	53
3.2. Analysis of histone acetylation and class I HDACs expression during human keratinocyte differentiation	54
3.3. Inhibition of the catalytic activity of class I HDACs in human keratinocytes by MS-275	57
3.3.1. Impact on acetylation and crotonylation of histone H3 and H4.....	57
3.3.2. Impact on keratinocytes' proliferation and differentiation.....	60
3.4. Generation of cell lines overexpressing catalytically inactive HDAC1 and wildtype HDAC1	66
3.4.1. Optimization of transfection of NHEK/SVTERT3-5 keratinocytes.....	66
3.4.2. FuGENE®-mediated transfection of keratinocytes to overexpress HDAC1 variants using CRISPR/Cas9.....	67
3.4.3. Electroporation-mediated transfection of keratinocytes to overexpress HDAC1 variants using CRISPR/Cas9.....	73
3.4.5. Impact of overexpression of HDAC variants on the expression of endogenous HDAC1 and HDAC2	81
3.4.6. Impact of overexpression of HDAC1 H141A and HDAC1 WT on total cellular deacetylase activity and histone acetylation	83
3.4.7. Knockdown of HDAC1 in keratinocytes	85
3.4.7. Knockdown of HDAC1 in keratinocyte cell lines overexpressing HDAC1 wildtype and HDAC1 H141A	87
3.4.8. Characterization of knock-in clones after shRNA knock-down	87
4. Discussion and Outlook.....	90
4.1. NHEK/SVTERT3-5 cell line can differentiate in 2D cell culture.....	90
4.1.2. Upregulation of the CDK inhibitor p21 correlated with the differentiation of NHEK/SVTERT3-5 cells.....	90
4.1.3. Terminal differentiation of NHEK/SVTERT3-5 cells resulted in changed acetylation of H3K56 and H4K8 histone marks	90

4.1.4. HDAC8 expression is upregulated in post-confluent NHEK/SVTERT3-5 cells	91
4.1.5. H4K8 histone crotonylation is down-regulated during terminal differentiation of NHEK/SVTERT3-5 keratinocytes	91
4.2. Treatment of NHEK/SVTERT3-5 keratinocytes with HDACi MS-275 differed regarding the stage of keratinocytes' differentiation	92
4.2.1. Class I HDAC inhibition caused accumulation of histone acetylation and H4K8 crotonylation in NHEK/SVTERT3-5 cells	92
4.2.2. Effects of class I HDAC inhibition on proliferating keratinocytes	93
4.2.3. Differentiated post-confluent cells reacted to MS-275 with increased sensitivity ..	93
4.3. Generation of transgenic keratinocyte-derived cell lines.....	93
4.4. Overexpression of catalytically inactive HDAC1 variant significantly reduced cellular HDAC activity.....	95
4.5. Set-up of a specific shRNA-mediated knock-down of endogenous HDAC1in human keratinocytes.....	95
5. Appendix	97
5.1. Vector map Cas9	97
5.2. Vector map guide RNA (gRNA).....	97
5.3. Vector map HDAC1 H141A.....	98
5.4. Vector map GFP	98
References.....	99

Abbreviations

APS	Ammonium persulfate
DAPI	4', 6-diamino- 2-pheylindole
DKO	Double knockout
DMSO	Dimethyl sulfoxide
EDTA	Ethylenediaminetetraacetic acid
EtBr	Ethidium bromide
EtOH	Ethanol
ES	Embryonic stem cell
FBS	Fetal bovine serum
hEGF	Human epidermal growth factor
NHEK	Normal human epidermal keratinocytes
NTC	Non template control
PBS	Phosphate-buffered saline
PFA	Paraformaldehyde
rcf	Relative centrifugal force
RT	Room temperature
TEMED	Tetramethylethylenediamine

1. Introduction

1.1. Epigenetics

1.1.1. From genetics to epigenetics

The beginnings of modern genetics date back to the end of the 19th century when the Mendelian work was rediscovered and newly assessed. During the next four decades, scientists tried to understand the link between the represented trait (phenotype) and “hereditary factors” today known as genes by performing crossing-experiments with *Drosophila melanogaster*. This led to some important discoveries, for example, the construction of first gene maps and the linkage analysis, studying of recombination (crossing-over), chromosomes and nature of the hereditary material. With the discovery of the DNA and its structure in the early 50’s new era of genetics began. Coevally also the term “epigenetics” evolved. At the turn of the 19th century and beginning of the 20th, epigenetics described steps in the development of an organism from a fertilized egg to a mature creature and had more in common with embryology and evolution than with genetics (Felsenfeld, 2007). With further investigations, this definition changed because the *Drosophila* genetics revealed that there must be some chemical modifications of genetical material that change the phenotype without altering the heritable material (Felsenfeld, 2007). A word “epigenetic” was derived from Greek words “epi” which stands for “in addition to, outside” and “genesis” that means “origin” or in combination “epigenesis” that was used for describing a developmental process of an organism and was used already in the 17th century (Deichmann, 2016). From this word, the derivative “epigenetics” was coined by the geneticist and developmental biologist Conrad Waddington in 1942. He formulated it as “the branch of biology which studies the causal interactions between genes and their products which bring the phenotype into being (Amini-nik et al., 2016). The definition of epigenetics changed gradually over the decades. In 1975 the geneticist Arthur Riggs and molecular biologist Robin Holliday (known for Holliday junction) proposed that DNA methylation could impact the gene expression (Deans & Maggert, 2015; Deichmann, 2016; Felsenfeld, 2007). Later, the work of Vincent G. Allfrey showed that histone modifications such as acetylation of lysines influence the charge of the histones and therefore the affinity of the DNA for histone binding (Sites, 2012) and speculations about the involvement of acetylation in transcriptional activation were made. A few years later also other histone modifications, for example, phosphorylation, methylation, were discovered but their functional relevance remained unknown. Discovery of nucleosomes by Kornberg and Thomas in 1974 facilitated the studying of histone modifications and disproved the argument that gene activation is correlated with “stripping of histones from the chromatin” (Felsenfeld, 2007). Till the millennium the epigenetic research was in a realm of shades. However, after the year 2000,

the number of publications published in this field has drastically risen. Nowadays the epigenetics attempts to explain the link and mechanisms between environmental influences (nutrition, exercise, pesticides, tobacco smoke, heavy metals, environmental pollutants etc.) on the gene regulation and development of diseases (cardiovascular, autoimmune, neurological and cancer etc.) to improve their prophylaxis and treatment. 1996 the geneticist Arthur Riggs proposed the new definition of the term “epigenetics” as “the study of mitotically and/or meiotically heritable changes in gene function that cannot be explained by changes in DNA sequence” (CSHL, 2004) which is still in use today.

1.1.2. Epigenetics

How is possible that identical twins do not look the same if they possess the same genetical material? Why some lifestyle habits can increase/decrease disease incidence? What causes the cells to differentiate? The answers to questions like these, epigenetics try to answer. Therefore, throughout the decades identical twins were used for studying these phenomena hence they possess the same genetical material (genotype) but differ in their phenotypes (appearance, disease susceptibility). A large twin study with 80 participants (age range from 3-74 years) from Spanish National Cancer Centre (CNIO) (Fraga et al., 2005) on changes in DNA methylation and histone H3 and H4 acetylation patterns showed that identical (monozygotic) twins are in early ages epigenetically identical. However, with increasing age, these patterns change, especially if the twins do not live in the same environment. As a result, the differences in phenotype between the twins are more remarkable. The importance and heritability of the epigenetic marks were shown in the studies of individuals who were born during the famine (1944-1945) in Western Netherlands also known as “Hongerwinter”. Individuals, who were prenatally exposed to famine had lower birth weight and were shorter. Later in their lives, they were more frequently suffering from obesity, hypertension, breast cancer, diabetes type II, and psychiatric diseases. Additionally, the offspring of famine exposed babies suffered neonatally from obesity, premature mortality and general poor health (Painter et al., 2008). The transgenerational effects of the environment (food availability) and the heritability of the epigenetic makeup were shown by Överkalix study (Bygren et al., 2014). Överkalix is a small parish located in the northernmost province of Sweden. Existence in this subarctic area highly depended on the harvest. This study showed that, if the paternal grandmother experienced fluctuations in food availability during the early childhood her granddaughter was affected by increased cardiovascular mortality later in life. However, not only the lack of food but also the increased intake of some foods or supplements could affect the epigenome and health of the offspring. DNA methylation is one of the epigenetic mechanisms of gene regulation. The increased intake of methyl donors like folic acid, vitamin B₁₂ and methionine alters these methylation patterns of the DNA. A recent study by Ryan et al. (Ryan et al., 2017) indicated that the offspring of male mice fed with methyl-donor rich diet

prior mating had decreased learning ability and impaired memory. These are only a few examples that illustrate why studying epigenetics is relevant. Finally, the understanding of epigenomes (or "epigenetic code") and their function could considerably improve comprehension of disease formation, its prevention and treatment.

1.1.3. Organization of genetic material

By definition, epigenetic changes do not involve changes in the genetic material. DNA (*deoxyribonucleic acid*) serves as a carrier of all genetic information of the cell in the form of a nucleotide sequence. For gene expression, this information is transcribed into RNA (*ribonucleic acid*) and lastly translated into proteins (or different types of RNAs) which have structural and functional roles in the cell. The DNA molecule is a long polymer; in the stretched form, its length would be in total around 2 meters. To fit this large molecule into only a few microns large cell nucleus (3-10 μm), the DNA needs to get highly compacted. In eukaryotic cells, the first level of DNA compaction is the spooling of DNA around the histone core that reduces its length for one-third. Histones are highly conserved basic proteins that are enriched for lysine and arginine amino acids. Structurally they are made of two domains: the histone fold motif and 15-30 unstructured N-terminal tails which can be covalently modified (Kimura, Matsubara, & Horikoshi, 2005). The histone fold consists of three alpha-helices flanked by shorted loops (Alva, Ammelburg, Söding, & Lupas, 2007). The histone core is made up of four histone proteins: H2A, H2B, H3, H4. Two copies of each dimer, H2A-H2B and H3-H4, are combined in an octamer with 147 base pairs of DNA wrapped around (Tsankova & Nestler, 2010). This basic unit of DNA compaction is called a nucleosome. Linker DNA and histone H1 connect the adjacent nucleosomes.

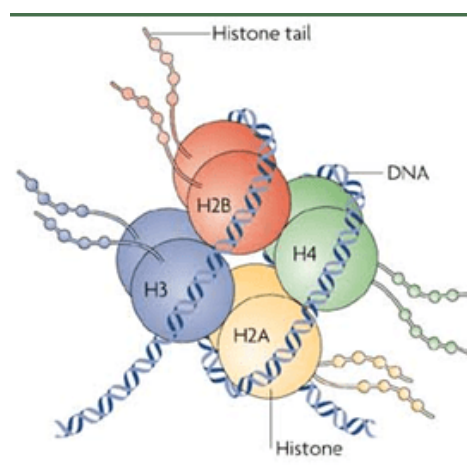


Figure 1: The nucleosome; the fundamental unit of the chromatin consists of four pairs of histone proteins, H2A, H2B, H3, H4, that build the histone core around which the DNA is spooled. Histone tails are the targets of different types of histone modifications. Figure taken from Tsankova & Nestler, 2010.

Between the DNA and the histone core, many types of interactions are established, like for example, hydrogen bonds, hydrophobic interactions, and, in particular, salt bridges. The positive charge of the arginine and lysine side chains in histone proteins neutralizes the negative charge of the DNA phosphodiester backbone. During the interphase, the DNA is organized with the corresponding histone and non-histone proteins in a loose form known as chromatin. However, during the mitosis or meiosis, the chromatin is compacted into more tightly packed chromosomes. The chromatin can adopt two structures. The open transcriptionally active form of the chromatin is euchromatin. Heterochromatin is tightly packed chromatin, mostly gene-poor region of chromatin where gene expression cannot occur. There are two types of heterochromatin: constitutive and facultative heterochromatin. The first type occurs in the regions of centromeres and telomeres. The second one can be found randomly in between euchromatic regions; its formation depends on the developmental or physiological state of the cell. The best example for the facultative heterochromatin is the X chromosome of female mammals. To maintain the cell homeostasis and to adapt to constant endogenous and environmental changes the cells need to react quickly by adjusting their gene expression program. Therefore, it is crucial that DNA is stored in the manner to be briskly available for transcriptional machinery (reviewed by Alberts et al., 2015).

Figure 2: Levels of DNA packing. *The first level of DNA compaction is the nucleosome. In the nucleosome DNA is wrapped around octameric histone core. Higher orders of DNA compaction are called "beads on the string", solenoid/30 nm fibre and chromatin loops. During the mitosis, DNA is in the most compacted form called chromosomes. Figure taken from Alberts et al., 2015.*

1.1.4. Epigenetic modifications

Gene expression consolidates highly dynamic and complex processes that are regulated at many levels. There are three main mechanisms of gene expression control: DNA methylation, histone modifications, and non-coding RNA expression that can target specific mRNAs (Handy, Castro, & Loscalzo, 2011; Perri et al., 2017).

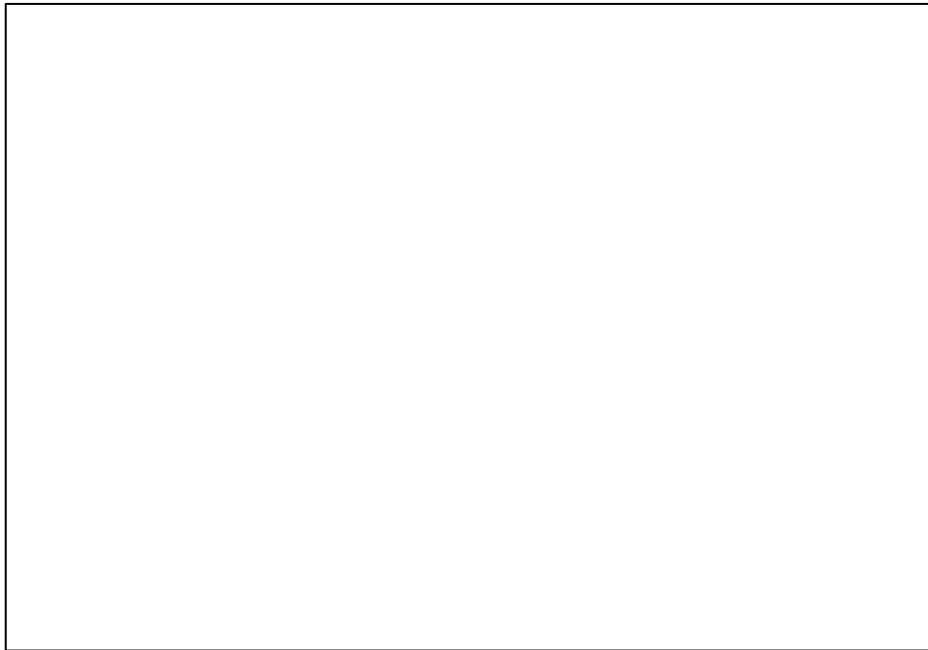
1.1.4.1. DNA methylation

One of the most important processes during early development is the erasure and the establishment of new DNA methylation patterns. These patterns are crucial for further cell differentiation of multipotent cells. Moreover, DNA methylation is of great importance in X-chromosome inactivation, genomic imprinting, silencing of mobile elements (transposons), cancer, ageing (Horvath, 2013), and in gene repression. During the methylation, methyl-groups (CH₃-) are transferred to 5' ends of cytosines by enzymes called DNA methyltransferases (Dnmt). Dnmt3a and Dnmt3b are responsible for *de novo* methylation and the Dnmt1 for the replicative maintenance methylation. In contrast, removal of methyl groups can occur actively or passively, like for example, through spontaneous deamination of methylated cytosine into thymine (Schübeler, 2015). Actively, the Tet enzymes (Tet 1-3) remove methyl groups from methylated cytosines. In somatic cells methylation is naturally found at CpG sites; these are pairs of cytosine and guanine nucleotides. Distal promoter regions of mammalian genes usually contain CpG islands which are sequences of clustered CpG sites. These CpG islands are at least 200 bp long, and they are made from 50 % or more of cytosine and guanine nucleotides (Illingworth & Bird, 2009). In general, DNA methylation is associated with gene silencing (Schübeler, 2015).

1.1.4.2. Histone modifications

Histone post-translational modifications of unstructured N-terminal histone tails or specific sites of globular histone core cause changes in chromatin structure, transcriptional activity and other processes involving chromatin. The nature of change is determined by the type of modification and its position. During the last decades, many histone modifications like histone methylation, acetylation, phosphorylation, crotonylation, sumoylation, ubiquitination, propionylation, butyrylation, formylation, citrullination have been identified. The first discovered and best-studied modifications are methylation and acetylation. Due to the improved sensitivity of advanced methods such as mass spectroscopy, new histone modifications can be easily detected and identified. Although, the interpretation of these new histone marks and their cross-talk remains poorly understood (Izzo & Schneider, 2010).

although the acetylation of histone H3 and H4 is characterized in more detail than of histone H2A and H2B (Ruijter, Gennip, Caron, Kemp, & Kuilenburg, 2003). Acetylation of the basic lysines in histone tails neutralizes their positive charge and consequently reduces the electrostatic affinity of histones for the negatively charged DNA (Gregory, Wagner, & Hörz, 2001; Moser, Hagelkruys, & Seiser, 2014). As a result, the DNA is more accessible for binding of transcription factors, RNA polymerase and other reader proteins which contain bromodomains. However, acetylation alone cannot cause changes that lead to more loosened chromatin and higher transcriptional activity; therefore, ATP-dependent chromatin remodeling complexes, like for example SWI/SNF complex, are needed (Gregory et al., 2001). In general, histone acetylation is associated with transcriptionally active genes. Later, it became also linked to DNA repair, cell-cycle progression, and gene inactivation (Verdone, Caserta, & Mauro, 2005). Histone acetylation is a reversible process, which requires enzymes that add acetyl groups (“writers”) and their opponents that remove them (“erasers”). The writers are called histone acetyltransferases (HATs) or more specifically lysine acetyltransferases (KATs) and the erasers histone deacetylases (HDACs). These enzymes show an affinity for both histone and non-histone proteins and are evolutionary highly conserved. Both HATs and HDACs are part of large multiunit protein complexes that are crucial for their activity and substrate recognition. HATs are divided among three major families: MYST and GNAT and p300/CBP (Sterner & Berger, 2000), whereas HDACs are classified into four classes depending on their homology to yeast enzymes. The altered balance between histone acetylation and deacetylation due to the impaired HAT or HDAC activity has been shown in many diseases. In many tumors, tumor suppressor genes, like p21, p53 or Rb, are hypoacetylated and therefore inactivated. On the contrary, oncogenes are usually found to be hyperacetylated in tumors and hence transcriptionally activated. Transcriptionally active promoters are usually marked with acetylated H3 at lysine residues 9, 18 and H4 acetylated at lysine 12 and 16 (Botchkarev, Gdula, Mardaryev, Sharov, & Fessing, 2012). The importance of reversible histone acetylation in the regulation of many cellular processes (Fig. 4) is significant.



Histone crotonylation

Figure 4: Acetylation and deacetylation performed by two antagonistic groups of enzymes, HATs and HDACs, have pivotal functions in many cellular processes. Lysine acetylation has a vast effect on the regulation of many cellular functions. Figure taken from Yang & Seto, 2007.

The recently discovered covalent histone modification by lysine crotonylation shows similarities to histone acetylation/deacetylation. This modification is abundantly found in all core histone proteins, despite lower concentrations of crotonyl-CoA compared to acetyl-CoA concentration (Wei et al., 2017). How the cells use different acyl groups to mark histone lysines is poorly understood. The regulation of these highly depends on the metabolic status of the cell. Histone acetyltransferase p300/CBP possess also crotonyltransferase function and HDACs (especially the class I) act as histone decrotonylases (Sabari et al., 2015; Wei et al., 2017). On the contrary, a paper published by Zhao group (Tan et al., 2011) demonstrated that HDAC 1, 2, 3, and 6 have little or no effect on lysine decrotonylation. Therefore, they propose that there must be distinct enzymes responsible for decrotonylation. Histone lysine crotonylation was found on several lysine positions at histones 3 or 4, like for example H3K9, H3K14, H3K56, and H4K8, though H3K18 is the most abundant crotonylation mark (Fellows et al., 2018). Transcriptional start sites (TSS) are enriched with crotonylation and hence associated with active promoters.

1.2. Histone deacetylases (HDACs)

Histone deacetylases (HDACs) or more precisely lysine deacetylases (KDACs) are pivotal regulators of chromatin and transcription. Moreover, they are involved in the regulation of several cellular processes, like for example cell differentiation, proliferation, apoptosis, cell division and DNA repair (Moser et al., 2014). These hydrolases are conserved from archaea, bacteria, to eukaryotes and primarily remove acetyl groups from lysine residues. In eukaryotes, HDACs are in principle associated with gene silencing. The interest in HDACs increased when their role in a variety of diseases (cancer, neurological disorders etc.) was revealed, and when they were recognized as potential targets for treatment with small molecule inhibitors. There are 18 HDACs known in humans that are divided between two families: the classical HDAC family and the SIRT family (Ruijter et al., 2003). The classical HDAC family can be divided into three classes. All members of this family contain a zinc ion in their catalytic site. Class I comprises HDAC1, HDAC2, HDAC3, and HDAC8 that are homologous to the yeast (*Saccharomyces cerevisiae*) enzyme Rpd3 (Reduced potassium dependency 3) protein. Class II is homologous to yeast Hda1 (Histone deacetylase 1) and is subdivided into class IIa (HDAC4, HDAC5, HDAC7, and HDAC9) and class IIb which contains HDAC6 and HDAC10. HDAC11 is the only member of class IV. The SIRT family or sirtuins that are referred to as class III, and do not belong to the classical HDAC family, comprise seven members (SIRT1-7). This family requires NAD⁺ for their catalytic activity and does not contain zinc. Some HDACs also have few different isoforms due to alternative splicing (Yang & Seto, 2009). Histone deacetylases deacetylate beside histone proteins also non-histone proteins which regulate cell cycle progression, differentiation, and apoptosis, like for example p21, p53, Rb, E2F, α -tubulin, MyoD and many other (Ropero & Esteller, 2007). HDACs cannot directly bind the DNA. Therefore, to accomplish their functions, they need to be part of large multiunit co-repressor complexes. HDAC1 and HDAC2 can be found as homo- or heterodimers in Sin3, CoREST or NuRD complexes. HDAC3 homodimerizes and is part of the NCoR (Nuclear receptor co-repressor)/SMRT (Silencing mediator of retinoid and thyroid receptors) complex. Homodimers of HDAC8 are not part of any complex (reviewed by Moser et al., 2014).

Figure 5: HDAC1 and HDAC2 are a part of three different multiunit co-repressor complexes called Sin3, NuRD and CoREST. *NODE complex comprises HDAC1 or HDAC2 in the embryonic stem cells. MiDAC complex was found in mitotic cells. These complexes comprise also SAP30 and SAP18 protein, histone binding proteins RbAp46 and RbAp58. (Zhang & Reinberg, 2001). HDAC3 forms homodimers which assemble into NCoR/SMRT complex, whereas HDAC8 does not require a complex for its activity after forming the homodimers. Figure taken from Moser et al., 2014.*

These co-repressor complexes not only fulfil the structural role, but they also act as interaction partners for transcriptional factors (NFκB, Bcl-6, MyoD, c-Myb etc.) and are able to recognize DNA regulatory elements (Mariadason, 2008). HDAC1 and HDAC2 can carry out their deacetylase activity only as a part of a complex. Localization, as well as tissue expression patterns of HDACs, differ within and between classes. HDAC1, HDAC2, and HDAC11 are localized primarily in the cell nucleus, whereas HDAC3, HDAC8 and class IIa HDACs shuttle between the nucleus and the cytoplasm. HDAC6 and HDAC10 are the only cytoplasmic HDACs (reviewed by Ruijter et al., 2003). Moreover, these two HDAC isoforms are the only ones to contain two catalytic sites (Dokmanovic, Clarke, & Marks, 2007). In contrast to class I HDACs that are ubiquitously expressed, class II and IV have shown tissue-specific expression patterns. Ablation of each class I HDAC member results in lethality of mice (Haberland, Montgomery, & Olson, 2011). The only member of class IV that belongs to the classical HDAC family, HDAC11, shows similarities to both class I and class II in its structure. The exact functions of the HDAC11 are not known yet, but some papers describe HDAC11 as most effective fatty acid deacetylase (Kutil et al., 2018; Moreno-yruela, Galleano, Madsen, & Olsen, 2017). Furthermore, HDAC11 probably has a diverse role in immunological processes (Yanginlar & Logie, 2018) and in the differentiation of proliferating bone cells (Blixt et al., 2017). Class II HDACs are involved in differentiation processes of specific tissues, like for example HDAC4 is enriched in bone tissue, HDAC5 and HDAC9 in muscles and heart, HDAC7 in

thymocytes. HDAC6 targets cytoskeletal proteins like α -tubulin (reviewed by Haberland, Montgomery, & Olson, 2011). The chaperone 14-3-3 and several phosphorylation events enable HDAC class II to shuttle between nucleus and cytoplasm. Sirtuins represent the NAD⁺-dependent class III of HDACs that is named after the yeast homolog Sir2 (Silent information regulator 2) (Dali-Youcef et al., 2007). Small molecule HDAC inhibitors (HDACi) like trichostatin A (TSA) which inhibit classical HDAC family do not inhibit sirtuins.

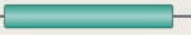
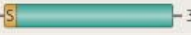
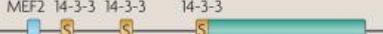
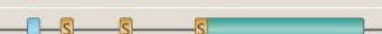
	Protein domains		Time of lethality	Phenotype	References
Class I	HDAC1	 482	E10.5	Proliferation defects	12,53
	HDAC2	 488	P1	Cardiac malformation	12,61
	HDAC3	 428	E9.5	Gastrulation defects	69–71
	HDAC8	 377	P1	Craniofacial defects	M.H. and E.O., unpublished observations
Class IIa	HDAC4	 1,084	P7–P14	Chondrocyte differentiation defect in growth plate	33
	HDAC5	 1,122	Viable	Exacerbated cardiac hypertrophy after stress	32
	HDAC7	 912	E11	Endothelial dysfunction	34
	HDAC9	 1,069	Viable	Exacerbated cardiac hypertrophy after stress	31
Class IIb	HDAC6	 1,215	Viable	Increased tubulin acetylation	43
	HDAC10	 669	ND	–	–
Class IV	HDAC11	 347	ND	–	–

Figure 6: Domain organization of the HDAC family. Numbers on the right side of the domain layout represent the total length of respective HDAC isoform in amino acids. Further right is listed the time of knock-out lethality and its cause. Figure taken from Haberland et al., 2011.

1.2.1. HDAC1 and HDAC2

HDAC1 and HDAC2 are members of the class I HDACs and exhibit high (87 %) amino acid sequence homology in mice (Yamaguchi et al., 2010). The explanation for this high homology could be that *Hdac1* and *Hdac2* probably have arisen from gene duplication and underwent only minor divergence (Khier et al., 1999; Moser et al., 2014). HDAC1 and HDAC2 are regulators of cell cycle, apoptosis, differentiation and metastasis (Hagelkruys, Sawicka, Rennmayr, Seiser 2011). The importance of HDAC1/HDAC2 activity for survival and proliferation was shown by the generation of the catalytically inactive HDAC1 and HDAC2 knock-in mice (Hagelkruys et al., 2016). Hagelkruys et al. have shown that mice which heterogeneously expressed catalytically inactive HDAC1 were viable and did not differ from the wild-type control mice. However, the heterogeneous expression of catalytically inactive HDAC2 led to the death of mice after a few hours after birth. This study led to the conclusion that HDAC2 can compensate for a loss of the HDAC1 activity but not *vice versa*. HDAC1 knockout mice are not viable and die during embryogenesis before day E10.5 due to proliferation failure and growth retardation (Lagger et al., 2002). On the other hand, conditional HDAC1 deletion in different tissues (brain, heart, muscles) is not lethal, probably due to the

compensatory mechanism by HDAC2. Beside that HDAC1 and HDAC2 are highly similar proteins they also share a homologous C-terminal domain with phosphorylation sites for casein kinase 2 (CK2) (Yang & Seto, 2009). Overexpression of HDAC1 is found in breast, prostate, esophageal, gastric, lung and colon cancer and it is in general associated with poor prognosis. HDAC1 and HDAC2 are vital for normal differentiation of keratinocytes (Connelly, Mishra, Gautrot, & Watt, 2011). A simultaneous double knockout (DKO) of *Hdac1* and *Hdac2* in the epidermis of the mice revealed perinatal lethality and disturbances of ectodermal/epidermal development. DKO mice showed impaired stratification of the skin, lack of hair follicles and failed limb separation, accompanied by altered histone acetylation patterns, like for example, increased acetylation of histone H3K9 (LeBoeuf et al., 2010). The dominant role of HDAC1 in the epidermis was identified by conditional 3 allele KO mice (Winter et al., 2013). HDAC1 promotes proliferation in early embryonic development. In later stages of developing its expression is downregulated to allow expression of specific genes needed for proper tissue formation (Brunmeir, Lagger, & Seiser, 2009; Tou, Liu, & Shivdasani, 2004). In addition, HDAC1 activity is required for replication and might be therefore expressed at lower levels in less proliferating, more differentiated cells.

1.3. Skin

The skin is the largest organ of the human body and accounts for around 15 % of the body mass (Kanitakis, n.d.). The primary function of the skin is protection and separation of the body's inwards from the environment. The undamaged skin provides a barrier which is impermeable for biological invaders (viruses, bacteria, parasites), chemical toxins and resistant to mechanical stress and UV radiation. Other crucial functions of the skin in the maintenance of the body's homeostasis are thermoregulation, immune defense, synthesis (Vitamin D), and sensory perception (S. H. Lee, Jeong, & Ahn, 2006). Structurally the skin can be divided into three main regions: epidermis, dermis and hypodermis or subcutis. They differ in cellular and tissue composition, but also in their function. The most superficial layer, epidermis, is the thinnest with a thickness ranging from 0.4 mm to 1.5 mm (depending on the body region). As the outermost layer, it represents the surface between the inner and outer body's environment and has a primary protective function. Underneath epidermis lies dermis that anchors epidermis and helps in thermo- and water regulation, due to the presence of blood and lymph vessels. Hypodermis consists mainly of adipose tissue that functions as a cushion, energy storage and insulating layer. Furthermore, this layer connects the skin with the bones and muscles and is highly vascularized, and plaited with nerves (Chu, n.d.).

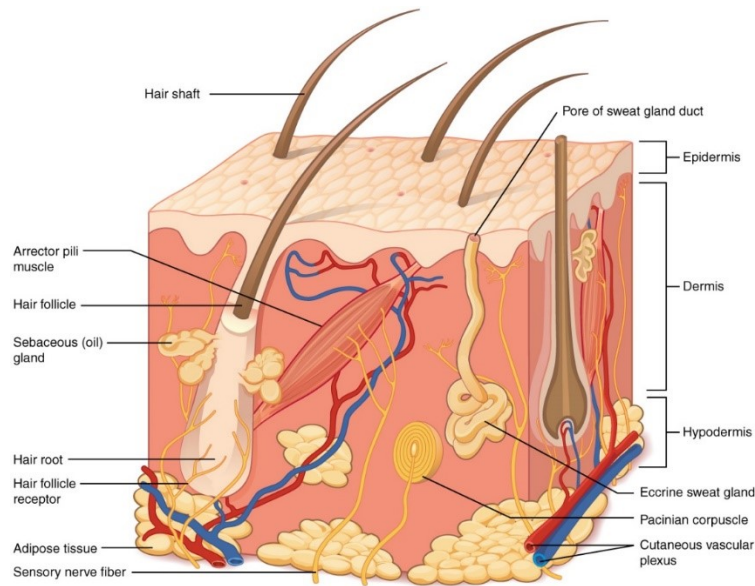


Figure 7: Cross section of the skin. Anatomically skin can be divided into epidermis, dermis, and hypodermis. The layers differ in their positioning, thickness, cell and tissue organization, and in their functionality. The epidermis is further divided into morphologically and functionally distinctive layers that provide a protective barrier. Figure taken from

1.3.1. Epidermis

Similarly, to how the skin is divided into different layers also the epidermis is stratified into a basal layer or *stratum basale* (also known as *stratum germinativum*), spinous layer (*stratum spinosum*), granular layer (*stratum granulosum*), *stratum lucidum*, and cornified layer (*stratum corneum*) (Yousef & Sharma, 2018). The proper layering of the epidermis is crucial for maintaining skin homeostasis and protective functions. The epidermis consists primarily (80 %) of keratinocytes (Kolarsick, Kolarsick, & Goodwin, 2011). Other cell populations like for example, dendritic cells, melanocytes, Langerhans' and Merkel's cells can also be found in the epidermis. The basal cells are columnar-shaped, mitotically active "stem cells" that are attached to the basement membrane by hemidesmosomes and form a monolayer. This layer of proliferating, undifferentiated cells produces with each cell division two new daughter cells; one of them remains in the stem cell population, and the other embarks on terminal differentiation (Telser, 2002). Above the basal layer lies squamous cell layer of polyhedral to fusiform-shaped cells. These cells are metabolically active, contain lamellar bodies, and connect with other cells by desmosomes. The epidermal lamellar bodies (LBs) are secretory organelles localized under the plasma membrane. They comprise of glycolipids, glycoproteins, antimicrobial peptides, and acid hydrolases (lipase, protease, glucosidase etc.) which are activated in the upper granular layer to form an impermeable membrane with barrier function (Menon, Lee, & Lee, 2018). Activation of these enzymes causes degradation of the nucleus and other cellular organelles in the granular layer. Lipids secreted by lamellar bodies serve as a "mortar" between the filaments and build hydrophobic protection. The spinous layer provides

resistance to mechanical stress due to many desmosomes that connect the neighboring cells and give the cells spindle-shaped appearance (Chu, n.d.). The last epidermal layer still containing living cells is the granular layer. The thickness of this layer varies depending on the body part and normally consists of two to three cell layers (Holbrook, 1989) however, it can be up to 10-times thicker on palms and soles. Keratinocytes in *stratum granulosum* change their shape from polyhedral to flattened and contain in their cytoplasm basophilic keratohyalin granules that are characteristic for this layer. Keratohyalin granules consist of cysteine- and histidine-rich proteins, like profilaggrin and involucrin. Profilaggrin is a precursor of filaggrin which is produced after the cleavage by serine proteases. The primary function of filaggrin is to crosslink the keratin filaments by disulfide bonds in the process of *keratinization*. The activation of the enzyme transglutaminase in the upper granular layer helps to covalently crosslink the non-keratin proteins in the formation of the cornified envelope (Candi, Schmidt, & Melino, 2005; Kopan, Traska, & Fuchs, 1987). Involucrin is responsible for the formation of the imperishable cell envelope underneath the plasma membrane (Kolarsick et al., 2011; McLean, 2016; Speed, n.d.). The degradative enzymes from lamellar bodies become highly active in the granular layer and result in the formation of the dead, keratinized cornified cells of the uppermost skin layer, *stratum corneum*. *Stratum lucidum* is a very thin layer between *stratum granulosum* and *stratum corneum* and can be found only on palms, soles and digits (Shen, Farid, & Mcpeek, 2008). Corneocytes of the cornified layer represent basal cells which successfully underwent the process of terminal differentiation. They are elongated, flat, nucleus-free horny cells filled with keratins and embedded in the lipid matrix (“bricks and mortar” model) produced mainly by lamellar bodies (Harding, 2004). The seemingly dead layer of cells fulfils many important functions, like providing a resistant barrier that enables protection against mechanical stresses, invaders, and excessive water loss but it also serves as a sensory interface between inner and outer body environment. Moreover, it plays a role in innate and adaptive immunity. The cornified layer is built of approximately 15 cell layers (palms and soles approximately 200 layers) (Kabashima, 2016). To prevent the exaggerated cornification, cells from the most outward cell layer are shed in the process of desquamation that is enabled by prior degradation of corneodesmosomes (Kolarsick et al., 2011).

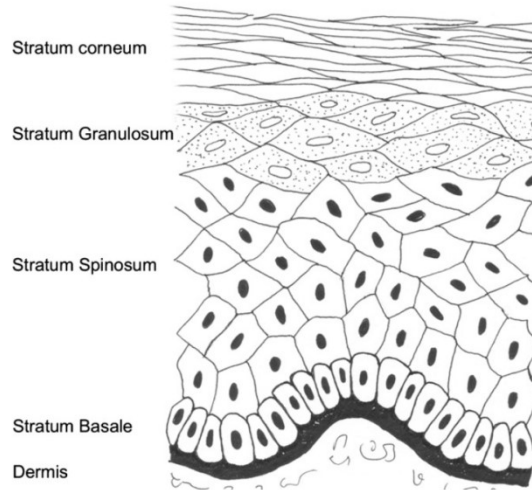


Figure 8: Layers of the epidermis. The epidermis consists of four or five cell layers of keratinocytes depending on the anatomical position. Basal cells mitotically divide and produce supplies of new cells which enter the process of terminal differentiation. Throughout this process, the shape and role of the keratinocytes progressively change. To ensure the normal layering and functionality of the skin, the autopoiesis¹ needs to be maintained. Figure taken from Wickett & Visscher, 2006.

1.3.2. Keratinocytes are expressing keratins and other proteins during differentiation

The major constituent of keratinocytes is keratin, which represents around 60-85 % of keratinocytes' dry mass (Elaine Fuchs, 1995; Wickett & Visscher, 2006). Keratins are water-insoluble proteins with a molecular weight of 40-70 kDa that dimerize to form the intermediate filaments, which together with microtubules and actin microfilaments build the cytoskeleton (Eichner, Sun, & Aebi, 1986). Keratins belong to a multigene family, and in humans, 54 keratin-encoding genes were identified (Moll, Divo, & Langbein, 2008) from which approximately 25 are expressed (Elaine Fuchs, 1988). In general, two types of keratinocytes are distinguished. When synthesized, the acidic, negatively charged type I pairs with basic, positively charged or neutral type II keratin. The favorable charge interaction of type I and type II keratins enables assembling of two α -helices to the coiled-coil structure of the intermediate filaments with a diameter of 10 nm. On the other hand, keratins of epidermis, hair, and nails are referred to as α -keratins with the molecular mass of 40-70 kDa and 8 nm diameter, whereas β -keratins of scales and feathers are only 3 nm thick and consist of smaller proteins with the molecular mass between 10-20 kDa (Fuchs, 1988). Keratins in the epithelial tissues are expressed in pairs, however, their expression patterns vary among different cell types and stages of differentiation (Keratins, 2016). For example, type II keratin 5 (58 kDa) and type I keratin 14 (50 kDa) are typically expressed by basal cells of *stratum basale*, type II keratin 1 (67 kDa) and type I keratin 10 (56 kDa) by the upper spinous and granular cells (Fuchs, 1994). The previously mentioned

¹ Autopoiesis represents a system that can self-maintain.

keratin pairs serve as so-called differentiation markers. Moreover, during wound-repair keratin 6 (type II) and 16 (type I) are expressed to promote proliferation and renewal. The expression of some keratins can be confined to specific body regions, for example, expression of keratin 9 is restricted only to soles and palms (Candi, Schmidt, & Melino, 2005; Fuchs, 1994).

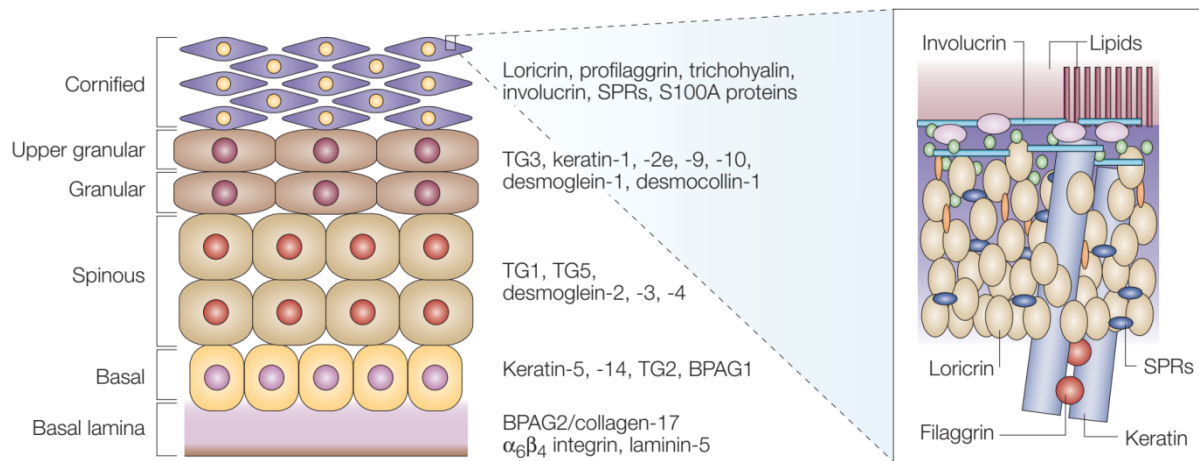


Figure 9: Overview of keratins and other structural proteins during the process of terminal differentiation. Basal keratinocytes express keratin 5 and 14, whereas granular keratinocytes produce primarily keratin 1 and 10, and in smaller amounts also keratin 2e. Keratin 9 expression is limited to palms and soles. TG = transglutaminase, SPRs = small proline-rich proteins, S100 proteins are calcium-binding proteins. Figure taken from Candi et al., 2005.

In the granular layer, besides keratins also other structural proteins, like filaggrin, involucrin, loricrin, trichohyalin, and small proline-rich proteins (SPRs) are synthesized and crosslinked by transglutaminases to build a resilient scaffold of corneocytes (Candi et al., 2005) embedded in lipid (ceramide) intercellular matrix.

1.4. HDAC inhibitors (HDACis)

Genetic mutations and other genomic alterations of the DNA sequence are not the only cause of diseases. For more than half of the century, we try to understand inheritable changes in gene expression that are not based on changes in the DNA sequence. These changes are known as epigenetic mechanisms (DNA methylation, histone modifications, non-coding RNAs). Environmental factors have a vast impact on these mechanisms. In many complex diseases like cancer, neurological and immune disorders it has been shown that an altered epigenetic code effects many cellular processes (Moosavi & Ardekani, 2016). HDAC inhibitors have been shown to restore some aberrant epigenetic modifications to their “normal” state. Therefore, they had been used for the treatment of neurological (Alzheimer’s, Parkinson’s disease), psychiatric (depression), immune disorders, and epilepsy prior to their beneficial effects in cancer treatment were discovered (Slingerland, Guchelaar, & Gelderblom, 2014). In the 1990s the link between HDAC inhibition and tumor proliferation was elucidated which led to increased interest in the application of HDACis in the cancer field (Hyun-Chung & Suk-Chul,

2011). The fact that HDACis induce cell cycle arrest, differentiation or apoptosis of cancer cells *in vitro* and *in vivo* impelled the HDACi research for cancer treatment even more (Eckschlager, Plch, Stiborova, & Hrabeta, 2017).

HDACis are small molecular compounds of natural or synthetic origin. Their chemical structure comprises of a Zn²⁺-binding domain, a linker and a hydrophobic group which allows interactions with proteins. Class III (sirtuins) are not inhibited by this type of HDACis. Based on their chemical properties they are grouped into five classes: short-chain fatty acids inhibitors (valproic acid (VPA), sodium butyrate), benzamides (entinostat (MS-275)), epoxyketones (trapoxin), hydroxamic acids (SAHA, trichostatin A (TSA)) and cyclic tetrapeptides (depsipeptide) which efficacies in HDAC inhibition range from milli-, to micro- and nanomolar doses *in vitro* (Katoch, Dwarakanath, & K Agrawala, 2013). Some other components like sulfonamide- and benzofuranone-containing molecules, α/β -peptides, and boronic acid-based structures were also described as HDACi (Marks, 2010). In general, two types of HDACis are distinguished: pan-HDACis and isoform-selective HDACis. Pan-HDACis (SAHA, TSA) are non-selective inhibitors that inhibit all Zn²⁺-containing HDACs (primarily class I, II). The major drawback for usage of pan-HDACis is the low target specificity of these inhibitors, affecting many off-target proteins (transcription factors, signalling mediators, non-histone proteins etc.) and pathways with the result of causing side-effects, like cardiotoxicity (Gryder, Sodji, & Oyelere, 2013). Nowadays the research is focused on discovery and development of selective HDACis that inhibit only specific HDACs, like for example only class I HDACs or even isoform-specific, for example solely HDAC1.

HDACis show promising results in treating hematological malignancies and very low or no efficacy in solid tumor treatment (SAHA, depsipeptide). Recently there are four FDA approved HDACis used in clinical cancer therapy: vorinostat (SAHA, approved 2006), romidepsin (depsipeptide/FK228, approved 2009) both approved for treatment of the cutaneous T cell lymphoma (CTCL); belinostat (PXD101, approved 2014) for treatment of relapsed peripheral T cell lymphoma and panobinostat (LBH589, approved 2015) for treating multiple myeloma (Chun, 2015; Singh, Bishayee, & Pandey, 2018). Vorinostat, belinostat and panobinostat inhibit HDAC class I, II, and IV, whereas romidepsin inhibits only HDAC class I. Currently, there are around 20 compounds from all chemical classes in different clinical phases in testing to get approval for therapy use (Singh et al., 2018). Moreover, also other natural compounds from different terrestrial and marine sources (bacteria, fungi, plants) are getting more and more attention due to their potential HDAC inhibitory effects and ubiquitousness. For example, butein, kaempferol (from *Aloe vera*) and resveratrol (from *Veratrum grandiflorum* or red grapes), or vitamin E and biotin, all of them exhibit HDAC inhibition and are found in our diet (Dashwood & Ho, 2008; Orlikova et al., 2012; Venturelli et al., 2013). Although the approved

HDACis demonstrated the most favorable risk-to-benefit ratio, their application elicits adverse effects (toxicities), like for example nausea, vomiting, diarrhea, headache, anorexia, phlebitis, asthenia etc. (Subramanian, Bates, Wright, Espinoza-Delgado, & Piekarz, 2010). Combinational therapies where HDACi are combined with other chemotherapeutic agents or radiotherapy are achieving promising results but also the development of isoform-specific HDACis is getting augmented attention.

1.4.1. HDACi mechanisms of action

Cell cycle arrest

The most prominent effect of HDACi treatment is cell cycle arrest by induction of p21 expression. p21 (also known as cyclin-dependent kinase inhibitor 1 or p21^{waf1/cip1}) is a universal cyclin kinases inhibitor that inhibits all members of the cyclin/CDK family (Xiong et al., 1993). HDAC1 reduces p21 expression. Both HDAC1 and p53 compete for the binding to the p21 promoter, whereas p53 promote p21 expression (p53-dependent response) and lead to inhibition of the cell cycle and differentiation (Inhibitor et al., 2003; Newbold, Salmon, Martin, Stanley, & Johnstone, 2014). Treatment with HDACi prevents HDAC1 to bind to the p21 promoter and causes acetylation of the p53 that prolongs its half-life and thus increases p21 transcription (Eckschlager et al., 2017).

Induction of apoptosis

HDAC inhibitors regulate the expression of pro- and anti-apoptotic genes and caspases that can induce apoptosis via the intrinsic or extrinsic apoptotic pathway. The intrinsic mitochondrial-induced apoptotic pathway is activated by increased transcription of pro-apoptotic genes like *Bim*, *Bax*, *Bid*, and *Bad* that cause the destruction of the mitochondrial membrane and consequently the release of cytochrome c which leads to the formation of apoptosome and activation of caspase 9 (Kroemer, Galluzzi, & Brenner, 2007; Mrakovcic, Kleinheinz, & Fröhlich, 2017). The extrinsic apoptotic pathway is launched by death receptors like TRAIL, Fas, TNF, TLA1 and their ligands (Hyun-Chung & Suk-Chul, 2011). Moreover, HDACis downregulate the expression of anti-apoptotic genes like BCL2A (Bolden et al., 2013).

Activation of autophagy

Autophagy enables cells the targeted degradation of cell components that are no longer needed (long-lived proteins) or are defective (misfolded proteins, malfunctioning organelles) by engulfing and fusing them with lysosomes into autolysosomes where the breakdown takes place. HDAC inhibitor studies have shown that HDACi can induce autophagy by acetylation of ATG (Autophagy-related) genes or by inhibiting the mTOR (mechanistic target of rapamycin) pathway. mTOR is the most important suppressor of autophagy, therefore, its inactivation by phosphorylation is of great importance in the autophagy induction of autophagic protein kinase ULK1 (Unc51 like autophagy activating kinase 1) (Gammoh et al., 2012). The HDAC inhibitor

SAHA (vorinostat) promotes induction of autophagy by both mentioned ways, either by repressing the mTOR pathway or by activating the expression of ATG genes (Eckschlager et al., 2017; Gammoh et al., 2012; Shulak et al., 2014).

Anti-angiogenic effect of HDACi

HDACis also exhibit anti-angiogenic effects. Growing tumors are in need to get more blood supply to survive. Therefore, the building of new blood vessels from pre-existing ones (angiogenesis) is one of the crucial cancer hallmarks (Hanahan & Weinberg, 2011). HDACis can modulate the down-regulation of pro-angiogenic genes, like vascular endothelial growth factor (VEGF) and endothelial nitric oxide synthase (eNOS) that have a highly mitogenic effect on endothelial cells (Eckschlager et al., 2017). On the other hand, HDACis promote acetylation of hypoxia-induced factor 1 α (HIF-1 α) which causes its destabilization. HIF-1 α is one of the major transcription factors (up-)regulating the expression of genes, like VEGF, involved in neovascularity as a response to hypoxic conditions (Ellis, Hammers, & Pili, 2010; Lin, McGough, Aswad, Block, & Terek, 2004).

The above-described actions of HDACis on tumor growth and progression are the most promising effects evoked by HDACi treatment (as monotherapy or in combination with other drugs). Besides these effects also some other, like the modulation of immune system/response (Haumaitre, Lenoir, & Scharfmann, 2009; Schotterl, Brennenstuhl, & Naumann, 2015), non-coding RNAs and stem cells were observed.

1.4.2. Entinostat (MS-275, SNDX-275)

In our experiments, we used the synthetic benzamide HDACi MS-275 for the treatment of keratinocytes. This chemical compound shows an anti-tumorigenic effect by inducing cell cycle arrest, differentiation and apoptosis ("Definition of entinostat - NCI Drug Dictionary - National Cancer Institute," n.d.). MS-275 inhibits class I HDACs, preferable HDAC1 and HDAC3 and shows no inhibition of HDAC8 ("MS-275 A HDAC1 and HDAC3 inhibitor | Sigma-Aldrich," n.d.). MS-275 is currently in phase II of clinical testing for malignant melanoma, colorectal and endometrial cancer, Hodgkin's disease, leukemia, pancreatic and ovarian cancer, renal cell carcinoma and non-small cell lung cancer, and in phase III for breast cancer ("Entinostat - Syndax Pharmaceuticals - AdisInsight," n.d.). In general, this HDACi is well tolerated, although following side effects of MS-275 therapy were observed: thrombocytopenia, anemia, vomiting, fatigue, hypophosphatemia and neurotoxicity. The half-life of MS-275 is relatively long, on average between 34 to 80 hours (Surolia & Bates, 2018), and the drug is soluble in DMSO.

1.5. Aim of the study

The class I HDACs, especially HDAC1 and its paralog HDAC2 have been shown to be essential regulators of epidermal differentiation and homeostasis (Markova, Karaman-

Jurukovska, Pinkas-Sarafova, Marekov, & Simon, 2007; Winter et al., 2013). Knockout studies have shown the importance of HDAC1 and HDAC2 for the viability of ES cells and mice. The mammalian skin is a multifunctional organ consisting of three layers. The uppermost, multi-layered part, epidermis, serves as the interface between the body's inner and outer environment. The skin is a suitable organ for observations of genetic manipulations due to immediate visual manifestation of genetic changes and is an excellent model for the well-orchestrated regulation of proliferation, differentiation and cell death.

The aim of this master project was to characterize the newly created human keratinocyte cell line NHEK/SVTERT3-5 with respect to the regulatory function of class I histone deacetylases. To this end, we investigated the expression of class I HDACs in proliferating and terminally differentiating primary human keratinocytes.

Next, we examined the effects of class I-specific HDAC inhibitor MS-275 on HDAC activity, histone acetylation and crotonylation, class I HDACs and p21 RNA and protein expression keratinocytes during proliferation and differentiation of these cells.

Additionally, we created a novel genetically engineered cell lines that mimic the effect of an HDAC1-specific inhibitor. This was achieved by the generation of NHEK/SVTERT3-5 cells overexpressing catalytically inactive HDAC1 or wild-type HDAC1 as control via CRISPR/Cas9. Furthermore, we wanted to abolish the expression of endogenous HDAC1 in wildtype NHEK/SVTERT3-5 cells and NHEK/SVTERT3-5 cells overexpressing catalytically inactive HDAC1 by targeted shRNA knockdown. The final goal of this master project was the comparison of the effect of the class I isoform-specific HDAC inhibitor MS-275 with individual inhibition of HDAC1 in the presence and absence of endogenous HDAC1 in growing and differentiated human keratinocytes.

The obtained data from these experiments with human cells complement and extend results from previous mice studies and might provide a rationale for the development of isoform-specific HDAC inhibitors.

2. Materials and Methods

2.1. Work with human cells

For our purposes, two cell lines were used: NHEK/SVTERT3-5 and HAP1. Recently developed diploid NHEK/SVTERT3-5 cell line was immortalized by transfection with SV40 early region plasmid and hTERT (Human telomerase reverse transcriptase) gene by retroviral transduction (Wagner et al., 2018; Weinmuellner et al., 2018). This cell line was derived from primary human epidermal keratinocytes and purchased by *Evercyte GmbH*. These adherent cells possess a cobblestone appearance and can be induced to differentiation; therefore, they can be used to produce 3D skin models. NHEK/SVTERT3-5 cells were cultured in serum-free keratinocyte growth medium supplemented with BPE (bovine pituitary extract), hEGF, insulin (recombinant human), hydrocortisone and GA-1000 (gentamicin, amphotericin B)

Walkersville, Inc.). The Keratinocyte growth medium 2 Ready-to-use (*PromoCell GmbH*) additionally contained epinephrine, transferrin (human), and CaCl_2 (0.5 M), but it did not contain GA-1000 therefore, 1 % Penicillin/Streptomycin was added. The G418 (geneticin, 50 $\mu\text{g}/\text{ml}$, *Roche*) was added throughout cultivation to the medium to maintain the expression of immortalization genes. The final Ca^{2+} concentration in *Lonza* KGM medium amounted 0.15 mM and in *PromoCell* KGM medium 0.06 mM. To induce the differentiation in keratinocytes, *PromoCell* medium was supplemented with CaCl_2 to the final concentration of 0.15 mM.

Adherent fibroblast-like HAP1 cells are near-haploid human cells derived from the male chronic myelogenous leukemia cell line KBM-7 (Carette et al., 2011). These malignant neoplastic cells are characterized by unlimited growth, and due to their haploid karyotype (exception chromosome 8 and 15), they are smaller than other human cells. The HAP1 cell line was purchased by *Horizon Genomics GmbH*. HAP1 cells were cultured in Iscove's Modified Dulbecco's Medium (IMDM, BioWhittaker®, *Lonza Walkersville, Inc.*) supplemented with 10 % FBS (*Sigma-Aldrich*), 1 % Penicillin/Streptomycin (*Sigma-Aldrich*), and 1 % L-Glutamine solution (*Sigma-Aldrich*). Both used cell lines required for their growth 37 °C and 5 % CO_2 .

2.1.1. Thawing of cells

To prevent cell lysis cells were rapidly thawed in a water bath (37 °C). Thawed cells were immediately pipetted into 5 ml of pre-warmed medium in 15 ml sterile tube, and centrifuged at 0.4 rcf for 3-5 minutes at RT. Subsequently, the supernatant was discarded, the cell pellet resuspended in an appropriate medium and transferred to a cell culture flask or petri-dish.

2.1.2. Cell passaging

When cells reached around 70 % (NHEK/SVTERT3-5) or 90 % confluency (HAP1), they needed to be split or expanded to a larger surface to sustain their normal growth and

homeostasis. The depleted medium was aspirated, and cells were washed once with 1x PBS. Cell detachment was achieved by incubating the cells with 1x Trypsin-EDTA (*Gibco® Life Technologies*) for 2-7² minutes in the incubator. Gentle tapping of the flask or pipetting the Trypsin-EDTA solution on cells helped by detachment. When > 90 % of cells detached, Trypsin-EDTA was diluted with medium³ (double amount of Trypsin-EDTA) or neutralized by Trypsin inhibitor (*PAN-Biotech GmbH*). Dissociated cells were transferred into 15 ml sterile tube and centrifuged at 0.4 rcf for 3-5 minutes at RT. The supernatant was cautiously aspirated, the cell pellet resuspended in appropriate volume of medium (depending on the splitting ratio) and seeded in the cell culture flask.

2.1.3. Cell counting

In some cases, an exact number of cells needed to be seeded or frozen, therefore cells were counted by using 0.4 % Trypan blue solution (*Thermo Fisher Scientific*) and Countess® Automated Cell Counter (*Thermo Fisher Scientific*). If necessary, also the cell viability was ascertained. The cell suspension was mixed with 0.4 % Trypan blue solution in 1:1 ratio and approximately 20 µl were pipetted into a Countess™ Cell Counting Chamber Slide (*Invitrogen*).

2.1.4. Cell freezing

Cells were trypsinized and centrifuged (see 2.1.2. Cell passaging). The cell pellet was resuspended in medium and mixed with the same volume of freezing medium (20 % DMSO⁴ (*Sigma-Aldrich*), 80 % medium). Due to the cytotoxicity of the DMSO cells were rapidly aliquoted into 1.5 ml cryovials and stored at -80 °C in the freezing container (*Nalgene®*). The next day aliquots were frozen in liquid nitrogen.

10x PBS

80 g NaCl

25.6 g Na₂HPO₄·7H₂O

2 g KCl

2 g KH₂PO₄

Filled up to 1 L and pH adjusted to 7.4 with NaOH.

2.1.5. Transfection of NHEK/SVTERT3-5 cells

One day prior to transfection around 0.3 x 10⁶ cells/well were seeded in a 6-well plate. Few hours before the transfection the medium was exchanged. Vector DNAs (0.2-1.5 µg) were mixed with reduced serum media (Opti-MEM™, *Life Technologies*) in 1.5 ml sterile tube. The FuGENE® HD transfection reagent (*Promega*) was prewarmed to RT and added to 1.5 ml

² Two minutes for HAP1 cells, seven minutes for NHEK/SVTERT3-5 cells.

³ FBS inhibits trypsin.

⁴ DMSO prevents the building of ice-crystals during the freezing process.

sterile tube, containing Opti-MEM and DNA. The transfection mix was incubated for 15 min at RT and subsequently dropwise added to cells. The plate was gently shaken to achieve the even distribution and incubated for 24 hours at 37 °C, 5 % CO₂. The transfection efficiency was determined 24 hours after transfection using an inverted microscope in fluorescent mode and calculated as a percentage of the total number of cells.

2.2. Work with RNA

2.2.1. RNA isolation

RNA was isolated from cells by using TRIzol® reagent (*Life Technologies*). Before isolation, all used surfaces and equipment (pipettes, racks, etc.) were cleaned with 1 M NaOH. Added volumes of the solutions during the entire procedure referred to 1 ml TRIzol® reagent.

The RNA isolation procedure was divided into five steps: cell lysis, phase separation, RNA precipitation, RNA wash and re-dissolving of RNA. Firstly, the medium was removed from the cell culture vessel (we used 6-well plate), the cells were washed once with 1x PBS (pre-cooled) and lysed with 1 ml TRIzol® reagent. Lysed cells were immediately transferred to 1.5 ml sterile tube on ice (no scratching needed) and 200 µl chloroform were added. The tube was vigorously shaken by hand for 15 seconds, incubated at RT for two minutes and subsequently centrifuged at 13.523 rcf for 10 minutes in a pre-cooled centrifuge (4 °C). To precipitate the RNA only the upper, aqueous phase was used. Therefore, this phase was transferred to a 1.5 ml sterile tube. After addition of 1 µl glycogen and 500 µl isopropyl alcohol, the tube was inverted several times, incubated at RT for 10 minutes, and afterwards centrifuged at 13.523 rcf for 10 minutes at 4 °C. The supernatant was discarded, the RNA pellet washed with 1 ml of 75 % EtOH and centrifuged at 5.283 rcf for 5 minutes at 4 °C. The supernatant was removed, and the pellet air-dried for around 10 minutes. The RNA pellet was dissolved in 100 µl sterile dH₂O with added RNase inhibitor (0.1 µl per 1 ml dH₂O; 40 U/µl, *Roche*). The tube was incubated in a thermomixer at 55 °C for 10 min while shaking (300 rpm). For the second precipitation 1 µl glycogen, 1/10⁵ volume of 3 M sodium acetate (pH 5.2) and 2.5⁶ volumes of 96 % EtOH were mixed with the RNA, and incubated overnight at -20 °C. The next day the sample was centrifuged at 13.523 rcf for 30 minutes at 4 °C. Subsequently, the supernatant was discarded, and the pellet washed with 1 ml 75 % EtOH by vigorous vortexing. The tube was once more centrifuged at 5.283 rcf for 5 minutes at 4 °C, and the supernatant discarded. Finally, the RNA pellet was dissolved in 40 µl sterile dH₂O supplemented with RNase inhibitor (see above) by

⁵ This volume is referred to 100 µl dH₂O used for RNA dissolving.

⁶ This volume is referred to 100 µl dH₂O used for RNA dissolving.

shaking in the thermomixer for 10 minutes at 55 °C. The RNA concentration was measured with NanoDrop™ One C (*Thermo Fisher Scientific*).

To evaluate the quality and concentration of the isolated RNA, RNA was run on the MOPS gel. RNA samples were prepared to contain 500 ng RNA and mixed with 2 µl EtBr-loading buffer. The mixture was filled up with dH₂O to 10 µl and heated to 65 °C for 5 minutes in the thermomixer. Afterwards, the RNA mixture was run on the MOPS gel for 20 minutes at 90 V in 1x MOPS buffer. The gel was visualized by using the ChemiDoc XRS+ system (*Biorad*).

MOPS gel

1.2 g agarose (SeaKem® LE Agarose, Lonza)
90 ml sterile dH₂O
10 ml 10x MOPS buffer
5.2 ml formaldehyde (added after boiling the gel)

10x MOPS buffer

0.2 M MOPS
50 mM sodium acetate (pH 5.0)
10 mM EDTA
(diluted in dH₂O and adjusted to pH 7.0 with NaOH, kept at 4 °C)

RNA loading buffer

15 ml deionized formamide
4.8 ml 37 % formaldehyde
3 ml 10x MOPS
2 ml dH₂O
2 ml glycerol
1.6 ml 10 % bromophenol blue
5 µl EtBr

2.2.2. Reverse transcription

The reverse transcriptase (RT) enzyme enables synthesis of the complementary DNA (cDNA) from an RNA template. 500 ng of isolated RNA was mixed with 4 µl 5x iScript Reaction Mix and 1 µl iScript Reverse Transcriptase from the iScript cDNA Synthesis Kit (*Biorad*). The reaction mix was filled up to 20 µl with nuclease-free water (included in the kit). The reaction of cDNA synthesis was carried out in a thermocycler according to this scheme:

Temperature (°C)	Time (min)
25	5
46	20
95	1
4	∞

2.2.3. Quantitative Real-Time PCR (qRT-PCR)

For qRT-PCR, the cDNA acquired by reverse transcription was diluted 1:10 with ultrapure H₂O. Per reaction 5 µl diluted cDNA, 10 µl Sso Advanced Universal SYBR Green Supermix (*Biorad*), 0.4 µl of 10 µM forward and reverse primer were mixed and filled up to 20 µl with sterile dH₂O. Each reaction was conducted in duplicates. The standard curve was obtained by serial dilutions of random cDNA. The primer annealing temperature was determined by gradient PCR in a temperature range between 55-65 °C. The data generated by *Biorad* iQ5 iCycler system were normalized to a housekeeping gene (*-Microglobulin*) and interpreted in accordance with the paper: *-time* (Pfaffl, 2001) using Excel and GraphPad Prism Software.

qPCR program

Temperature (°C)	Time (s)	Cycles
95	180	1
95	3	NC
AT	20	NC
72	6	NC
60-95	Melting curve	1
20	∞	1

The primer annealing temperature (AT) and the number of cycles (NC) depended on primer-pair, determined by gradient PCR.

qPCR Primer pairs				
Gene	Primer label		AT/NC	Company
<i>Hdac1</i>	hRT_Hdac1_for	CCAAGTACCACAGCGATTGAC	60/40	<i>Sigma-Aldrich</i>
	hRT_Hdac1_rev	TGGACAGTCCTCACCAACG		
<i>Hdac2</i>	hRT_Hdac2_for	TGAAGGAGAAGGAGGTTCGAA	60/40	<i>Sigma-Aldrich</i>
	hRT_Hdac2_rev	GGATTATCTTCTTCCTTAACGT		
<i>Hdac8</i>	hRT_Hdac8_for	TTTTCCCAGGAACAGGTGA	60/40	<i>Sigma-Aldrich</i>
	hRT_Hdac8_rev	AGCTCCCAGCTGTAAGACC		

2.3. Work with DNA

2.3.1. Isolation of genomic DNA from keratinocytes by phenol-chloroform extraction

To isolate the DNA from cells the cell medium was removed, and cells were washed once with 1x PBS. The cells were scraped off the flask using 5 ml 1x PBS, transferred into a sterile 15 ml tube and centrifuged at 3428 rcf for 30 minutes at RT. Afterwards, the supernatant was discarded, and the cell pellet resuspended in around 250 µl DNA lysis buffer. Lysed cells were transferred to a 1.5 ml sterile tube, and 8 µl of proteinase K (20 mg/ml) was added. The tube was incubated in the thermomixer at 55 °C overnight slightly shaking (350 rpm). The next day proteinase K was inactivated at 95 °C for 5 min and the sample was refilled to 250 µl with dH₂O (volume loss due to evaporation). 250 µl phenol/chloroform/isoamyl alcohol⁷ (25:24:1; *Sigma-Aldrich*) was added, and the tube was vigorously vortexed. After the centrifugation at 15.871 rcf for 10 minutes at 4 °C, 200 µl of the upper phase were transferred into a new 1.5 sterile tube, 20 µl of 3 M sodium acetate (pH 5.2; *Thermo Fisher Scientific*), 1 µl glycogen and 500 µl 96 % EtOH were added and thoroughly mixed. The tube was incubated for ≥ 1 hour at -20 °C and centrifuged for 30 minutes at full speed, 4 °C. The supernatant was discarded, the pellet was washed once with 1 ml 70 % EtOH and repeatedly centrifuged at full speed for 10 minutes. After removal of the supernatant, the pellet was air-dried for around 10 minutes and resuspended in 100 µl dH₂O by shaking in a thermomixer at 55 °C for 10 min. The DNA concentration was measured with NanoDrop™ One C (*Thermo Fisher Scientific*).

DNA lysis buffer

200 mM NaCl

100 mM Tris (pH 8.0)

5 mM EDTA (pH 8.0)

0.1 % SDS

2.3.2. Direct-PCR DNA isolation

For this procedure, the cell pellet (in 1.5 ml sterile tube) that was obtained from trypsinized, washed and centrifuged cells was resuspended in 200 µl Direct PCR® Lysis Reagent (*Peqlab*) supplemented with 4 µl proteinase K (20 mg/ml) and incubated overnight at 56°C, 350rpm. Hereafter, the proteinase K was inactivated at 80 °C for 45 min, and the DNA extracts were used for PCR. To isolate the DNA from cells attached to a 96-well plate, the medium was discarded, and the cells were washed twice with 1x PBS. Afterwards, 100 µl Direct PCR® Lysis Reagent with added 2 µl proteinase K was added to each well. The cell culture plate was

⁷ Phenol/chloroform/isoamyl alcohol saturated with 10 mM Tris (pH 8.0), 1 mM EDTA

sealed with StarSeal sealing tape (Aluminium PCR Sealing Foil; *Starlab*) and incubated for 3 hours at 56 °C. Thereafter, the proteinase K was inactivated at 80 °C for 45 min.

2.3.3. Polymerase chain reaction (PCR)

Per reaction 12.5 µl OneTaq® Quick-Load® 2X Master Mix (*NEB Inc.*) was mixed with 1 µl DNA template and 0.5 µl of forward and reverse primer (10 µM). The reaction mix was filled up to 25 µl with PCR grade H₂O. All PCRs were performed in T100™ Thermal Cycler (*Biorad*). Primer annealing temperatures were determined by gradient PCR.

PCR program

Temperature (°C)	Time (s)	Cycles
95	300	1
95	30	NC
AT	30	NC
72	240*	NC
72	420	1
20	∞	1

The primer annealing temperature (AT) and the number of cycles (NC) depended on primer-pair. Elongation time* was adjusted according to the fragment size expected to be amplified.

2.3.4. Agarose gel electrophoresis

To confirm the specific amplification of the desired DNA fragment, the PCR product was separated on an agarose gel, which concentration (1.2-1.8 %) depended on the fragment size of the amplicon. The agarose gel was prepared by mixing and boiling the SeaKem® LE Agarose (*Lonza Inc.*) in 100 ml 1x TAE buffer (for example 1.5 g agarose was weighed for 1.5 % agarose gel). To visualize the PCR product, DNA stain (peqGREEN 1.5 µl/100ml gel; *Peqlab*) was added to the gel. Since the OneTaq® Quick-Load® 2X Master Mix already contained the loading buffer no additional buffer was added to the PCR product. Depending on the size of the PCR product, 7 µl of an appropriated DNA ladder (1 kb or 100 bp; *NEB Inc.*) was loaded on the gel. The gel was run for around 45 minutes at 90 V in 1x TAE buffer. After the completed run, DNA was visualized by ChemiDoc XRS+ system (*Biorad*).

50x Tris-acetate-EDTA (TAE) buffer

242 g Tris base

57.1 ml glacial acetic acid

100 ml 0.5 M EDTA

Filled up to 1 L with dH₂O and stored at RT.

2.4. Work with proteins and histones

2.4.1. Harvesting cells for protein and histone extraction

Cells were scraped off the cell culture flask on the ice and transferred with the medium into sterile 15 ml tube. The tube was centrifuged in a pre-cooled swing-out centrifuge (4 °C) for 5 minutes at 811 rcf. The supernatant was discarded, the cell pellet was washed with 5 ml 1x PBS (for histones 10 mM sodium butyrate added to 1x PBS) and repeatedly centrifuged for 5 minutes at 811 rcf. Subsequently, the supernatant was completely removed, and the cell pellet was frozen in liquid nitrogen (long-term) or stored at -80 °C (short-term).

2.4.2. Preparation of protein isolates (freeze/thaw method)

Hunt buffer supplemented with protease inhibitors was used for cell lysis. The cell pellet was thawed on ice and resuspended in appropriate volume of the Hunt buffer (150 µl/100 mm dish). For lysis, the cells were transferred to a sterile 1.5 ml tube that was snap-frozen in liquid nitrogen and thawed (37 °C) for three times, followed by centrifugation at 13.523 rcf for 30 minutes at 4 °C. The supernatant was transferred to a new sterile 1.5 ml tube, and the concentration of the protein isolate was measured using the Bradford assay. After determination of the concentration, the supernatant and the pellet were frozen at -20 °C.

Hunt buffer

20 mM Tris/HCl (pH 8.0)

100 mM NaCl

1 mM EDTA

0.5 % NP-40

Protease inhibitors were added before use.

Protease inhibitors

50x PI (cOmplete protease inhibitor cocktail tablet; 1 tablet dissolved in 1 ml dH₂O; *Roche*)

100x β-glycerophosphate disodium hydrate

100x sodium fluoride

200x aprotinin

1000x sodium molybdate

1000x sodium orthovanadate (prior to use activated at 95 °C for 5 minutes)

1000x PMSF (phenylmethane sulfonyl fluoride)

2.4.3. Histone acid extraction

Histone extraction was conducted in three steps: cell lysis, acid extraction and acetone precipitation. Cell pellet obtained after cell harvest (see 2.4.1. Harvesting cells for protein and

histone extraction) was resuspended in 1 ml lysis buffer and centrifuged for 5 minutes at 18.407 rcf, 4 °C. The supernatant was removed, and the pellet was washed with 1 ml wash buffer four times by repeating the centrifugation step and removal of the supernatant. Afterwards, the pellet was dissolved in 20-30 µl dH₂O (amount depended on the pellet size) and 2 µl of concentrated H₂SO₄ was added. The tube was incubated on ice for one hour and subsequently centrifuged for 20 minutes at 18.407 rcf, 4 °C. The supernatant (= 1 volume) was transferred to a new 1.5 ml tube, 10 volumes of acetone were added and precipitated overnight at -20°C. The next day, the sample was centrifuged for 20 minutes at 18.407 rcf, 4 °C. Subsequently, the supernatant was discarded, the pellet air-dried and resuspended in dH₂O. Bradford protein assay was used to determine the concentration of isolated histones.

Lysis buffer

100 mM Tris-HCl

50 mM sodium bisulfite

1 % Triton X-100

10 mM MgCl₂

8.6 % sucrose

pH adjusted to 6.5

Protease inhibitors were added before use.

Wash buffer

100 mM Tris-HCl

13 mM Na₃EDTA

pH adjusted to 7.4

Protease inhibitors were added before use.

2.4.4. Extraction of insoluble proteins from keratinocytes

Lysis protocol using Hunt buffer is suitable only for soluble proteins and ineffective to lyse high molecular weight, and membrane-bound proteins such as keratins, involucrin, or filaggrin. Therefore, protein pellets that were left over after protein extraction (see 2.4.2. Preparation of protein isolates) were separately collected and stored. For lysis, cells were thawed on ice and resuspended in SDS lysis buffer using different buffer volumes, depending on the size of the pellet (50 µl – 150 µl). The mixture was denatured and reduced at 95 °C for 5 min, by slightly shaking at 350 rpm on the thermoshaker, and thereupon centrifuged for 10 min at 18.407 rcf, RT. Afterwards, the supernatant was transferred to the new 1.5 ml tube and used for Coomassie blue staining or SDS-PAGE.

SDS extraction buffer

2 % SDS

50 mM Tris-HCl (pH 7.4)

200 mM DTT (Dithiothreitol, *PanReac Applichem*, 154,25 g/mol) – due to instability always added freshly

Filled up with dH₂O.

2.4.5. Bradford assay

Bradford protein assay was used to measure the total protein concentration in a solution. Protein Assay Dye Reagent Concentrate (*Biorad*) was diluted 1:5 with dH₂O and mixed with 1 µl sample in 1.5 ml tube. The absorption was measured against the blank value at 595 nm with NanoDrop™ One C (*Thermo Fisher Scientific*) by using cuvettes. Absorption values were multiplied with 10 to obtain concentrations in µg/µl.

2.4.6. Sodium dodecyl sulfate-polyacrylamide gel electrophoresis (SDS-PAGE)

SDS-PAGE was used to separate molecules by their molecular weight in an electric field. The molecules migrate through the polyacrylamide gel; the smallest ones faster than the bigger ones. Anionic detergent Sodium dodecyl sulfate (SDS) covers proteins' intrinsic charges and provides them with an overall negative charge. The proteins with the same charge can then be separated by their molecular weights. For our purposes, we used 12.5 % or 16 % resolving polyacrylamide gels of 0.75 mm thickness. Before loading samples on the gel, samples were mixed with the 2x Laemmli buffer and denatured for 5 minutes at 95 °C. The Laemmli buffer contains 2-mercaptoethanol that reduces disulfide bonds and consequently, breaks them so that proteins become linear. The length of the linearized proteins corresponds to their molecular weight. As a marker Precision Plus Protein All Blue (10-250 kDa, *Biorad*) was used. We loaded 7 µl marker and 20 µl sample on a gel and ran the gel in a 1x Running buffer for 60-75 minutes, at 20 mA. Histones were separated on 16 % gel and proteins on 12.5 % gel.

Resolving gel	12.5 %	16 %
30 % Polyacrylamide	4.35 ml	3.73 ml
1 M Tris (pH 8.8)	3.9 ml	2.6 ml
H ₂ O	2.1 ml	560 µl
20 % SDS	52.5 µl	35 µl
20 % APS	90 µl	56 µl
TEMED	7.5 µl	5 µl

Stacking gel **5 %**

30 % Polyacrylamide	510 μ l
1 M Tris (pH 6.8)	375 μ l
H ₂ O	2.1 ml
20 % SDS	15 μ l
20 % APS	28 μ l
TEMED	7.5 μ l

30 % Acrylamide

30 % acrylamide

0.8 % N, N' methylenebisacrylamide

Resine beads (*Biorad*)

Stored at 4 °C, protected from light.

2x Laemmli buffer

4 % SDS

20 % glycerol

10 % 2-mercaptoethanol

0.0004 % bromphenol blue

0.125 M Tris-HCl

10x Running buffer

14.4 % glycine

3 % Tris-HCl

1% SDS

2.4.7. Coomassie blue staining

After the completed run of the polyacrylamide gel, in some cases, the gel was occasionally stained with Coomassie blue to detect proteins and visualize their relative amounts. Due to high sensitivity, this technique was used to more precisely adjust the loading amount of the proteins for SDS-PAGE if the sample volume was scarce. The gel was fixed in 100 ml fixing solution for 30 minutes and afterwards stained in 100 ml staining solution for 20 minutes. The stained gel was de-stained in Destainer I for 0.5-5 minutes and subsequently in Destainer II until only bands, without background, could be seen. Finally, the gel was rinsed twice for 5 minutes in dH₂O and scanned for quantitative evaluation.

Fixing solution

10 % glacial acetic acid

40 % EtOH (10 ml glacial acetic acid/40 ml EtOH/50 ml dH₂O)

Staining solution

made up of two solutions that are mixed 1:1

Stock Solution I

0.2 % Brilliant Blue G (*SERVA Electrophoresis GmbH*)

90 % EtOH

Stock Solution II

20 % acetic acid

Destainer I = Fixing solution

Destainer II

10 % glacial acetic acid

20 % EtOH

Filled with dH₂O to 100 ml.

2.4.8. Wet blot transfer

The transfer of separated proteins after SDS-PAGE to the nitrocellulose membrane was performed by wet blot transfer. The polyacrylamide gel with proteins was placed onto 0.2 µm nitrocellulose membrane (*Protran* , *GE Healthcare*), enclosed from the sides with one sheet Whatman® 3MM paper and supporting pads in a transfer cassette. The nitrocellulose membrane, Whatman® 3MM paper and pads were soaked before use in Wet blot transfer buffer. The transfer of proteins from the gel to the membrane was conducted in the Mini Trans-Blot® Electrophoretic Transfer Cell (*Biorad*), filled with Wet blot transfer buffer, for two hours, at 250 mA, 4 °C. The quality of the protein transfer was assessed by staining the membrane with Ponceau S for 5-10 minutes and destaining it with dH₂O.

Wet blot transfer buffer

25 mM Tris base

190 mM glycine

20 % methanol

(pH adjusted to 8.3)

10x Ponceau S

30 % trichloroacetic acid

30 % sulfosalicylic acid

2 % Ponceau S

Diluted in dH₂O

2.4.9. Antibody incubation

To prevent the unspecific binding of the antibodies, the blotted membrane was incubated in the blocking solution for minimally 30 minutes and thereupon in the primary antibody overnight at 4 °C while shaking. The primary antibody was diluted in blocking solution. The following day the membrane was washed three times for 5 minutes with 1x PBS/0.1 % Tween-20 and afterwards incubated with secondary antibody for at least one hour at RT while shaking. The horse-radish peroxidase-coupled secondary antibody was diluted 1:10.000 in 1x PBS/0.1 % Tween-20. Ultimately, the membrane was repeatedly washed three times for 5 minutes in 1x PBS/0.1 % Tween-20.

Blocking solution

1 % Milk powder

1 % Polyvinylpyrrolidone (PVP)

10 % 10x PBS

0.1 % Tween-20

0.02 % Sodium azide

Dilutes in dH₂O and adjusted to pH 7.4.

Primary antibody	Dilution	Origin	Company
p21 sc-6246	1:500	mouse	<i>Santa Cruz</i>
p53 do-7	1:20	mouse	<i>Seiser lab</i>
HDAC1 Sat13	1:1000	rabbit	<i>Seiser lab</i>
HDAC1 10E2	1:1000	mouse	<i>Seiser lab</i>
HDAC2 3F3	1:1000	mouse	<i>Seiser lab</i>
HDAC2 7029-50	1:5000	rabbit	<i>Abcam</i>
HDAC3 ab7030	1:2500	rabbit	<i>Abcam</i>
HDAC8 ab187139	1:10.000	rabbit	<i>Abcam</i>
β-actin A5316	1:5000	mouse	<i>Sigma</i>
Lamin B SC-6216	1:1000	goat	<i>Santa Cruz</i>

DNase1/L2	1:400	goat	<i>Anna Spiegel*</i>
DNase1/L2	1:500	rabbit	<i>Anna Spiegel*</i>
KRT1 165-P	1:5000	rabbit	<i>Covance</i>
KRT5	1:5000	rabbit	<i>Covance</i>
Loricrin PRP-145P	1:2000	rabbit	<i>Covance</i>
Involucrin	1:1000	rabbit	<i>Covance</i>
H3K56ac ab676307	1:5000	rabbit	<i>Abcam</i>
H4K8ac Sat198	1:20.000	rabbit	<i>Seiser lab</i>
H3 c-terminal ab1791	1:20.000	rabbit	<i>Abcam</i>
H3K18cr ab195475	1:1000	rabbit	<i>Abcam</i>
H4K8cr ab201075	1:1000	rabbit	<i>Abcam</i>

*kindly gift from Dermatology department of the Anna Spiegel Institute (*Medical University Vienna*)

2.4.10. Immuno-detection by enhanced chemiluminescence (ECL)

Detection of the requested protein was enabled by a chemiluminescence imaging system (*Fusion FX, Vilber Lourmat*) and by using the Western Blotting Detection Reagents (*GE Healthcare*). Both detection reagents were mixed in a 1:1 ratio and distributed over the membrane for approximately one minute. The membrane was wrapped in the transparent plastic cover and placed in the imaging system. The photos of the membrane that was exposed to the light were taken for different long intervals.

2.4.11. Activity assay of histone deacetylases

The proteins were extracted as described in 2.4.2. Preparation of protein isolate (freeze/thaw method). The total protein amount needed for this assay was around 20 µg. The protein extract was filled up to 20 µl with Hunt buffer containing protease inhibitors (control only Hunt buffer with protease inhibitors). 2 µl of ³H-acetate-labeled chicken erythrocyte histone mix was added, and the mixture was incubated for one hour at 30 °C while shaking at 300 rpm. Afterwards, 35 µl Histone Stop Solution and 800 µl Ethyl acetate were added. The 1.5 ml tube was vortexed for 15 seconds and centrifuged in a swing bucket centrifuge at 10.000 rpm for 4 minutes. Subsequently, 600 µl of the upper organic phase was transferred into a measuring tube with 3 ml Scintillation solution. The tube was slightly shaken and ready to measure the radioactive signal by Liquid Scintillation Analyzer (*Packard*).

Histone Stop solution

0.4 M Sodium acetate

1 M HCl

Scintillation solution

5 g/l PPO (2,5-Diphenyloxazole)

0.5 g/l POPOP ((1,4-bis(5-phenyloxazol-2-yl) benzene)

Filled up with toluene.

2.4.12. MTS proliferation assay

MTS assay is a colorimetric method to assess the proliferation or metabolic activity of the viable cells. The reduction of the tetrazolium compound [3-(4,5-dimethylthiazol-2-yl)-5-(3-carboxymethoxyphenyl)-2-(4-sulfophenyl)-2H-tetrazolium, inner salt; MTS] and an electron coupling reagent (phenazine ethosulfate; PES) by NADH or NADPH dehydrogenase enzymes into formazan can be measured at 490 nm. The cells were seeded in 96-well plate (around 4000 cells per well) and incubated at 37 °C, 5 % CO₂ overnight. The next day the cells were treated with MS-275 HDACi (0.1 μM, 1 μM, 10 μM) for 24h, DMSO was used as a control. After 24 hours the cell medium was exchanged, and 20 μl of MTS reagent was added to the cells for 3 hours, at 37 °C. Afterwards, the absorption at 490 nm was measured with ELISA reader (*Perkin Elmer*).

2.5. Generation of keratinocyte cell lines overexpressing HDAC1 wildtype and HDAC1 H141A using CRISPR/Cas9 technology

2.5.1. Electroporation of the NHEK/SVTERT3-5 cells

NHEK/SVTERT3-5 cells were grown in T175 flasks. When the cells reached around 70 % confluency, they were used for electroporation. This method was performed at the *Vienna BioCenter Core Facilities GmbH (VBCF)* by Krzysztof Chylinski and Philipp Czermak. In the first attempt, cells were electroporated with plasmids coding for the Cas9 protein, guide RNA (gRNA), GFP-Blasticidin resistance plasmid, and HDAC1 (either wild-type or mutant) encoding AAVS1-targeting vector (provided by Verena Moos). In the second attempt Cas9 protein (5 μg), synthetically synthesized gRNA (12 μg) and AAVS1 plasmids coding for HDAC1 (either wild-type or mutant) were used for electroporation. The cells were electroporated under the following conditions: 1150 V, 30 seconds, 2 pulses.

The plasmids coding for HDAC1_WT and HDAC1_H141A contain a FLAG-tag in their C-terminal domain. They were previously shown to work in the HAP1 cell line and were made by Verena Moos.

DNA/RNA	Concentration ($\mu\text{g}/\mu\text{l}$)
Cas9	0.57
gRNA	0.56
GFP-Blasticidin	0.46
Hdac1_WT	0.67
Hdac1_H141A (mutant)	1.25

The concentration of synthesized gRNA (g996; T7-gAAVS): 5.07 $\mu\text{g}/\mu\text{l}$.

1. Electroporation		
DNA/RNA	Hdac1 WT (μl)	Hdac1 H141A (μl)
Cas9	7.89	7.89
gRNA	5.36	5.36
GFP-Blasticidin	1.30	1.30
Hdac1_WT	4.48	-
Hdac1_H141A	-	2.40
H ₂ O	0.90	3.00

2. Electroporation		
	Hdac1 WT (μl)	Hdac1 H141A (μl)
Cas9 protein (5 μg)	2.00	2.00
gRNA (g996 T7-gAAVS, 12 μg)	2.37	2.37
Hdac1_WT plasmid	14.93	-
Hdac1_H141A plasmid	-	8
H ₂ O	13.63	13.63
10x PBS	1.60	-
10x Buffer	2.00	2.00

2.5.2. Clonal dilution and expansion of cell lines

Electroporated cells were selected with Blasticidin for 24 hours and tested for the insert presence by nested PCR, and for the successful cut by Cas9 protein using sequencing and a PCR. Part of these electroporated cells was frozen, another part was used for PCR tests and clonal dilutions. Cells used for clonal dilutions were diluted employing serial dilution method so that in each well would have been approximately 5 cells. The cells were seeded in 96-well plates and placed in the incubator for a week while being daily observed under the microscope. After approximately 10 days, only single-cell colonies were chosen for further cultivation and screening. The single-cell colonies were split into three 96-well plates; one plate was used for cultivation, the second one for screening, and the third as a backup. After the nested PCR screen of the whole cell batch, the single-cell colonies were screened for containing the

transgene (either HDAC1 WT or HDAC1 H141A). The PCR positive clones were stepwise expanded to 24-well, 12-well and 6-well plate and then additionally screened with another PCR-screen for the presence of the transgene with primers binding in different regions of AAVS-locus and transgene. Cell clones positive for both PCRs were finally expanded to 60 mm and 100 mm cell culture dishes. Cellular proteins were extracted and tested for the presence of the FLAG-tag protein by Western blot analysis. Cell transfer from one plate to other was performed as described in 2.1.4. Cell passaging with minor alterations. Due to small volumes, vigorous pipetting of the trypsin solution helped to detach the cells from the well's surface. Trypsin should not be applied to the cells for longer than 7 minutes. To prevent cell death, trypsin inhibitor was used for trypsin neutralization. The resuspended cells were subsequently transferred to 1.5 ml tubes and placed into 15 ml falcon tubes (without cap) in the centrifuge. Cells were centrifuged for 5 minutes at 0.4 rcf at RT, the supernatant was discarded, and cells resuspended in fresh medium. 10 μ l of cell suspension was mixed with 10 μ l 0.4 % Trypan blue solution and pipetted into the cell counting chamber used by counter Countess® Automated Cell Counter (*Thermo Fisher Scientific*). For clonal dilutions, we calculated the total number of cells and μ l of cell suspension needed, to seed around 5 cells per each well. Due to the unequal distribution of seeded cells, not every well contained exactly 5 cells, moreover some cells also died or did not form colonies.

2.5.3. Validation of knock-in and screening of cell clones (PCR, Western blot, IF)

The screening of clones was performed by running different PCRs (nested, indel, and screening/direct PCR). All these PCRs were used to test for the presence of the transgene at AAVS locus, with the primer pair binding either outside of the likely integrated transgene or within it. The difference between a screening and a direct PCR was in primer pairs used. In the screening PCR, primer pair bound within the transgene (if inserted), and in the direct PCR in the right and left homology arm of the AAVS locus. These two PCRs provided a hint which clones could possibly contain the transgene, however, they were sometimes reciprocal. The most accurate and reliable methods to detect the inserted transgene were Western blotting and immunofluorescence labeling of the expressed FLAG-tagged HDAC1 protein. The immunofluorescence technique showed to be the method of choice in High-Throughput-Screening (HTS).

2.5.4. Screening of cell clones by immunofluorescence labeling

This method was established to easier and faster screen for potentially positive single colonies (clones) by immune-detection of FLAG-tagged protein in 96-well plate. The cell medium was aspirated from the wells, and the cells were washed once with 1x PBS. After removing the PBS, the cells were incubated in 4 % paraformaldehyde (PFA) for 20 minutes at 4 °C. The PFA was disposed in special waste, and the cells were repeatedly washed twice with 1x PBS,

followed by a 15-minute incubation in 1x PBS/0.1 % Triton X-100 at RT. To block unspecific epitopes, 1x PBS/0.1 % Triton X-100/10 % goat serum was added to cells for at least 30 minutes at RT. Subsequently, the mix of primary antibody (anti-FLAG; 1:500) and 1x PBS/0.1 % Triton X-100/10 % goat serum was pipetted to the cells, and the plate was incubated overnight at 4 °C on a rocking shaker. The next day the cells were washed 3x 10 minutes with 1x PBS/0.1 % Tween-20 followed by second antibody incubation (Alexa red 11003, goat α -mouse; 1:500) in 1x PBS/0.1 % Tween-20/10 % goat serum/DAPI (1:2000) for at least one hour at RT. Due to the light sensitivity of the secondary antibody, the plate was wrapped in tinfoil. After that, the cells were washed again 3x 10 minutes with 1x PBS/0.1 % Tween-20 and once with 1x PBS. Immunofluorescence-labeled cells were visualized and photographed using an Olympus CKX53 inverted microscope.

2.5.5. Immunofluorescence labeling of cells grown on coverslips

The same procedure applies for immunofluorescence staining of cells grown on coverslips. The coverslips were additionally mounted onto glass slides with the antifade reagent (ProLong™ Gold, *Invitrogen*). Pictures of coverslips were taken using the VS120 virtual slide systems (*Olympus BX61SV*) and *Olympus VS-ASV* software.

2.6. Work with bacteria

2.6.1. Inoculation of overnight culture

Transformed bacterial cells were plated on pre-warmed LB-agar plates with an appropriate antibiotic, and incubated overnight at 37 °C. The next day single colonies were picked with a pipette tip and dropped into 2-4 ml LB medium supplemented with the corresponding antibiotic. These bacterial pre-cultures were incubated at 37 °C in a shaking incubator (180 rpm) for 6 hours. Afterwards, 100 ml LB medium with the antibiotic were inoculated with pre-cultures and incubated at 37 °C, overnight while shaking. The bacterial plates were stored with agar-side up at 4 °C. Cloning, transformation and preparation of competent bacteria were done by Verena Moos.

2.6.2. Preparation of bacterial glycerol stocks

To prepare stocks with bacteria carrying the desired plasmid, 500 μ l of bacterial culture was mixed with 50 % glycerol in a ratio 1:1 in a cryovial that was subsequently stored at -80 °C. This method enables the storage of bacterial stocks for many years.

2.6.3. Midiprep plasmid purification

Larger quantities of plasmid DNA were purified and collected using the Plasmid Midi Kit (*Qiagen*) according to the manufacturer's instructions. Bacterial overnight cultures were harvested by centrifugation at 3428 rcf for 15 min at RT. The supernatant was cautiously

removed, and the bacterial pellet was resuspended in 4 ml Resuspension buffer. Bacterial cells were lysed by addition of 4 ml Lysis buffer and vigorously inverting the Falcon tube several times followed by incubation at RT for 5 minutes. Subsequently, 4 ml Neutralization buffer was added, the Falcon tube was repeatedly inverted and incubated on ice for 15 minutes. After that, lysed bacterial cells were centrifuged at 22.000 rcf for 30-45 minutes at 4 °C, and meanwhile, the purification column was equilibrated with 4 ml Equilibration buffer. The supernatant was applied to the column, and the bound plasmid DNA was washed twice with 10 ml Wash buffer. The DNA was eluted from the column with 5 ml Elution buffer and precipitated by addition of 3.5 ml isopropanol and centrifugation at 5000 rcf for 1 hour at 4 °C. The supernatant was thoroughly discarded, and the precipitated DNA was washed with 2 ml of 70 % EtOH while centrifuging at 5000 rcf for 20 minutes at 4 °C. Ultimately, the supernatant was removed, DNA pellet air-dried and resuspended in an appropriate volume (depending on pellet size) dH₂O.

LB medium (autoclaved, for 1 liter)

10 g Tryptone

5 g Yeast-extract

5 g NaCl

Filled up with dH₂O, pH adjusted to 7.5 with NaOH.

LB agar

see LB medium; 15 g/l Bacto agar added.

Ampicillin (stock 100 mg/ml)

Final concentration used in LB medium/plates: 100 µg/ml.

2.7. shRNA-mediated knockdown of HDAC1 in NHEK/SVTERT3-5 cells

Knockdown of targeting endogenous HDAC1 was performed with three different shRNAs in NHEK/SVTERT3-5 cells and newly generated NHEK/SVTERT3-5-derived knock-in cell lines. The complete procedure of generating these knockdown cell lines was conducted by Oliver Pusch (Department of Cell and Developmental Biology, Center for Anatomy and Cell Biology, Medical University of Vienna) according to the Wiederschain & Ph, n.d. protocol. Importantly, HDAC1 shRNA3 targets only the endogenous but not the transgenic murine HDAC1 mRNA.

The creation of knockdown cell line stably expressing the shRNA that binds to the complementary mRNA sequence of the target gene requires the following steps to be performed (taken from Wiederschain & Ph, n.d.):

1. Transformation and amplification of *pLKO-Tet-On vector*
2. Design of shRNA oligos

The oligo sequences used for knockdown of HDAC1 are depicted below and were selected from MISSION® shRNA Library (*Sigma-Aldrich*).

Histone deacetylase 1

RefSeq NM_004964.2

Organism human

Symbol HDAC1

Oligo	Sequence
hHDAC1-1_S	ccggGCCGGTCATGTCCAAAGTAATctcgagATTACTTTGGACATGACCGGCttttttg
hHDAC1-1_AS	AATTcaaaaaGCCGGTCATGTCCAAAGTAATctcgagATTACTTTGGACATGACCGGC
hHDAC1-2_S	ccggCGGTTAGGTTGCTTCAATCTActcgagTAGATTGAAGCAACCTAACCGttttttg
hHDAC1-2_AS	AATTcaaaaaCGGTTAGGTTGCTTCAATCTActcgagTAGATTGAAGCAACCTAACCG
hHDAC1-3_S	ccggCCTAATGAGCTTCCATACAATctcgagATTGTATGGAAGCTCATTAGGttttttg
hHDAC1-3_AS	AATTcaaaaaCCTAATGAGCTTCCATACAATctcgagATTGTATGGAAGCTCATTAGG

Histone deacetylase 2

RefSeq NM_001527.3

Organism human

Symbol HDAC2

Oligo	Sequence
hHDAC2-1_S	ccggGACGGTATCATTCATAAATActcgagTATTTATGGAATGATACCGTCttttttg
hHDAC2-1_AS	AATTcaaaaaGACGGTATCATTCATAAATActcgagTATTTATGGAATGATACCGTC
hHDAC2-2_S	ccggGCTGTGAAGTTAAACCGACAActcgagTTGTCGGTTTAACTTCACAGCttttttg
hHDAC2-2_AS	AATTcaaaaaGCTGTGAAGTTAAACCGACAActcgagTTGTCGGTTTAACTTCACAGC
hHDAC2-3_S	ccggCAGTCTCACCAATTTTCAGAAAActcgagTTTCTGAAATTGGTGAGACTGttttttg
hHDAC2-3_AS	AATTcaaaaaCAGTCTCACCAATTTTCAGAAAActcgagTTTCTGAAATTGGTGAGACTG

Histone deacetylase 3
RefSeq NM_003883.3
Organism human
Symbol HDAC3

Oligo	Sequence
hHDAC3-1_S	ccggCCTTCCACAAATACGGAAATTctcgagAATTTCCGTATTTGTGGAAGGtttttg
hHDAC3-1_AS	AATTcaaaaaCCTTCCACAAATACGGAAATTctcgagAATTTCCGTATTTGTGGAAGG
hHDAC3-2_S	ccggCAAGAGTCTTAATGCCTTCAActcgagTTGAAGGCATTAAGACTCTTGttttttg
hHDAC3-2_AS	AATTcaaaaaCAAGAGTCTTAATGCCTTCAActcgagTTGAAGGCATTAAGACTCTTG
hHDAC3-3_S	ccggGCCTGACAATGGTACCTATTAActcgagTAATAGGTACCATTGTCAGGCttttttg
hHDAC3-3_AS	AATTcaaaaaGCCTGACAATGGTACCTATTAActcgagTAATAGGTACCATTGTCAGGC

Histone deacetylase 8
RefSeq NM_018486.2
Organism human
Symbol HDAC8

Oligo	Sequence
hHDAC8-1_S	ccggGCGTATTCTCTACGTGGATTTctcgagAAATCCACGTAGAGAATACGCtttttg
hHDAC8-1_AS	AATTcaaaaaGCGTATTCTCTACGTGGATTTctcgagAAATCCACGTAGAGAATACGC
hHDAC8-2_S	ccggAGTCGCTGGTCCCGGTTTATAActcgagTATAAACCGGGACCAGCGACTttttttg
hHDAC8-2_AS	AATTcaaaaaAGTCGCTGGTCCCGGTTTATAActcgagTATAAACCGGGACCAGCGACT
hHDAC8-3_S	ccggCTGAGGAGTGGTGCCTATAATctcgagATTATAGGCACCACTCCTCAGtttttg
hHDAC8-3_AS	AATTcaaaaaCTGAGGAGTGGTGCCTATAATctcgagATTATAGGCACCACTCCTCAG

Figure 10: Design of shRNAs for HDAC1 knock-down. Black letters correspond to the shRNA sequence in sense and anti-sense direction, blue one's label loop sequence, green one's cloning site and red letters mark a spacer.

3. Oligo annealing and ligation into *pLKO-Tet-On* vector
4. Transformation and ligation in competent Stbl3 *E. coli* cells
5. Screening for positive clones
6. Sequencing of positive clones
7. Lentiviral packaging
8. Titering of lentiviruses
9. Infection of target cell line for stable shRNA-expression
10. Induction of shRNA-expression and knockdown

3. Results

3.1. Characterization of the immortalized human epidermal keratinocyte cell line NHEK/SVTERT3-5

3.1.1. Expression of differentiation markers by NHEK/SVTERT3-5

Keratinocytes *in vivo* undergo the process of terminal differentiation that is vital for proper layering of the skin (Watt, 1989). The recently created cell line NHEK/SVTERT3-5 possess the characteristics of primary keratinocytes. It can inducibly differentiate and displays the morphologic features of primary keratinocytes in 2D and 3D culture (Wagner et al., 2018; Weinmuellner et al., 2018). Depending on the stage of terminal differentiation, keratinocytes express different keratins, which can be used as differentiation markers. According to the provider (*Evercyte*), the NHEK/SVTERT3-5 cell line expresses keratin 1 (*KRT1*), keratin 2 (*KRT2*), keratin 10 (*KRT10*), and loricrin in a 3D skin model. In our experiments, we confirmed the expression of specific differentiation markers also in 2D conditions.

In vitro, these cells start to differentiate after the proliferation phase (if the cell culture medium is supplemented with calcium (≥ 0.1 mM)) at 80 % confluency. At lower Ca^{2+} concentrations (≤ 0.1 mM) cells do not start to differentiate (Bikle, Xie, & Tu, 2013). To verify the ability of the NHEK/SVTERT3-5 cell line to differentiate, cells were collected at three different time points; at 70 % confluency (pre-confluent), on day 5 (d-5) and day 9 (d-9) after reaching the complete confluency (day 0). Cells were lysed in Hunt buffer (see chapter 2.4. Work with proteins and histones) and centrifuged to obtain the soluble cytoplasmic extract. The pellet was further treated with SDS-containing buffer to solubilize also keratins and membrane-bound proteins. Cell pellet extracts and whole cell extracts were used to assess the expression of keratin 1 (early differentiation marker) and DNase1L2 (late differentiation marker) in harvested cells.

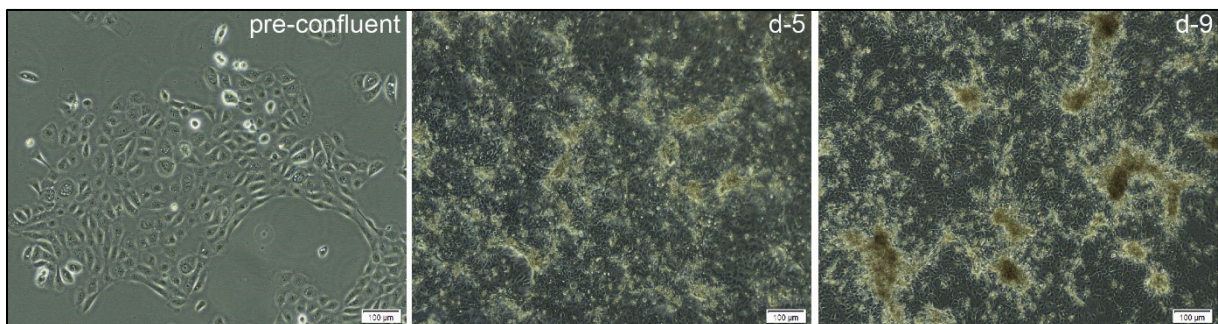


Figure 11: NHEK/SVTERT3-5 cell line in pre-confluent (growing) and post-confluent phase (d-5, d-9). Pre-confluent cells conform to basal cells from the basal layer of the epidermis. These cells are still in the growth phase and versatile. d-5 and d-9 cells represent a mixture of basal cells and differentiated cells *In vitro*. These cells build multilayered colonies and express differentiation markers. The upper cells of the colonies are terminally differentiated keratinocytes undergoing cell death (Sun & Green, 1976). Magnification: pre-confluent 10x, d-5 and d-9 4x.

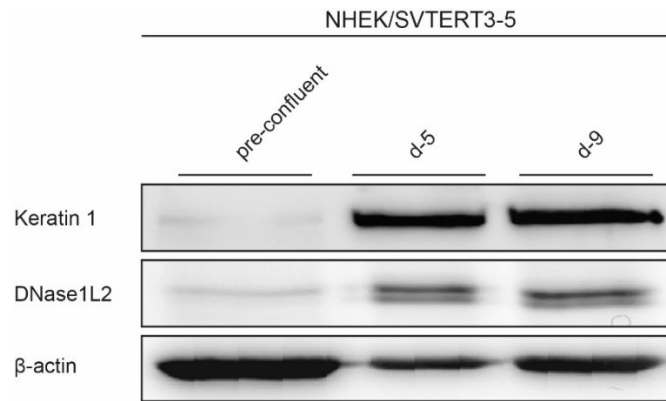


Figure 12: Immunoblot analysis of keratin 1 and DNase1L2 in pre-confluent and post-confluent NHEK/SVTERT3-5 cells. Only post-confluent (d-5, d-9) cells expressed differentiation markers keratin 1 and DNase1L2. β -actin served as loading control.

As shown in Figure 12, NHEK/SVTERT3-5 cells express the differentiation markers, keratin 1 and DNase1L2 that are naturally expressed by keratinocytes in *stratum spinosum* and *stratum granulosum* of the epidermis.

To substantiate the immunoblot analysis, mRNA expression of differentiation markers was analyzed by RT-qPCR. The data have shown significantly higher levels of keratin 1, DNase1L2, and S100A9 in post-confluent (d-5, d-9) cells compared to pre-confluent ones (Fig. 12). S100A9 is a calcium-binding protein associated with differentiation. Through the progression of differentiation of primary keratinocytes, caused by elevated extracellular Ca^{2+} concentration, the expression of S100A9 was shown to be induced (Martinsson, Yhr, & Enerbäck, 2005).

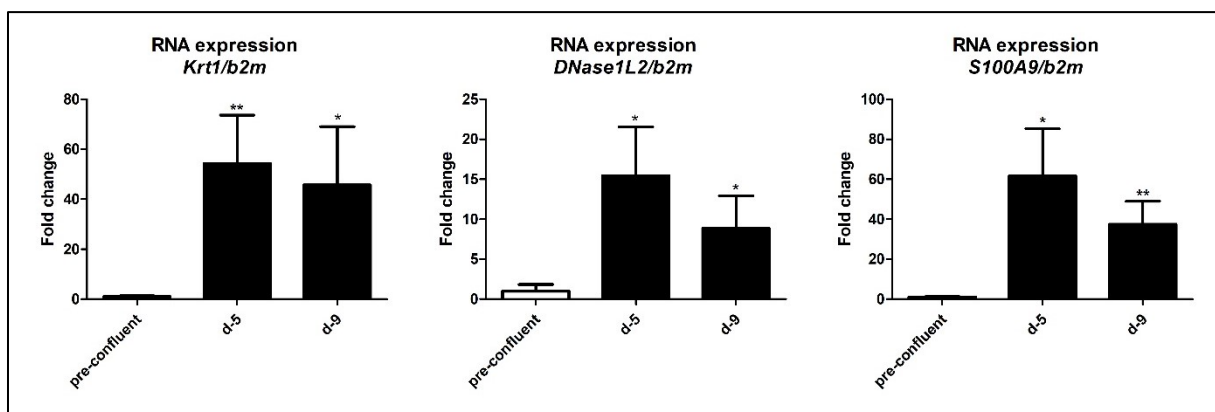


Figure 13: Relative mRNA expression levels of differentiation markers keratin 1 (KRT1), DNase1L2 and S100A9 in NHEK/SVTERT3-5 cells. Significantly increased mRNA levels of these differentiation markers in d-5 and d-9 cells confirmed the differentiation in these cells, and the ability of the NHEK/SVTERT3-5 cell line to correctly differentiate in vitro. $n = 3$. Left: $P = 0.0088, 0.0294$. Middle: $P = 0.0151, 0.0308$, Right: $0.0116, 0.0054$. Unpaired t -test, two-tailed. Error bars indicate SD. Housekeeping gene b2m (β -microglobulin) was used as a reference gene in comparative gene expression analysis.

3.1.2. p21-induced growth arrest in post-confluent keratinocytes

The differentiation of keratinocytes is regulated by the CDK inhibitor p21 (CDKN1A). Independently of the cell cycle regulation, p21 promotes differentiation of basal keratinocytes and growth arrest of differentiated cells (Devgan, Nguyen, Oh, & Dotto, 2006). Elevated expression levels of p21 were detected in d-5 and d-9 cells which corroborate the promoting function of p21 on keratinocyte differentiation. Also, Chaturvedi et al., 1999 observed low p21 expression in pre-confluent keratinocytes, and its induction in post-confluent keratinocytes, as a consequence of p21-induced growth arrest.

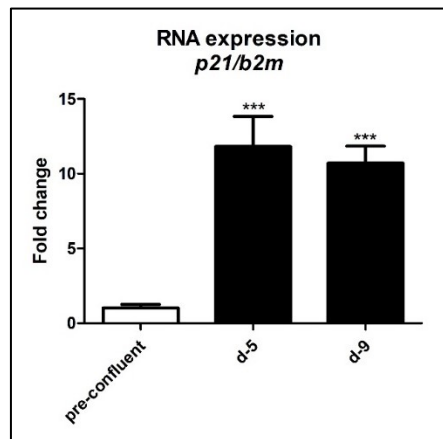


Figure 14: **Relative mRNA expression of the CDK inhibitor p21 in NHEK-SVTERT3-5 cells.** Significantly increased p21 mRNA levels suggest the suppressive function of p21 on proliferation in differentiated (d-5 and d-9) keratinocytes. $n = 3$. $P = 0.0008, 0.0001$. Unpaired *t*-test, two-tailed. Error bars indicate SD. The housekeeping gene *b2m* (β -microglobulin) was used as a reference gene in comparative gene expression analysis.

3.1.3. Keratin 5 is a marker of proliferating, pre-confluent keratinocytes

Keratin 14 (KRT14) together with its partner keratin 5 (KRT5) are proliferation markers of mitotically active basal keratinocytes. *In vivo*, the expression of *KRT5/KRT14* gradually decreased with ongoing differentiation and was replaced by other keratins such as keratin 1, 2, 10, 23, and 78 (Alam, Sehgal, Kundu, Dalal, & Vaidya, 2011, Ehrlich et al. 2018, Fischer et al. 2014, Langbein et al. 2016). qRT-PCR analysis specific for *KRT5* detected similar mRNA expression in pre- and post-confluent keratinocytes, showing that *KRT5* levels did not significantly change during differentiation.

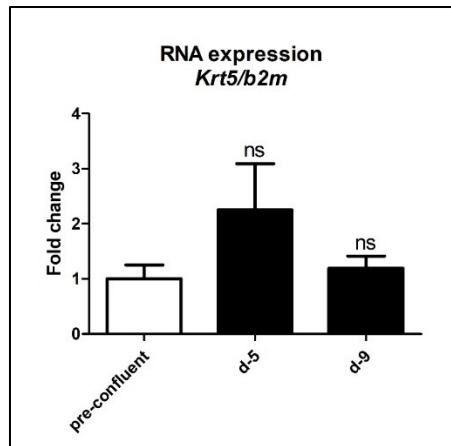


Figure 15: Relative mRNA expression levels of keratin 5 (KRT5) in NHEK/SVTERT3-5 cells. q-RT-PCR of pre- and post-confluent keratinocytes showed KRT5 expression in pre and post-confluent keratinocytes. $n = 3$. $P = 0.0675$, 0.3799 . Unpaired t-test, two-tailed. β -microglobulin) was used as a reference gene in comparative gene expression analysis.

3.2. Analysis of histone acetylation and class I HDACs expression during human keratinocyte differentiation

Histone acetylation is targeted and tightly regulated by the activities of HAT and HDAC enzymes. The current master thesis aims to test the effects of modulating the catalytic activity of HDACs during proliferation and differentiation of keratinocytes. Therefore, expression of class I HDACs, as well as acetylation of histones, were analyzed during keratinocyte differentiation. Histones were prepared by acid extraction and acetone precipitation. The extent of acetylation of two known class I targets, H3K56ac and H4K8ac, was analyzed with specific antibodies using Western blotting. For loading control, an antibody against the histone H3 C-terminus was applied.

Compared to proliferating keratinocytes the level of H3K56 acetylation was found to be unchanged or slightly increased in 5 days post-confluent cells. With proceeding terminal differentiation of keratinocytes (day 9), H3K56 acetylation level further increased. The acetylation level of histone H4 at position K8 showed the opposite effect during differentiation since it was significantly decreased compared to pre-confluent cells. It seems that the terminal differentiation of keratinocytes results in divergent effects on histone acetylation i.e. increased H3K56 acetylation and decreased H4K8 acetylation.

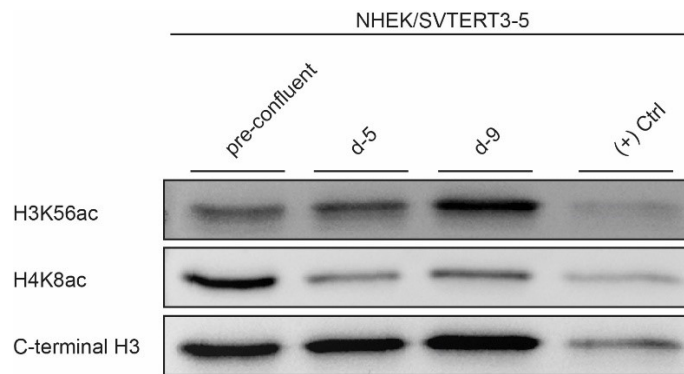


Figure 16: Immunoblot analysis of histone acetylation at histone marks H3K56 and H4K8 in pre-confluent and post-confluent keratinocytes. Terminal differentiation resulted in increased acetylation of histone H3 at lysine 56, whereas pre-confluent cells showed higher acetylation of histone H4 at lysine 8. H3 c-terminal was used as a loading control. HeLa histone extracts were used as a positive control.

Next, we analyzed the expression of class I deacetylases during the differentiation of NHEK/SVTERT3-5 keratinocytes. Soluble extracts of pre-confluent, growing and post-confluent, differentiated cells were used to determine the protein levels of HDAC1, HDAC2, HDAC3 and HDAC8. HDAC1 and HDAC2 showed decreased protein expression with ongoing terminal differentiation of keratinocytes. No changes were observed in protein levels of HDAC3, whereas HDAC8 displayed increased protein expression during terminal differentiation.

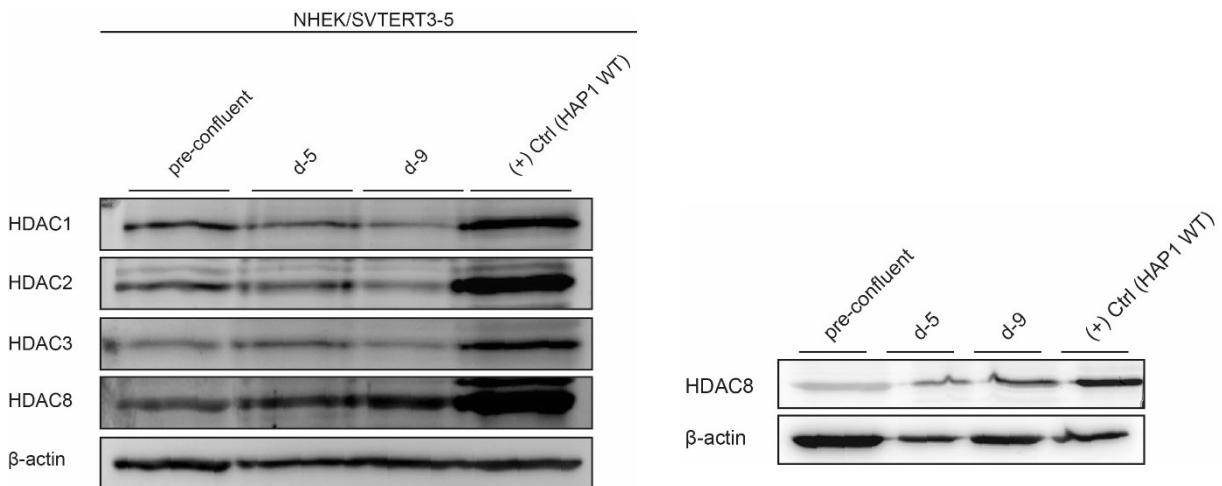


Figure 17: Immunoblot analysis of class I HDACs in pre- and post-confluent NHEK/SVTERT3-5 keratinocytes. HDAC1 and HDAC2 showed reduced expression in differentiated keratinocytes, whereas HDAC3 was found to be essentially unchanged. However, the expression of HDAC8 was induced during the keratinocyte differentiation. The right panel shows a Western blot repeat of the HDAC8 immunodetection. Increase in HDAC8 expression is induced by differentiation of keratinocytes. β -actin was used as a loading control.

For determination of mRNA expression, cells were seeded in 6-well plates and harvested with TRIzol® at three different times points: pre-confluent, d-5, and d-9. After reverse transcription of RNA into cDNA, the qPCR analysis for *HDAC1*, *HDAC2*, and *HDAC8* was performed.

As shown in Figure 18, the mRNA levels of *HDAC1* and *HDAC2* showed no alteration between proliferating and differentiated cells which contrasts with results obtained from Western blotting. This indicates that downregulation of HDAC1 and HDAC2 during keratinocyte differentiation occurs preferably at the protein level than transcriptional. In contrast, HDAC8 mRNA levels in post-confluent d-9 keratinocytes were modestly but significantly increased and coincided with elevated HDAC8 protein expression.

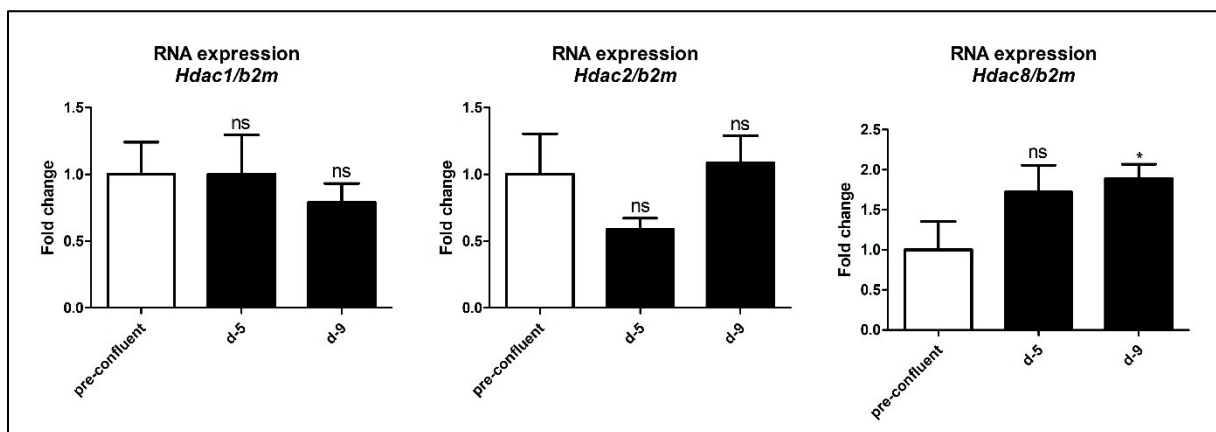


Figure 18: Relative mRNA expression of HDAC1, HDAC2, and HDAC8 during proliferation and differentiation in NHEK/SV3T3-5 cells. *n* = 3. Left: *P* = 0.9886, 0.2650. Middle: *P* = 0.0822, 0.7112. Right: *P* = 0.0637, 0.0181. Unpaired *t*-test, two-tailed. Error bars indicate SD. Housekeeping gene *b2m* (*-microglobulin*) was used as a reference gene in comparative gene expression analysis.

Crotonylation represents an acetylation-like, newly discovered post-translational histone modification associated with active gene expression. Deletion or down-regulation of HDAC1/HDAC2 leads to increase in histone crotonylation. Known sites for lysine acetylation overlap with sites of lysine crotonylation. Moreover, HDAC1/HDAC2 are not only deacetylases but also decrotonylases (Kelly et al., 2018). Histone crotonylation stays low in G1-phase of the cell cycle and gradually increases during S-phase (Fellows et al., 2018).

Acid extractions of histones from harvested keratinocytes in pre-confluent and differentiated (d-5, d-9) state were used to analyze crotonylation of histones H3 and H4. These histone extracts were used for immunoblotting and antibody detection with H3 and H4-specific antibodies. As shown in Figure 19, Western blot analysis displayed a strong decrease of H4K8 crotonylation and unchanged to slightly increased H3K18 crotonylation during proceeding differentiation of keratinocytes.

In summary, histone acetylation (Fig. 16) and crotonylation (Fig. 19) have shown diverse expression patterns, where some histone lysines display an increase of acetylation or crotonylation, whereas others exhibited a decrease or even lack of these post-translational modifications.

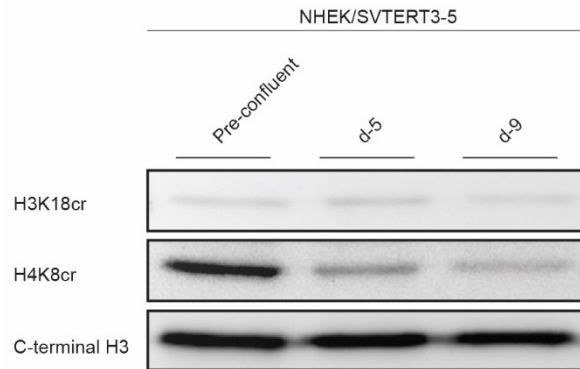


Figure 19: Immunoblot analysis of histone crotonylation during the keratinocyte differentiation. Changes in crotonylation of histones H3 and H4 were observed during keratinocyte differentiation. An antibody against the H3 C-terminus was used as loading control.

3.3. Inhibition of the catalytic activity of class I HDACs in human keratinocytes by MS-275

3.3.1. Impact on acetylation and crotonylation of histone H3 and H4

In the first set of experiments, it was aimed to determine the consequences of class I HDAC inhibition on the level of histone acetylation and crotonylation. Since histones are direct targets of HDACs, these trials should function as controls for the catalytic inhibition of class I HDACs. Additionally, the observed results should demonstrate whether histone acetylation can be influenced at all stages of differentiation by HDACi.

The NHEK/SVTERT3-5 keratinocytes were therefore seeded into 15 cm cell culture dishes (confluency 30-40 %) and treated with increasing concentrations of the HDACi MS-275. The impact of HDACi was tested on both proliferating and differentiating keratinocytes. Accordingly, proliferating keratinocytes were treated with vehicle (DMSO) or increasing concentrations of MS-275 and harvested after 24 hours at 70-80 % confluency. For treatment of keratinocytes undergoing differentiation, cells were grown to 100% confluency and then treated with MS-275 every second day for in total 5 days (d-5) or 9 days (d-9). After the cell harvest, the keratinocytes were prepared for acid histone extraction (see 2.4. Work with proteins and histones) followed by Western blot analysis using antibodies against different histone acetylation and crotonylation sites.

As shown in Figure 20 proliferating keratinocytes responded to increasing HDACi concentrations with a dose-dependent increase in acetylation of H3K56 and H4K8. Treatment of differentiating keratinocytes with 10 μM MS-275 ended in massive cell death and detachment of cells. Therefore, only keratinocytes treated with 1.0 μM and 0.5 μM MS-275 were further studied. Compared to proliferating cells, differentiated keratinocytes reacted to the lowest MS-275 concentration (0.5 μM) with pronounced histone acetylation. However, the effects were less noticeable when using 1.0 μM MS-275 concentration.

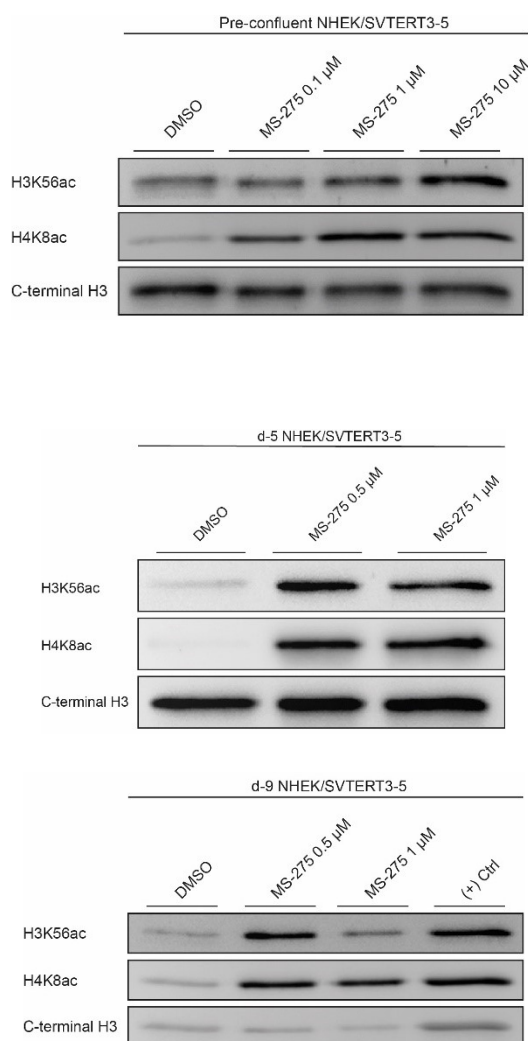
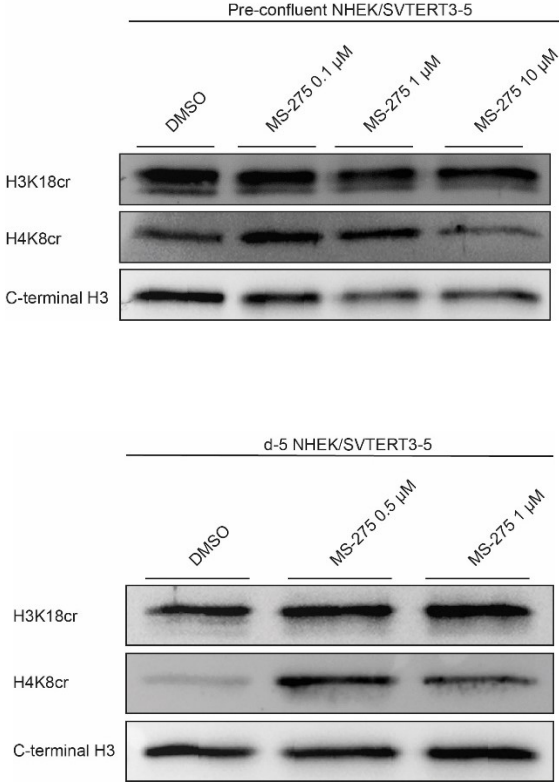


Figure 20: Immunoblot analysis of histone acetylation upon MS-275 treatment in pre-confluent and post-confluent keratinocytes. An antibody specific for H3 C-terminus was used as loading control. HAP1 WT sample was used as a control.

Treatment with increasing concentrations of MS-275 showed an effect on acetylation of histones. Acetylation and crotonylation are functionally similar post-translational modifications, and their addition or removal to histone and non-histone proteins is catalyzed by the same

enzymes. Therefore, we decided to examine also crotonylation of histones H3 and H4 from treated keratinocytes.

Western blot analysis of lysates obtained from HDACi-treated proliferating keratinocytes revealed hardly any regulation of histone crotonylation (H3K18cr, H4K8cr), which contrasted with the results found for histone acetylation (Fig. 21). However, when differentiating cells were treated with MS-275, H4K8 crotonylation strongly increased. In accordance with histone acetylation, the effects were less pronounced when cells were treated with 1.0 μ M MS-275. Due to the inequalities of loaded histone amounts from late-differentiated keratinocytes (d-9), the suggestive increase of crotonylation (H4K8cr) cannot be fully judged. The impact of MS-275 treatment on the H3K18 crotonylation was found to be modest, as hardly any increase could be observed in d-5 keratinocytes. Inequalities in amounts of loaded samples from late-differentiated keratinocytes (d-9) and in general low signal intensities prevented a clear statement about the regulation of H3K18cr in these cells.



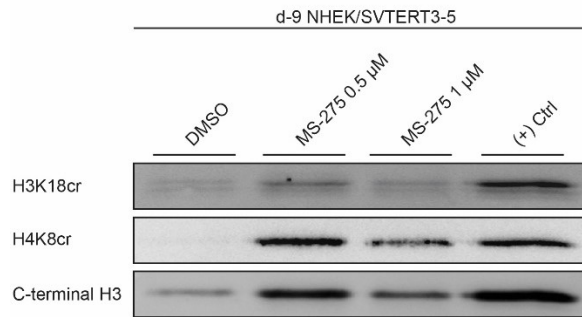


Figure 21: Immunoblot analysis of crotonylation in MS-275 treated keratinocytes. Treatment of cells with MS-275 induced crotonylation of histone H3 and H4. An antibody specific for H3 C-terminus was used as loading control. HeLa cells were used as positive control.

3.3.2. Impact on keratinocytes proliferation and differentiation

Having shown, that MS-275 inhibits HDACs in keratinocytes, resulting in increased levels of histone acetylation, I aimed to determine the phenotypical consequences of HDAC inhibition. To investigate the impact of class I HDACs on proliferating keratinocytes, NHEK/SVTERT3-5 cells were treated for 24h with MS-275, and effects on cellular morphology, metabolic activity, and expression of HDACs as well as markers for keratinocyte proliferation, differentiation, and cell cycle were analyzed. As seen in Figure 22, the treatment of keratinocytes with increasing concentration of MS-275 did not alter cell morphology, indicating that even high MS-275 doses do not have immediate toxic effects.

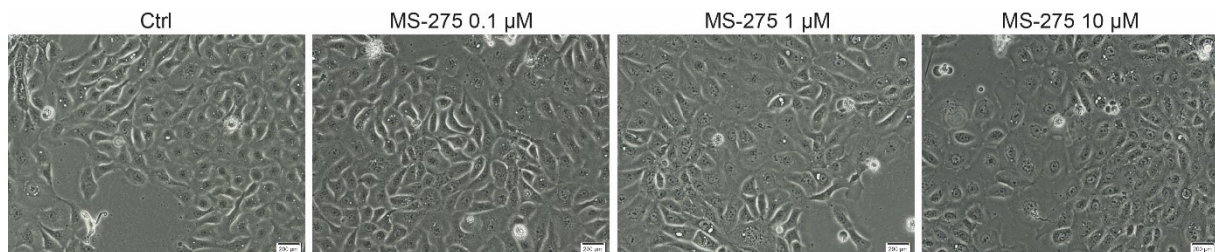


Figure 22: Pre-confluent NHEK/SVTERT3-5 keratinocytes after 24h-treatment with increasing concentrations of HDACi MS-275. No changes in cell morphology or increased apoptosis were observable. Magnification: 20x, bright-field.

The cells' metabolic capacity was analyzed using MTS cell proliferation assay, where the reduction of the MTS compound into formazan resulted in the colorimetric shift which was measured as an absorption change. The analyzed data displayed a reduced proliferation of pre-confluent keratinocytes treated with 10 μ M MS-275, and no difference in metabolic activity of keratinocytes treated with 0.1 μ M and 1.0 μ M MS-275 concentration.

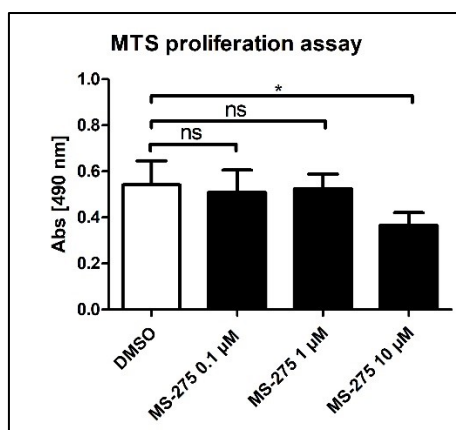


Figure 23: The metabolic rate of NAD^+ to $NADH$ conversion measured by MTS colorimetric assay. The free electron is accepted by intermediate electron acceptor (PMS) which can easily penetrate the cell membrane and reduce MTS tetrazolium compound to formazan in the cell culture medium. Treatment of cells with HDACi MS-275 inhibits NAD^+ to $NADH$ conversion and cell metabolism with the result of reduced proliferation. Only the highest MS-275 concentration led to a significant decrease in cells proliferation. $n = 5$. $P = 0.6153, 0.7565, 0.0103$.

To test whether the treatment of pre-confluent NHEK/SVTER3-5 keratinocytes with HDACi MS-275 can induce changes in gene expression of class I HDACs itself, as well as in HDACs' target genes, the keratinocytes were treated with 1.0 μM and 10 μM MS-275 concentrations for 24h and harvested for RNA isolation and further processing.

The treatment of pre-confluent keratinocytes with 10 μM MS-275 induced *HDAC1* mRNA expression by 2-fold (Fig. 24, upper panel). On the contrary, mRNA levels of *HDAC2* and *HDAC8* remained unaffected, independently of the MS-275 concentration. This indicates that increased levels of histone acetylation upon MS-275 treatment are rather caused by inhibition of catalytic activity of HDACs, than by downregulation of these enzymes. Upregulation of *p21* expression in MS-275-treated keratinocytes repeatedly showed the connection between HDAC inhibition and modulation of the cell cycle (Fig. 24, middle panel). Genes that are associated with cellular proliferation, such as *EPGN* and *KRT5*, were found to be downregulated upon HDACi treatment. Moreover, *KRT1*, as a marker for early differentiation was found to be downregulated too, indicating that keratinocytes respond to MS-275 treatment with increased cell cycle arrest without induction of terminal differentiation. Similarly, *DNase1L2*, a marker for late differentiation was not induced by MS-275 treatment.

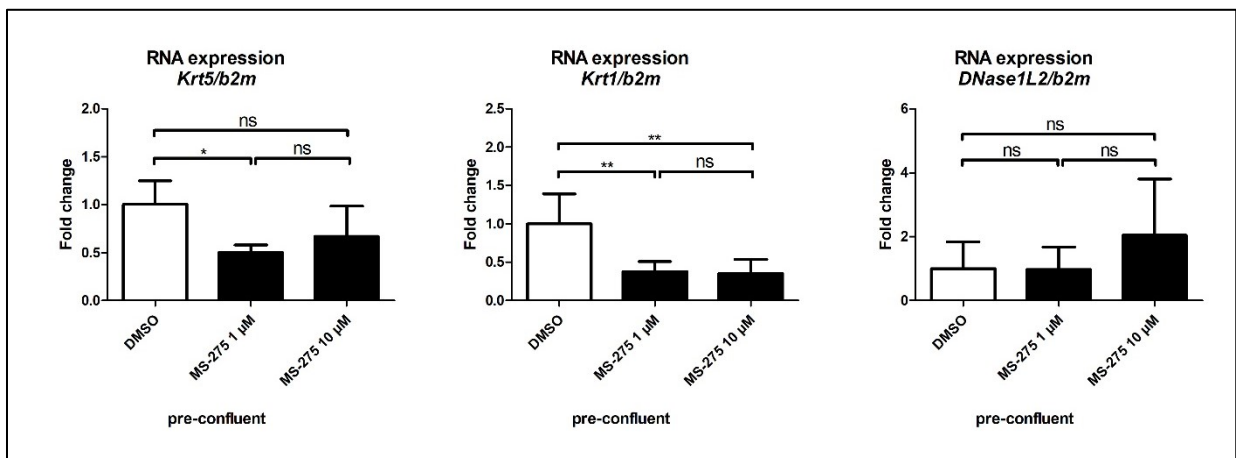
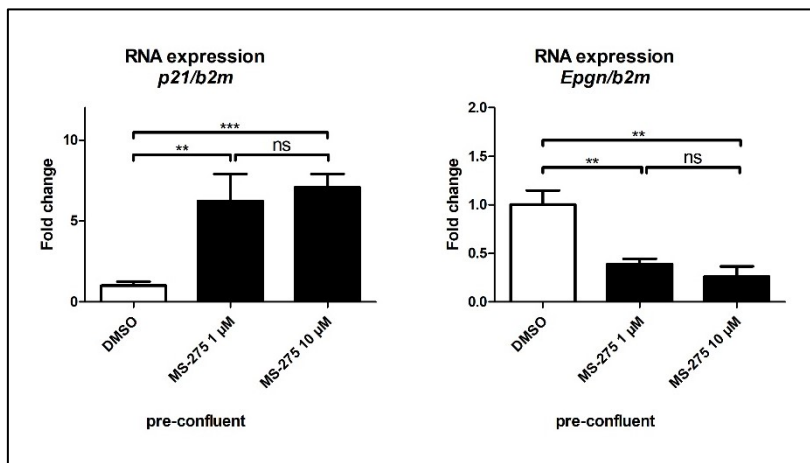
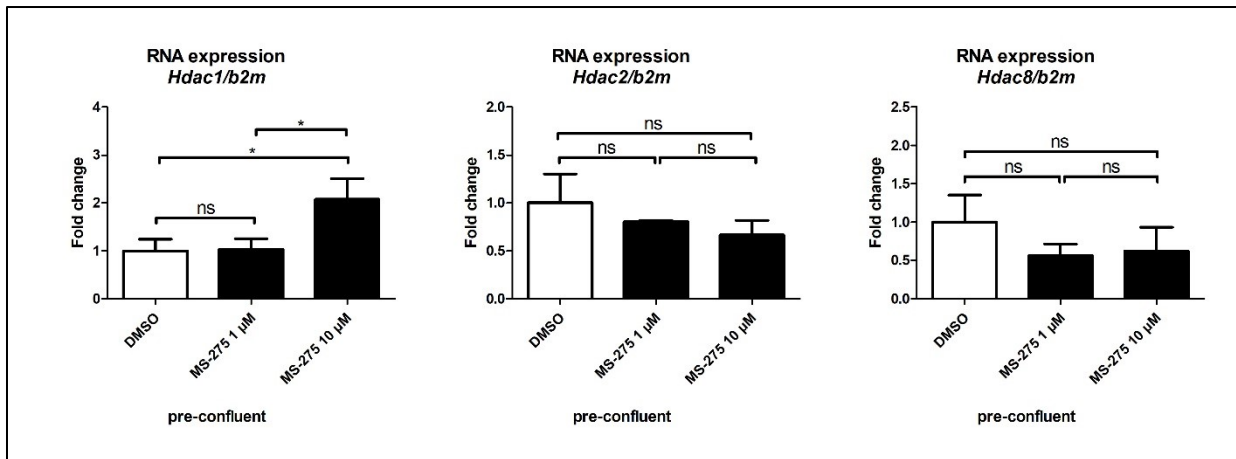


Figure 24: Relative mRNA expression levels of HDAC1, HDAC2, HDAC8, cell cycle regulator p21, and other proliferation and differentiation markers in MS-275 treated pre-confluent NHEK/SV3TERT3-5 keratinocytes. DMSO was used as a control. $n = 3$. $P < 0.05$. Error bars represent the standard deviation. -microglobulin (b2m) was used as reference gene for qPCR data analysis. In the next step, protein lysates were used to analyze alterations in protein expression of HDAC1, HDAC2 and cell cycle regulators p21 and p53 (Fig. 24). The HDAC1 and HDAC2 protein expression is not affected by increasing MS-275 concentrations. However, as seen from the mRNA data, the p21 expression is also induced on protein level in a dose-dependent manner. Protein levels of p53 were found to be unchanged in keratinocytes, that contrasts with a study published by (Choi et al., 2015), where p53 levels were found to be decreased in tumor cells after inhibitor treatment.

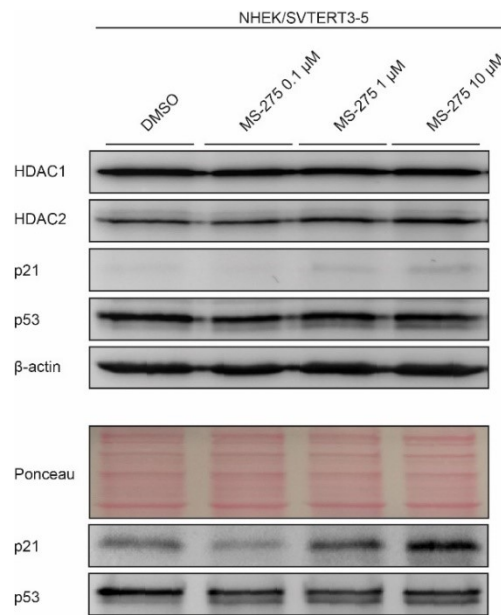


Figure 25: Immunoblot analysis of HDAC1/HDAC2 and cell cycle regulators (p21, p53) during the treatment of proliferating (pre-confluent) keratinocytes with increasing MS-275 concentration. HDAC1, HDAC2, and p53 exhibit no regulation on protein level upon increasing MS-275 concentrations. The Western blotting was repeated for p21 and p53 (bottom panel), Ponceau used as a loading control.

The influence of class I HDAC' inhibition during terminal differentiation was investigated by observing the cells and taking their photos throughout the treatment. The keratinocytes seeded in 6-well plates were treated with MS-275 and daily monitored until their harvest at day 5 or day 9 after reaching complete confluency.

Post-confluent keratinocytes reacted to HDACi treatment differently than pre-confluent, proliferating cells. Differentiated cells are more sensitive to the treatment with MS-275 because even the lowest HDACi concentration used (0.5 μM) caused the abnormal formation of many small autophagic-like vacuoles inside the d-9 keratinocytes (Fig. 27). At 1.0 μM MS-275 concentration cells started to die massively, and at the highest concentration (10 μM MS-275) all cells appeared apoptotic. Nonetheless, it seemed that d-5 keratinocytes were not affected at the lowest (0.5 μM) concentration, although the increased death rate was observed at 1.0 μM and 10 μM MS-275 concentrations.

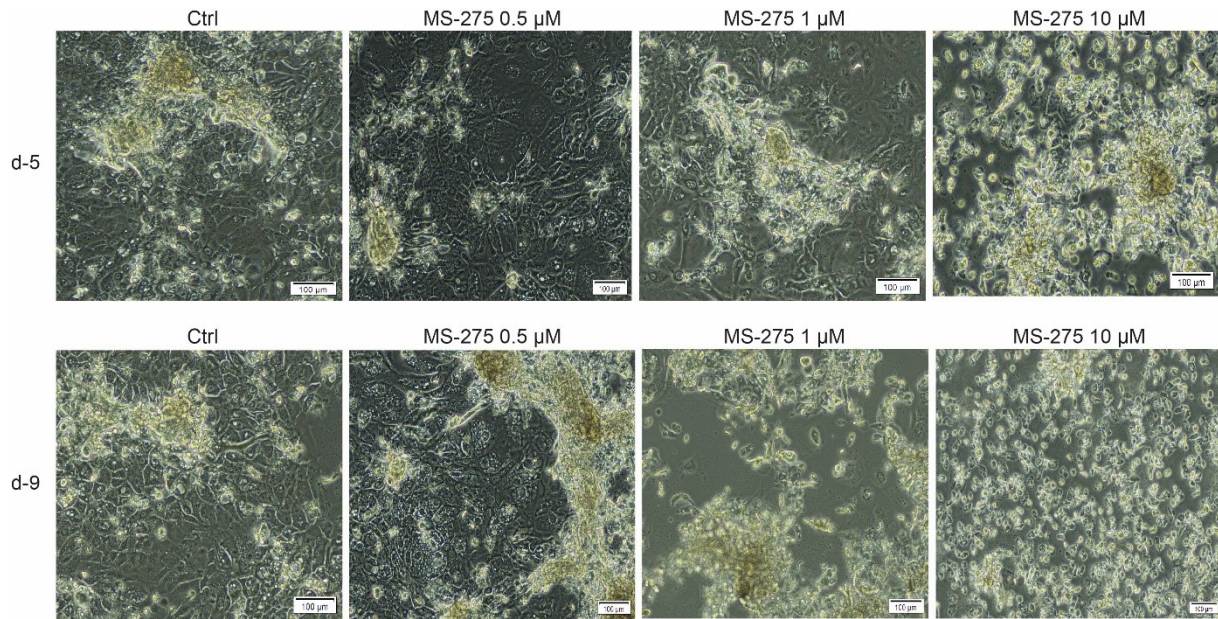


Figure 26: Treatment of post-confluent keratinocytes with increasing concentrations of MS-275 HDACi. *d-5* keratinocytes seemed to be less sensitive to increased HDACi concentration than more differentiated *d-9* cells. At the highest HDACi concentration (10 μM) both *d-5* and *d-9* keratinocytes appear apoptotic. Magnification: 10x, bright-field.

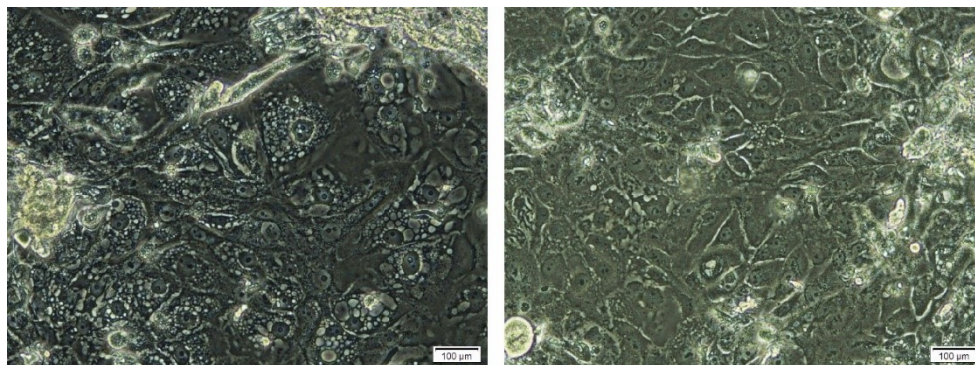


Figure 27: Vacuoles inside *d-9* keratinocytes treated with 0.5 μM MS-275 (left) and a respective control (right). Magnification: 20x, bright-field.

To compare the visual changes with molecular ones, we isolated RNA from keratinocytes treated with 1 μM MS-275 and analyzed the transcriptional levels of target genes. No samples could be obtained from *d-5* and *d-9* keratinocytes treated with 10 μM MS-275 concentration because the cells died before the harvesting day.

Analysis of qRT-PCR data showed that MS-275 treatment of *d-5* differentiated keratinocytes resulted in moderately reduced mRNA expression of HDAC1 (not significant) and significant 2-fold reduction of HDAC2 and HDAC8. This reduction was further pronounced in *d-9* treated cells, where mRNA levels of HDAC1, HDAC2, and HDAC8 were respectively reduced 2-fold, 4-fold and 4-fold. Moderate reduction of mRNA levels was also detected for *p21* and *EPGN* in

both, d-5 and d-9 treated keratinocytes. The greatest reduction of mRNA levels was detected in genes associated with early and late keratinocyte differentiation, such as keratin 1 (*KRT1*) and *DNase1L2*, indicating that HDAC activity is essential for transcription of at least some differentiation-associated genes.

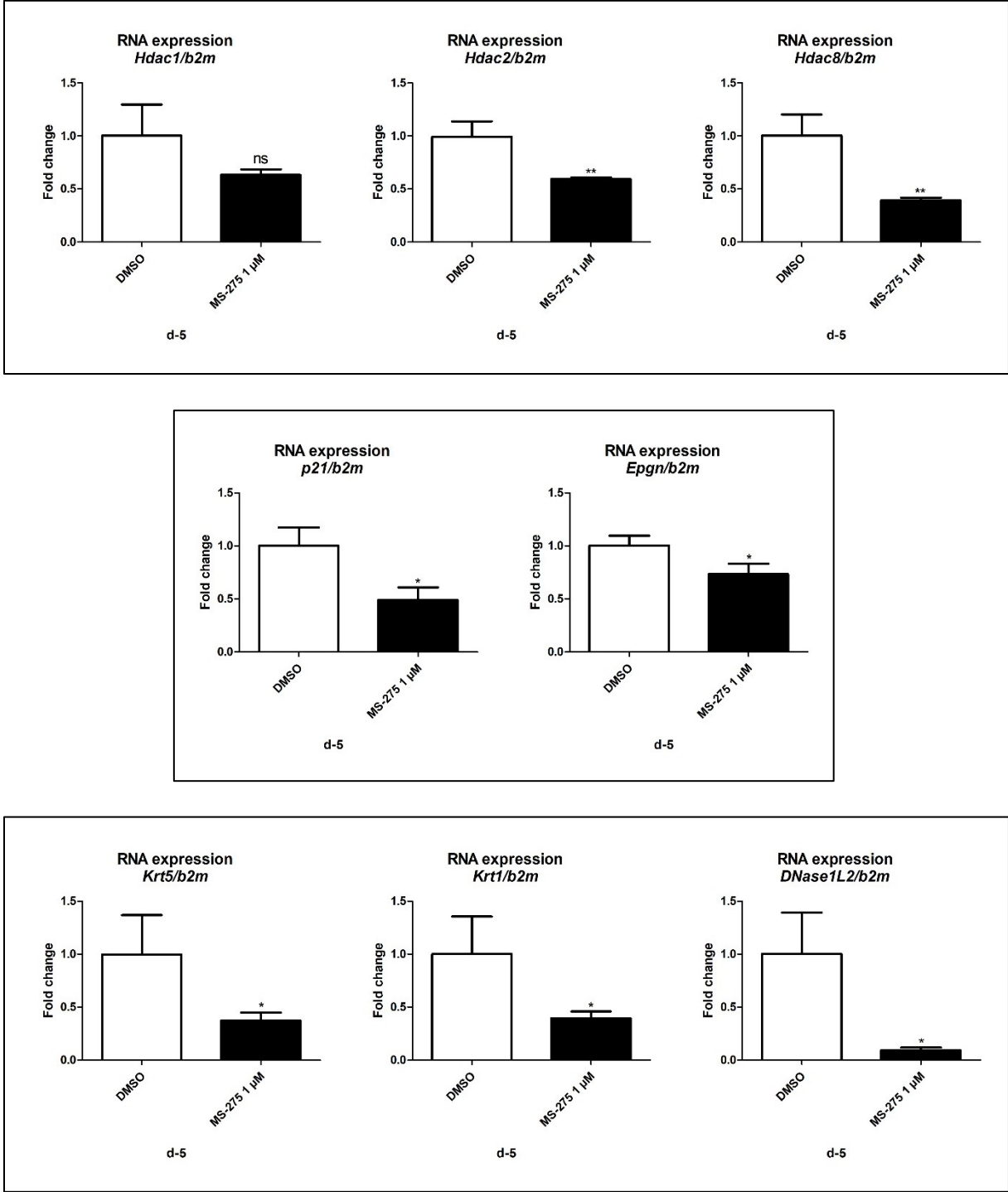


Figure 28: Relative mRNA expression levels of HDAC1, HDAC2, HDAC8, p21, EPGN and differentiation-specific keratins in post-confluent d-5 keratinocytes. The HDACi MS-275 significantly reduced expression levels of all tested genes. DMSO was used as a control. $n = 3$. $P < 0.5$. Error bars represent the standard deviation. -microglobulin (*b2m*) was used as reference gene for qPCR data analysis.

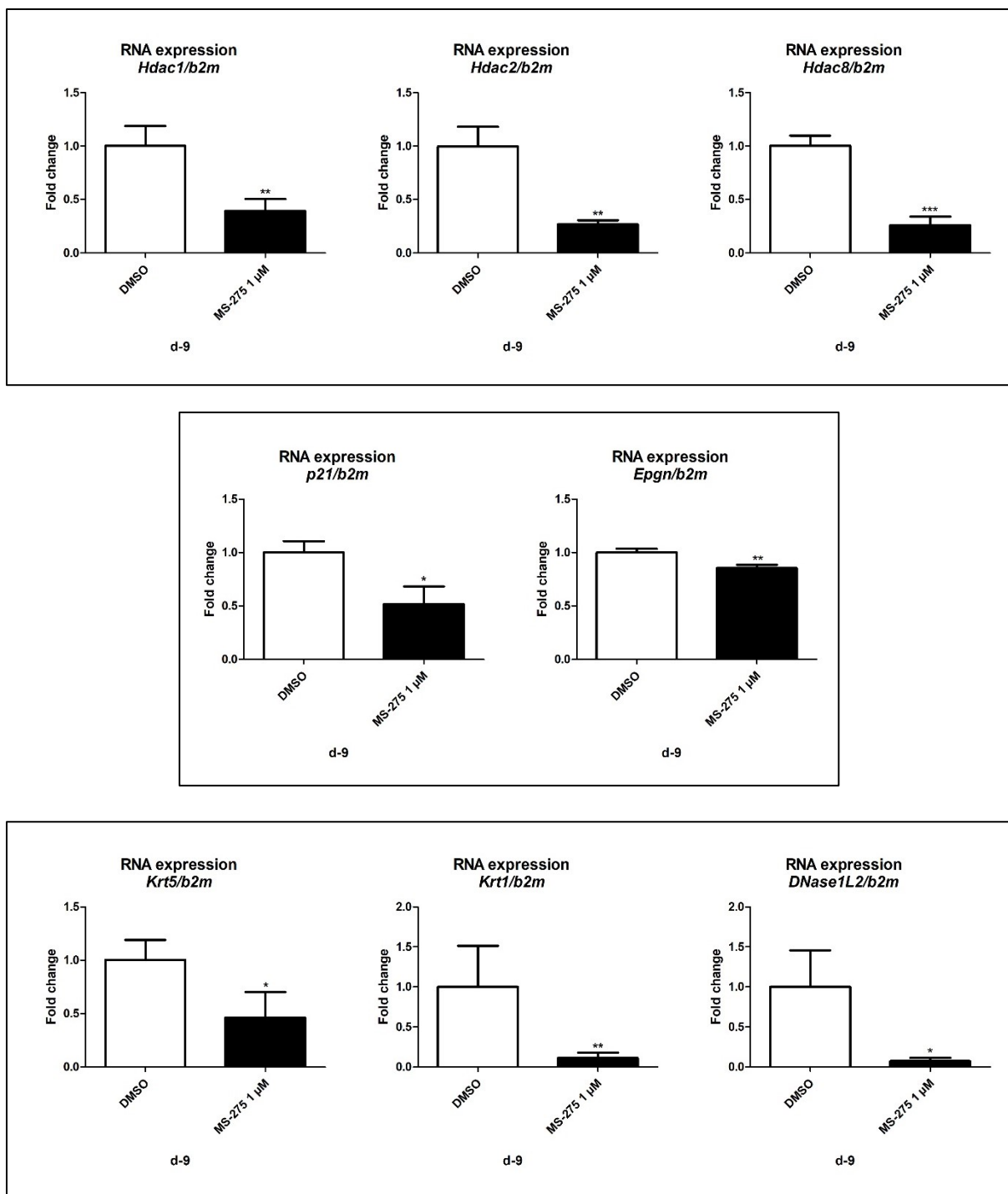


Figure 29: Relative mRNA expression levels of HDAC1, HDAC2, HDAC8, p21, Epgn and differentiation-specific keratins in post-confluent d-9 keratinocytes. DMSO was used as a control. $n = 3$. $P < 0.5$. Error bars represent the standard deviation. -microglobulin (b2m) was used as reference gene for qPCR data analysis.

3.4. Generation of cell lines overexpressing catalytically inactive HDAC1 and wildtype HDAC1

3.4.1. Optimization of transfection of NHEK/SVTERT3-5 keratinocytes

In general, primary cells, such as keratinocytes are difficult to transfect. Since NHEK/SVTERT3-5 closely resembles human primary keratinocytes, we hypothesized that this

might also be true for this cell line. Therefore, we tested several common transfection agents such as TurboFect™ (*Thermo Fisher Scientific*), SuperFect® (*Qiagen*), FuGENE® (*Promega*) and jetPEI™ (*Polyplus transfection*) for their transfection efficiency. To identify transfected cells, a plasmid containing a GFP expression construct fused to a nuclear localization signal (NLS) was used. As a result, nuclei adopted green fluorescent color that could easily and directly be visualized by an inverted fluorescence microscope. The highest transfection efficiency and the lowest cell toxicity for NHEK/SVTERT3-5 keratinocytes were achieved with the FuGENE® reagent. Additionally, the best DNA [µg] to transfection reagent [µl] ratio needed to be determined. By using the ratio of 2-3 µg of DNA to 6-8 µl of FuGENE® reagent, we achieved the highest transfection efficiency that was about 30 % (Fig. 30).

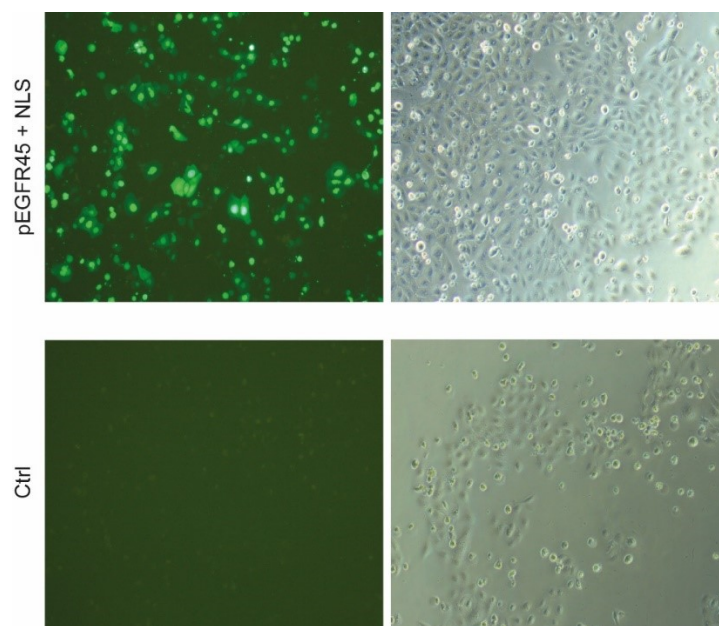


Figure 30: *Transfection efficiency of a vector encoding GFP with nuclear localization signal (NLS) in NHEK/SVTERT3-5 keratinocytes. As a control, we transfected the keratinocytes with FuGENE reagent without the addition of the GFP plasmid. Magnification: 100x.*

3.4.2. FuGENE®-mediated transfection of keratinocytes to overexpress HDAC1 variants using CRISPR/Cas9

The goal of this experiment was to create stably transfected NHEK/SVTERT3-5 keratinocyte cell lines overexpressing either active HDAC1 WT or inactive HDAC1 H141A enzyme. Therefore, we used the FuGENE® transfection reagent and CRISPR/Cas9 tools. The keratinocytes were transfected with four different vectors coding for guide RNA (gRNA), Cas9 endonuclease, blasticidin resistance with GFP, and the respective sequence for FLAG-tagged HDAC1 WT or HDAC1 H141A. The guide RNA guided Cas9 endonuclease to protospacer (target sequence) and PAM (Protospacer Adjacent Motif) sequence within the AAVS locus where the cut was made, and the cassette with the gene of interest could be inserted by the homologous recombination (Ceasar, Rajan, Prykhodzhiy, Berman, & Ignacimuthu, 2016). The

AAVS locus used for insertion represents a safe harbor locus which has two important features: the insertion and the expression of the gene of interest do not affect the expression of other genes, and the open chromatin configuration allows efficient and stable gene expression.

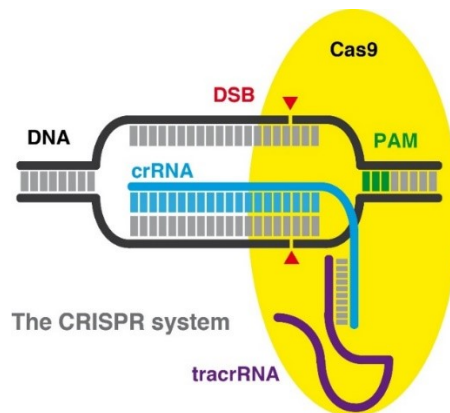


Figure 31: The CRISPR/Cas9 genome editing mechanism was discovered in bacteria where it is used as an anti-phi phages. For the genome editing purposes, single guide RNA (sgRNA) was created by connecting the bacterial CRISPR RNA (crRNA) with trans-activating crRNA (tracrRNA). The sgRNA can be designed to specifically bind the target region (protospacer). Cas9 makes a double-strand break (DSB). The CRISPR/Cas9 tool can be used for knock-in, conditional or permanent knock-out, an introduction of point mutations etc. Figure taken from <http://www.user.cnb.csic.es/~montoliu/CRISPR/> (7.12.2018).

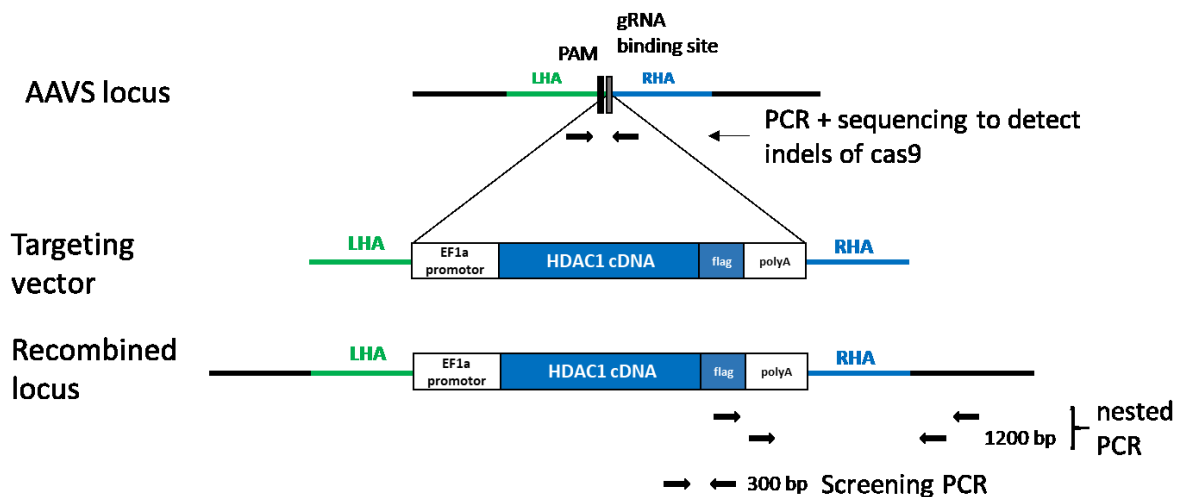


Figure 32: The figure represents the genomic safe harbor locus AAVS and a targeting construct after the successful recombination. The arrows indicate the binding sites of the primers and the length of the respective PCR products from different types of PCRs. LHA: left homologous arm, RHA: right homologous arm.

One day after transfection of keratinocytes, the cell medium was exchanged and Blasticidin was added to the medium for one additional day. This step selects for in-principle transfectable cells. The surviving cells were tested for the correct binding of the gRNA and Cas9-double-strand breakage using a PCR as we can see from the Figure 33 the two bands confirmed the successful binding of gRNA, cut and insertion of the target gene (either HDAC1 WT or HDAC1

H141A) into the AAVS locus. The second small band, which is also present in the negative control corresponds to the second unmodified AAVS1 allele.

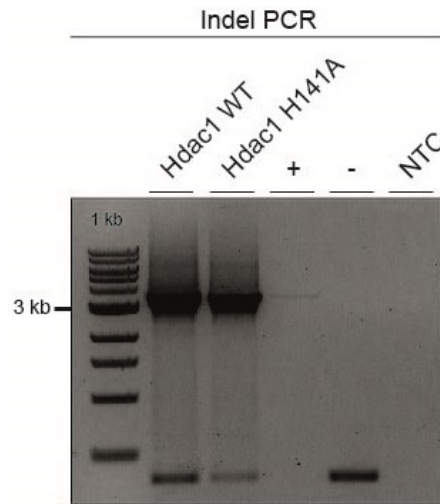


Figure 33: PCR for detection of the integrated transgene in AAVS locus. The primer-pair bound in the left- and right-homology region of the inserted cassette. The size of the integrated construct is 3530 bp. If there would be no gene insertion, the amplified product would only be 354 bp long (negative Ctrl). The transfected keratinocytes contain the gene of interest, either HDAC1 WT or HDAC1 H141A. Pos. control: HAP1 HDAC1 2S. Neg. control: HAP1 cells. NTC (Non-template control): ultrapure H₂O. Primer pair: AAVS-gRNA-F/R.

To verify the successful knock-in of NHEK/SVTERT3-5 transfected keratinocytes at the correct locus, a nested PCR strategy was used. As shown in Figure 32, a primer pair that binds on the one hand in the FLAG region of the insert and on the other outside of the right homology arm (RHA) of the AAVS locus was used for the analysis of the transfected cell batch. The presence of the bands for HDAC1 WT and HDAC1 H141A in the second nested PCR confirmed the gene insertion at the AAVS locus because the 5' end primers could bind to and amplify the region of the insert.

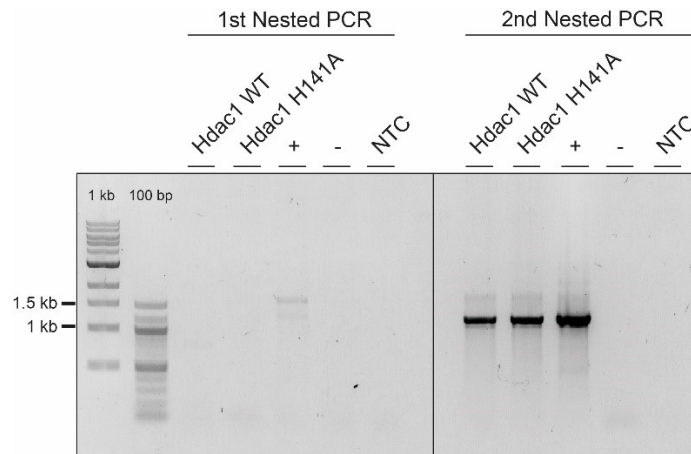


Figure 34: Nested PCR verified the successful knock-in of NHEK/SVTER3-5 keratinocytes. The nested PCR was conducted in two steps. The primer pairs used in first and second nested PCR bind inside the inserted gene and outside of the inserted gene, in the RHA. The product of second nested PCR with a size of 1200 bp, confirmed the successful amplification and binding of the primers. Pos. control: HDAC1 DD gRNA. Neg. control: HAP1 WT cells. NTC (Non-template control): ultrapure H₂O. The primer pair (1st n

Next, the transfected keratinocytes were seeded in 96-well cell culture plates in a way that in each well would be on average one cell to obtain single cell clones. The cells in the wells were further propagated for approximately 14 days, and single cell colonies were screened for the presence of the transgene (either *Hdac1 WT* or *Hdac1 H141A*).

The primer pair used for the screening of the clones binds to the HDAC1 ORF and the FLAG sequence inside the transgene (Fig. 32). As a positive control, we used genomic DNA from previously created HAP1 cell lines expressing FLAG-tagged HDAC1 WT or HDAC1 2S mutant that were generated by the same strategy (HAP1 HDAC1 WT and HAP1 HDAC1 2S). As a negative control, DNA from unmodified Hap1 cells was used (HAP1).

Screening PCR

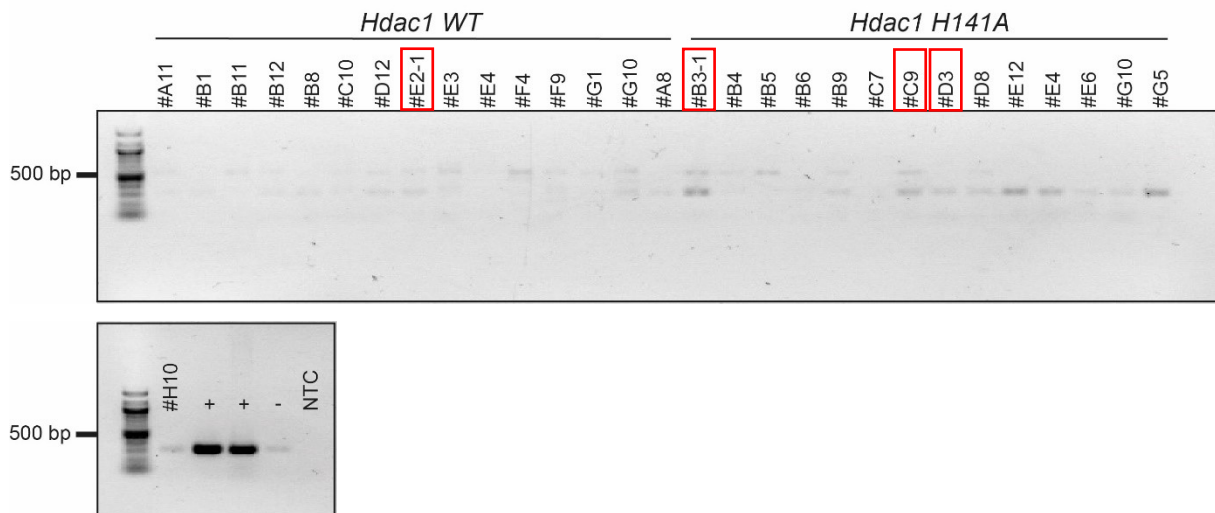


Figure 35: Screening PCR of the single cell colonies in the 96-well plate. The size of the amplified PCR product is 304 bp. The red rectangles represent the clones which were chosen for FLAG immunoblot detection. Pos. controls: HAP1 HDAC1 WT and HAP1 HDAC1 2S. Neg. control: HAP1. NTC (Non-template control): ultrapure H₂O. Primer pair: qRT_mHdac1_F1/qRT_FLAG_R1.

Parallel to the screening PCR also the quality control (QC) PCR was run, to assess the quality of the isolated DNA.

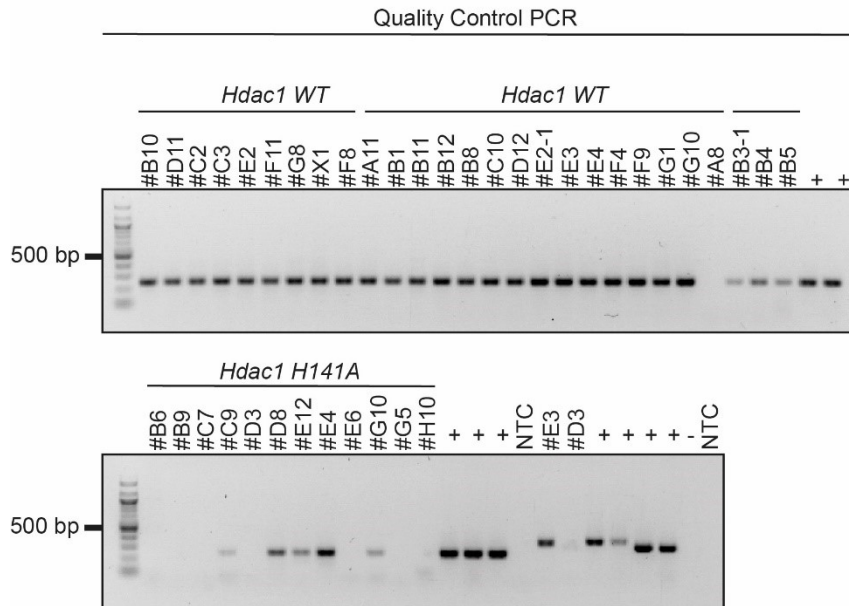


Figure 36: QC PCR of single cell colonies (clones) to assess the DNA quality. The primer pair used for this PCR binds in the genomic DNA and produces the PCR product of 244 bp. Pos. controls: HAP1 HDAC1 WT and HAP1 HDAC1 2S. Neg. control: HAP1. NTC (Non-template control): ultrapure H₂O. Primer pair: AAVS-gRNA-F/R.

To screen all single-cell colonies from the 96-well plates, two rounds of screening and QC PCR were performed. The clones with the adequate genomic DNA quality and a sign to contain the

transgene (encircled in red) were selected and expanded further until they could be grown in 10 cm dishes.

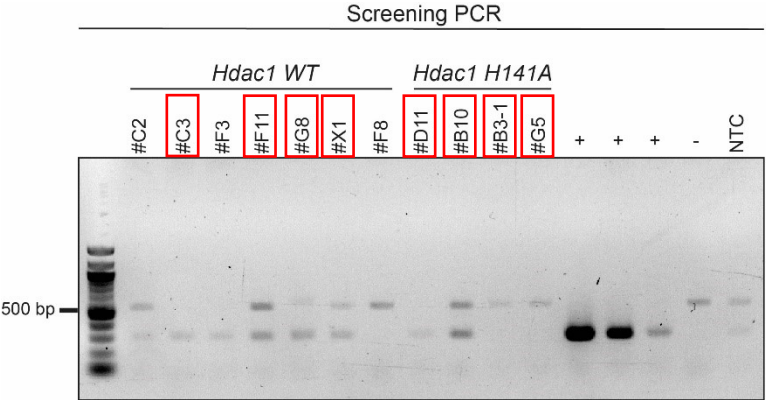


Figure 37: Screening PCR of the single cell colonies in the 96-well plate. The size of the amplified PCR product is 304 bp. The red rectangles represent the clones which were chosen for FLAG immunoblot detection. Pos. controls: AAVS HDAC1 WT, HAP1 HDAC1 WT, 4454 (tg/+mouse DNA), HDAC1 AAVS1 HAP. Neg. control: 4454 and HAP1. NTC (Non-template control): ultrapure H₂O. Primer pair: qRT_mHdac1_F1/qRT_FLAG_R1.

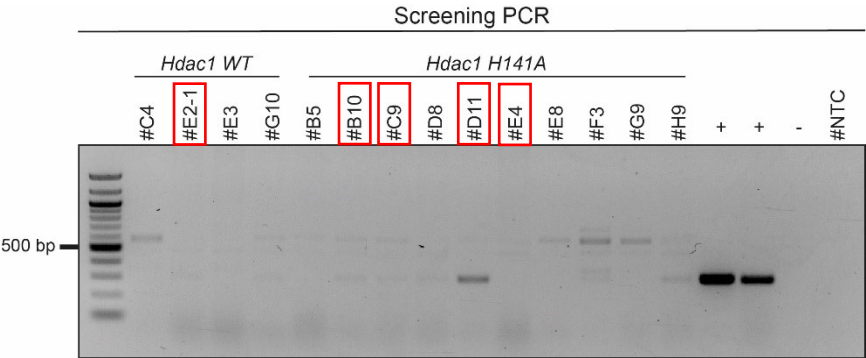


Figure 38: Screening PCR of the single cell colonies in the 96-well plate. The size of the amplified PCR product is 304 bp. The red rectangles represent the clones which were chosen for FLAG immunoblot detection. Pos. controls: SVTERT3-5 DNA AAVS-HD1, HAP1 HDAC1 2S. Neg. control: HAP1. NTC (Non-template control): ultrapure H₂O. Primer pair: qRT_mHdac1_F1/qRT_FLAG_R1.

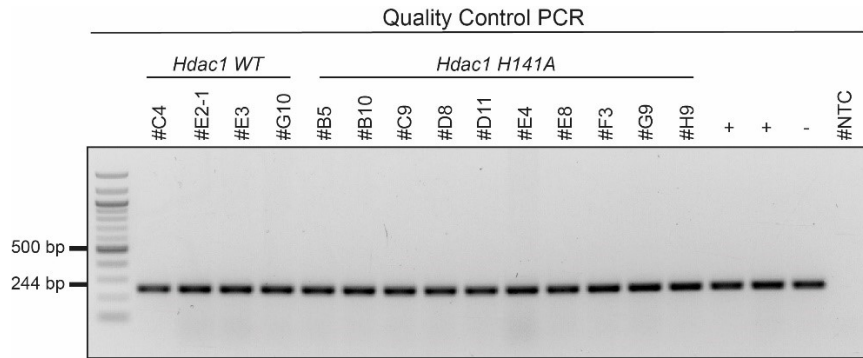


Figure 39: QC PCR of single cell colonies (clones) to assess the DNA quality. The primer pair used for this PCR binds in the genomic DNA and produces the PCR product of 244 bp. Pos. controls: SVTERT3-5 DNA AAVS-HD1, HAP1 HDAC1 2S. Neg. control: HAP1. NTC (Non-template control): ultrapure H₂O. Primer pair: h_p21_1/h_p21_2.

Based on screening and QC PCRs single clones were trypsinized and further propagated to 10 cm dishes. Cells were harvested, lysed and subjected to Western blot analysis to test whether cells express FLAG-tagged transgenic HDAC1 variants. However, from the chosen clones, none was positive for the FLAG-tag (Fig. 40).

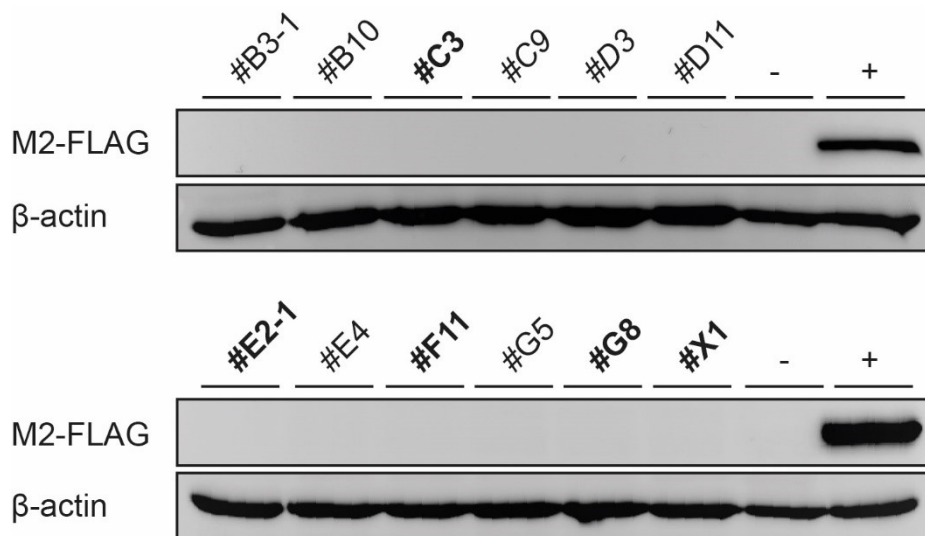


Figure 40: Immunoblot analysis of clones for the presence of the transgene using anti-FLAG antibodies. Pos. control: HAP1 HDAC1 WT A11 P7.

3.4.3. Electroporation-mediated transfection of keratinocytes to overexpress HDAC1 variants using CRISPR/Cas9

The endeavor of creating two new cell lines, expressing either HDAC1 WT or HDAC1 H141, using the NHEK/SVTERT3-5 keratinocytes and the FuGENE® transfection did not lead to any cell clones containing the desired transgene. Therefore, we decided to repeat the process but using electroporation instead of the transfection method. The electroporation is a highly efficient delivery method and can be used for cells which are difficult to transfect (primary cells) or show high rates of cell death due to the toxicity of the transfection agent. Additionally,

instead of cas9 plasmid, a cas9 protein was transfected with the goal to increase the likelihood of gene targeting (personal information Krzysztof Chylinski, VBC facility).

The electroporation of vectors coding for gRNA, blasticidin resistance with GFP and the desired transgenes coupled to FLAG-tag together with either Cas9 plasmid or Cas9 protein was performed by the VBC facility (Krzysztof Chylinski, Philipp Czermak) using conditions described in the Material and Methods section. The electroporation was lethal for many cells. Remaining cells were treated with blasticidin for 24 hours, resulting in an enrichment of successfully transfected cells. Aliquots of the transfected cell batch were collected during splitting and tested for successful gene targeting using indel PCR and nested PCR.

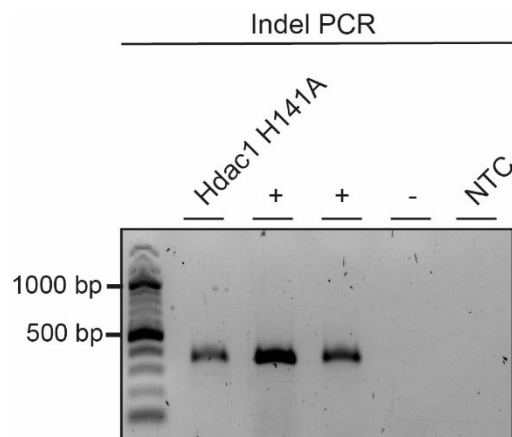


Figure 41: *Indel PCR* shows the successful binding of gRNA and double-strand break by Cas9 endonuclease for HDAC1 H141A electroporated NHEK/SVTERT3-5 keratinocytes.

In the next step, the electroporated cells were tested as a batch for the presence of the transgene at the AAVS locus with nested PCRs. The primer pairs used for nested PCR bound inside the transgene and outside of the right homology arm (RHA) genomic sequence (Fig. 32). The bands seen at the second nested PCR confirm the presence of the transgene (either HDAC1 WT or HDAC1 H141A) at the AAVS locus of the electroporated NHEK/SVTERT3-5 keratinocytes.

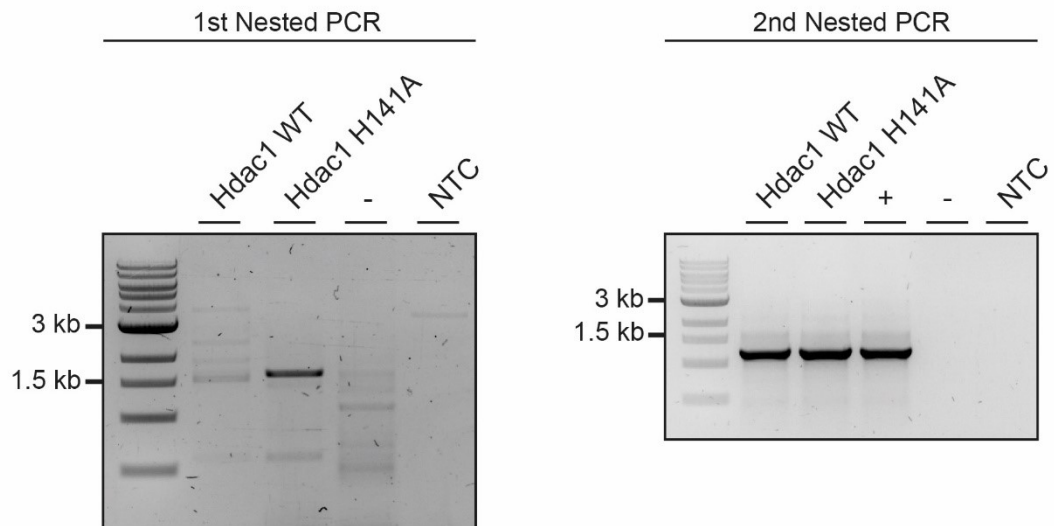


Figure 42: Nested PCR of the batch after electroporation. Nested PCR enabled to detect the integration of the transgene in AAVS locus. Since nested PCR is performed in two rounds with two different primer pairs, this results in vast amounts of PCR product. The primer pairs are selected to bind in the transgene region and in RHA of the AAVS locus. PCR product size: 1200 bp. 1st primer pair `_AAVS1_R2`. 2nd primer pair used:

Next, a limiting dilution approach was set up in order to cultivate single clones as described in chapter 2.5.2. Selection of wells colonized by single cells colonies was done by using the microscope. To test for the presence of the transgene, the screening PCR with primer pair binding within the transgene was utilized (Fig. 32). The screening was performed for in total of 768 *Hdac1* WT clones and 912 *Hdac1* H141A clones. In parallel, also the quality of the genomic DNA from the tested clones was examined.

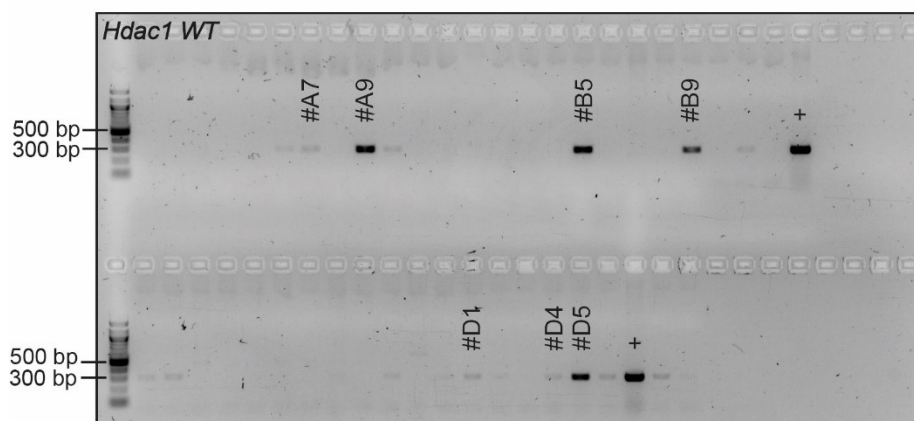


Figure 43: Screening PCR of single cell clones for containing the HDAC1 WT transgene. The primer-pair used bonded in HDAC1 transgene and FLAG-tag region. The expected length of the PCR product was 304 bp.

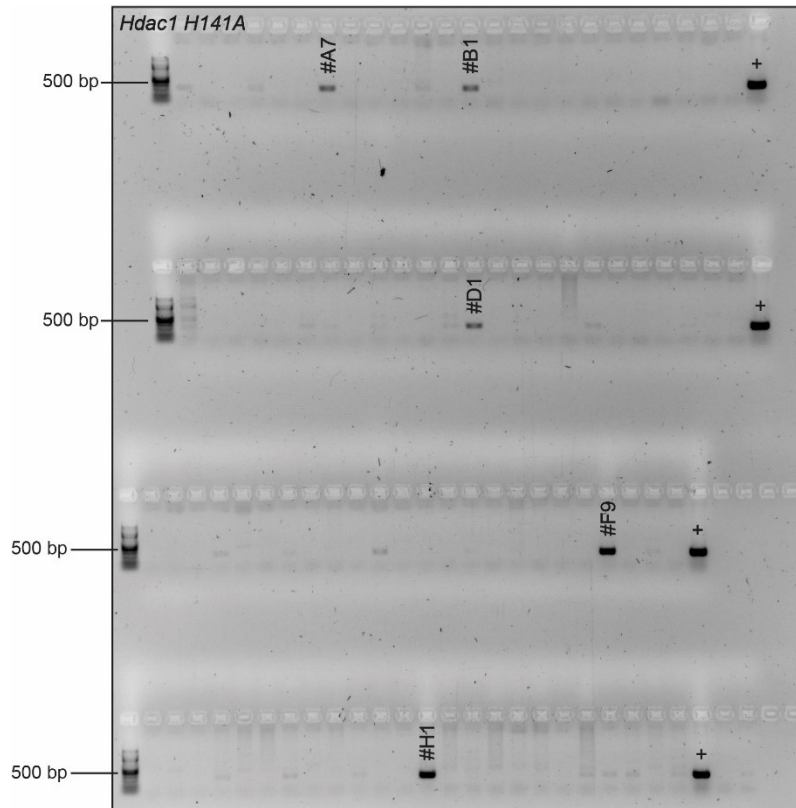


Figure 44: Screening PCR of single cell clones for carrying the HDAC1 H141A transgene. The primer pair used, bind to the HDAC1 transgene and the FLAG-tag region, respectively. The expected length of the PCR product was 304 bp.

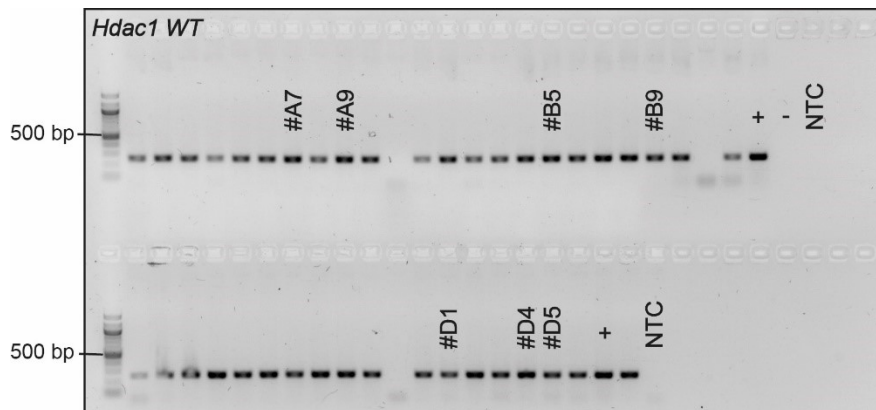


Figure 45: QC PCR of clones tested for HDAC1 WT transgene. The primer pair used for this PCR binds to the p21 gene. The expected length of the PCR product was 244 bp.

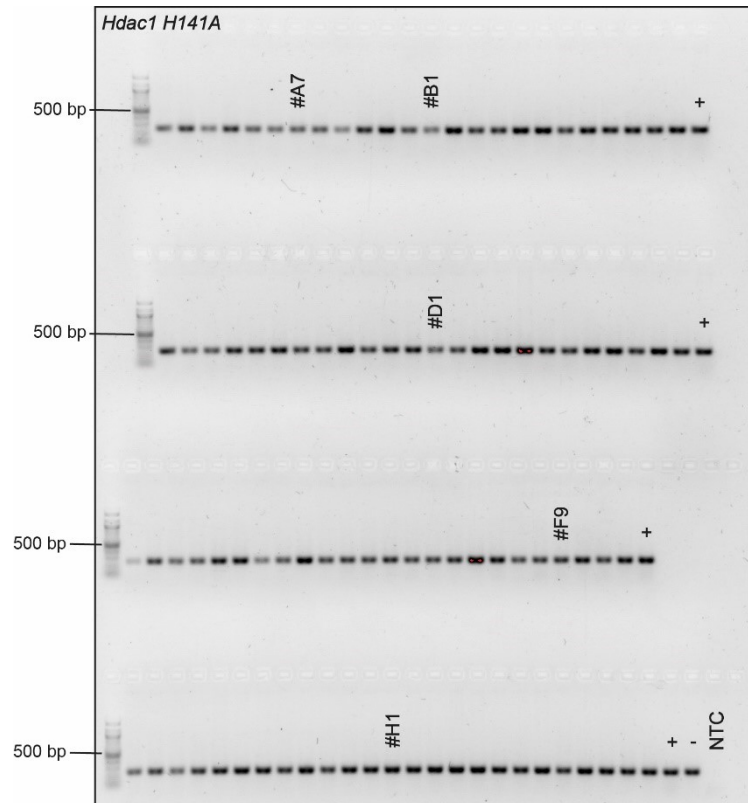


Figure 46: QC PCR of clones tested for HDAC1 H141A transgene. The primer pair used for this PCR binds to the *p21* gene. The expected length of the PCR product was 244 bp.

Finally, 9 *Hdac1* WT clones and 7 *Hdac1* H141A were positive for the respective transgene. To confirm the screening results for the seemingly positive clones, some of these clones were chosen for another round of screening PCR with different primer pair binding within the LHA and RHA of the AAVS locus.

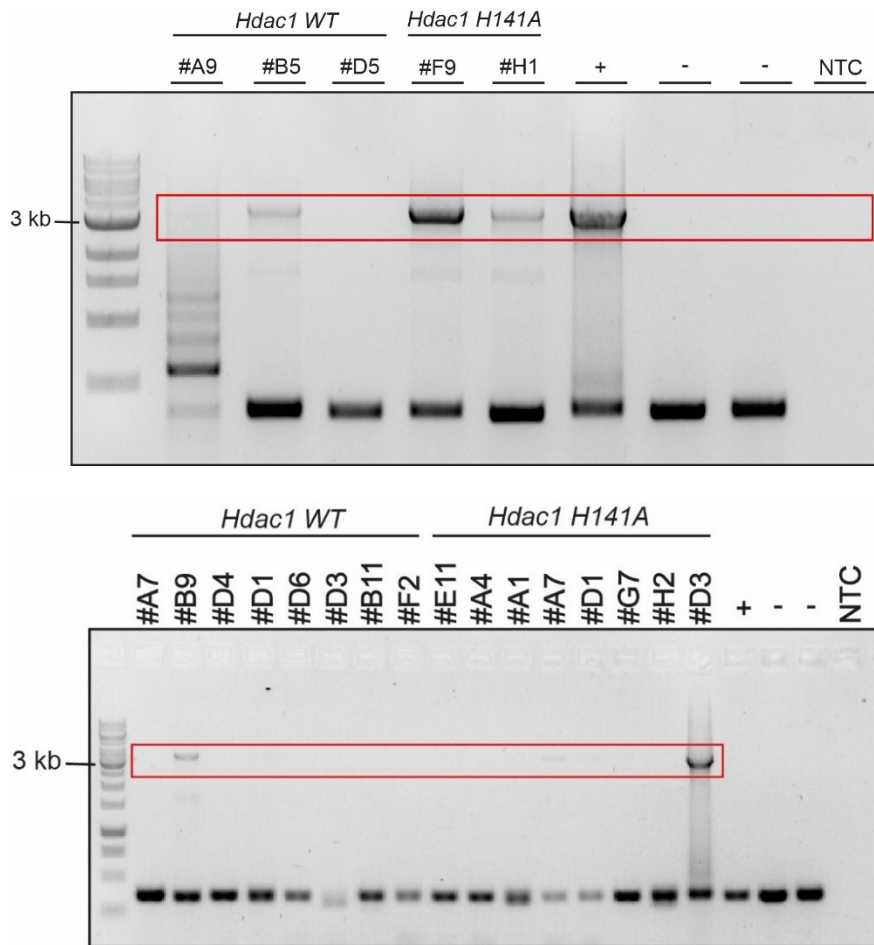


Figure 47: Additional screening of seemingly positive clones with direct PCR method (described in chapter 2.3.2.). The primers bind to the LHA and RHA of the AAVS locus. If the transgene integrated into the locus, the PCR product had a length of 3530 bp (red rectangle).

Because also the direct PCR did not give a reliable proof for successful transgene insertion, the decision was made to pick some clones which were positive both in screening and direct PCR to detect the FLAG tag of the transgene by Western blot analysis. In this way, we could detect the FLAG-tagged HDAC1 protein in clones #A7, #B5, and #H1.

The immunodetection of the transgene's FLAG tag revealed that two clones (#A9, #B5) expressed HDAC1 WT and that only a single clone (#H1) expressed HDAC1 H141A (Fig. 48). In addition, when the blot was re-probed with an antiserum against HDAC1, the presence of transgenic HDAC1 variants in the same cell lines was detected. The expression levels of the transgenic HDAC1 was slightly higher than the expression of the endogenous HDAC1 protein in the non-targeted cell lines.

To support the Western blot results and to test for the purity of the positive clones the immunofluorescence analysis was used by applying the anti-FLAG antibody.

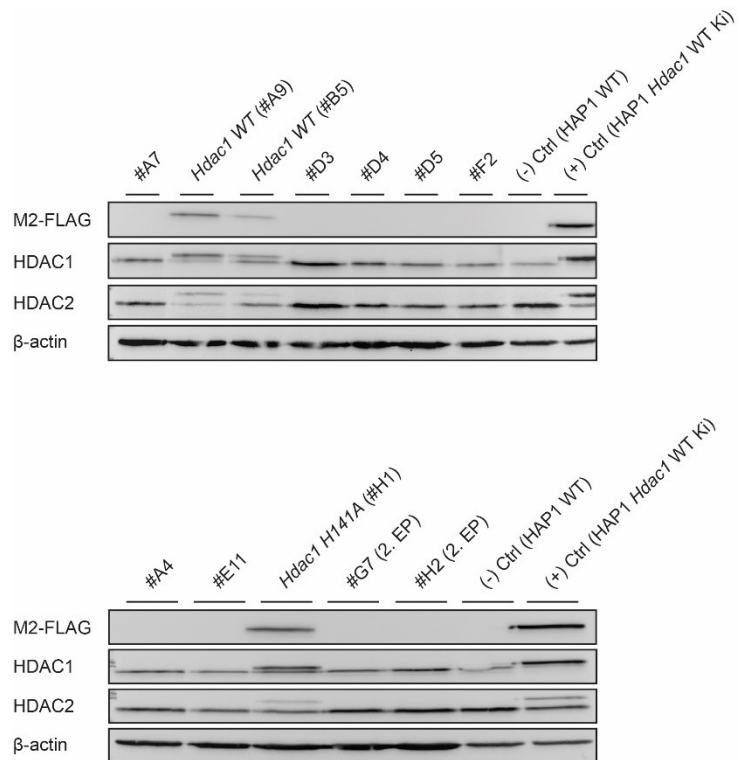


Figure 48: Immunoblot analysis of seemingly positive clones. The clones positive in screening and direct PCR were tested for their FLAG-tag, HDAC1, and HDAC2 protein expression. From all the tested clones three clones expressed the transgene; from them, two clones expressed HDAC1 WT and one HDAC1 H141A. Endogenous HDAC1 expression changed due to the overexpression of the transgene, as well as the expression of HDAC2. - actin was used as a loading control.

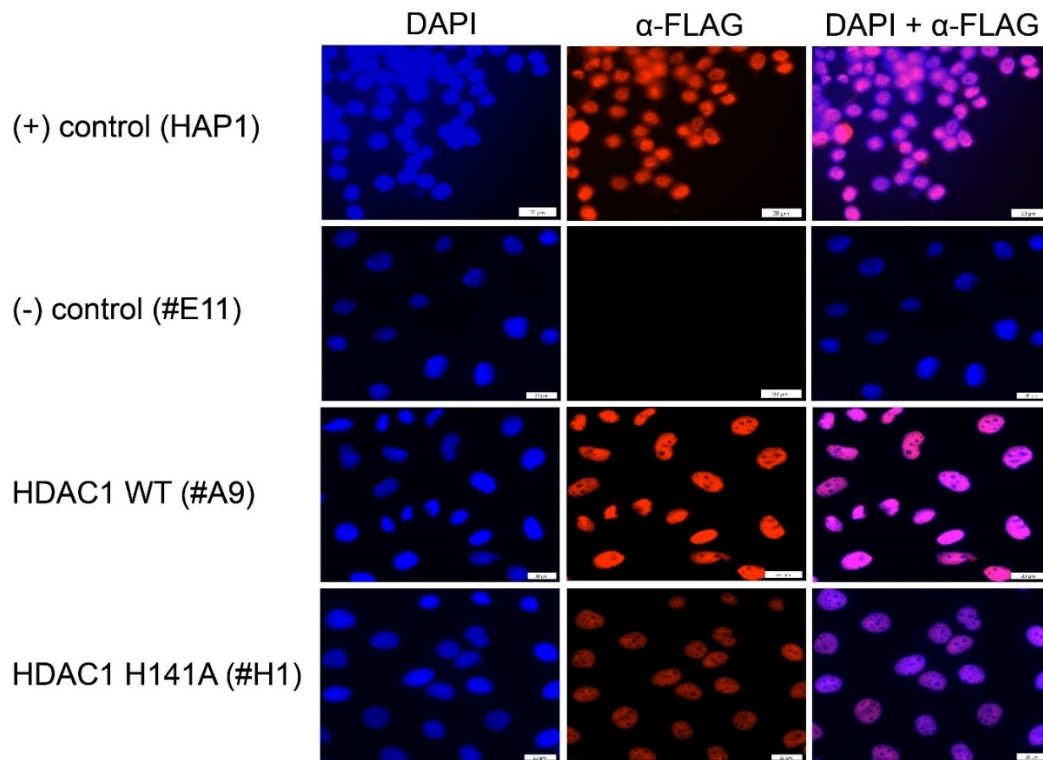


Figure 49: Immunofluorescence detection of FLAG-tagged HDAC1 WT and HDAC1 H141A. The first column shows colored nuclei of keratinocytes with DAPI staining. The second column shows FLAG-HDAC1 expressing nuclei, and the third column displays the merge of DAPI and anti-FLAG pictures. Based on this staining it can be concluded that clones #A9 and #H1 indeed express the transgene in all cells. Magnification: 40x.

As shown in Fig. 49, all cells that displayed a DAPI positive (blue) nuclear signal were also found to exhibit a positive nuclear fluorescence (red), conferring 100 % purity of the cell lines. The control cell line, #E11, without integrated transgene, showed no red fluorescence signal. The above presented immunofluorescent FLAG-positive clones were grown on the coverslip. The FLAG-tag positive clone #B5 did not grow on the coverslip, therefore we grew it in 3.5 cm dishes, and performed the staining in the dish.

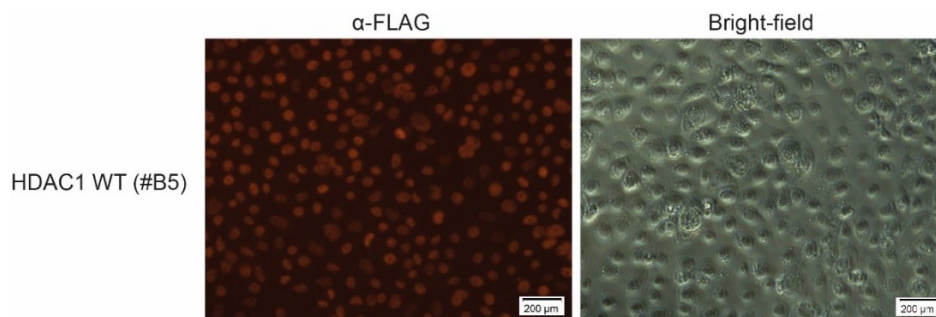


Figure 50: Immunofluorescence detection of the FLAG-tagged HDAC1 WT protein. The #B5 cells did not grow on the coverslip, therefore, they were grown and stained with anti-FLAG antibody in the 3.5 cm dish. Magnification: 10x.

The FLAG-tag immunofluorescence staining also visually affirmed the presence of the respective HDAC1 transgene in these clones. Moreover, the nuclear signal confirmed the correct intracellular localization.

3.4.5. Impact of overexpression of HDAC variants on the expression of endogenous HDAC1 and HDAC2

As previously seen from the immunoblots, the expression of endogenous HDAC1 and HDAC2 was slightly reduced upon the overexpression of the respective transgene (HDAC1 WT or HDAC1 H141A). The qPCR data showed significantly elevated mRNA levels of HDAC1 in all knock-in clones. Interestingly, upon the HDAC1 overexpression, the clones #B5 (HDAC1 WT) and #H1 (HDAC1 H141A) demonstrated increased HDAC2 expression. These observations are reciprocal with immunoblots (Fig. 48), and with a compensatory mechanism known for HDAC1 and HDAC2. The knock-in also affected HDAC8, resulting in induced RNA expression.

Detection of HDAC1 by an antibody, recognizing the N-terminus of HDAC1, unveiled the

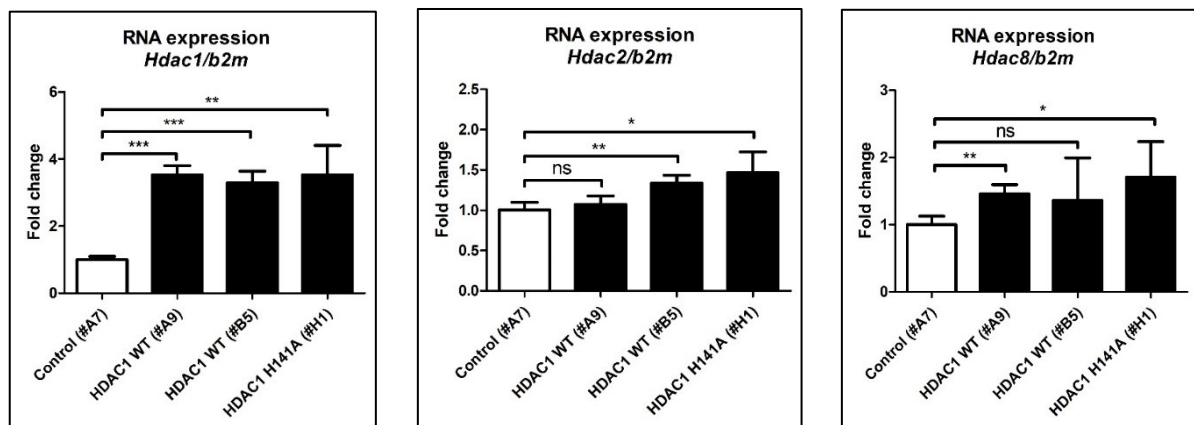


Figure 51: Relative mRNA expression levels of HDAC1, HDAC2, and HDAC8 in cell clones containing the respective transgene (either HDAC1 WT or HDAC1 H141A). b2m was used as a reference gene. n = 3. P < 0.5.

relationship between reduced expression of the endogenous HDAC1 in response to overexpression of the HDAC1 transgene (either HDAC1 WT or HDAC1 H141A). As discerned from the immunoblots the expression of the transgene was higher than from endogenous HDAC1. A cross-talk between HDAC1 and HDAC2 was previously reported (Winter et al. 2013). If HDAC1 is ablated, HDAC2 is upregulated to compensate for the loss of HDAC1. Likewise, to previous findings, HDAC2 expression is decreased in all three knocked-in cell clones, and especially in clone #A9.

The CDK inhibitor p21 is known as the major cell cycle regulator and its expression has been shown to be induced in the absence of HDAC1 (Zupkovitz et al., 2010). qRT-PCR revealed, that p21 mRNA is expressed at significantly decreased levels in clones overexpressing HDAC1

WT (#A9 and #B5, Fig. 52). However, no significant reduction of the p21 transcript was found in keratinocytes overexpressing catalytic inactive HDAC1 (#H1).

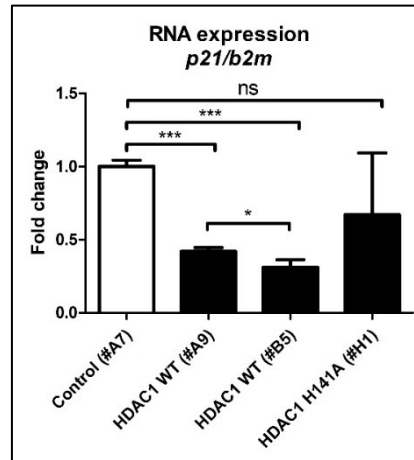


Figure 52: Relative mRNA expression levels of p21 in cell clones containing the respective transgene (either HDAC1 WT or HDAC1 H141A). b2m was used as a reference gene. n = 3. P = < 0.5.

In the next step, the expression of HDAC1, HDAC2 and p21 was compared between pre-confluent and post-confluent knock-in cell clones. The FLAG expression of pre-confluent knock-in cell clones showed decreased transgene expression in #B5 clone in comparison to #A9. This minor difference also could be observed at HDAC1 expression between #A9, #H1 and #B5. All three knock-in clones displayed notably reduced HDAC2 expression levels. The p21 protein expression was surprisingly increased only in the HDAC1 WT clone #A9 that contradicts the observations made by analyzing the qPCR data.

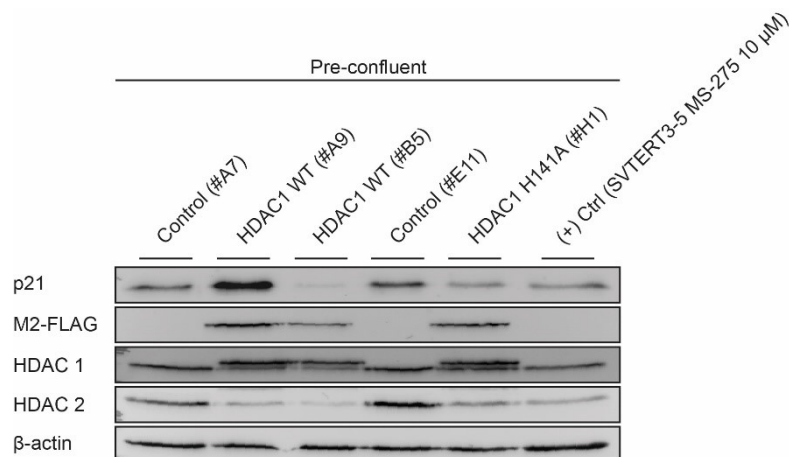


Figure 53: Immunoblot analysis of FLAG-tag positive clones (#A9, #B5, and #H1) and their controls (#A7, #E11). As previously seen in Figure 48, the FLAG-tag expression of the clone #B5 was slightly decreased compared to the other two FLAG-tag positive clones (#A9, #H1). HDAC1 overexpression resulted in a reduction of HDAC2 expression in all three FLAG-positive clones. Interestingly the p21 expression was increased in HDAC1 WT overexpression clone #A9, although HDAC1 normally represses its expression. -actin was used as a loading control.

The post-confluent cells with the respective transgene showed considerable overexpression of the transgene over the expression of the endogenous HDAC1 (see HDAC1 panel, Fig. 53) and diminished protein expression levels of HDAC2. This is most probably due to the fact that the endogenous Hdac1 promoter is responsive to differentiation signals whereas the EF1a promoter driving the transgenes is constitutively active. The post-confluency of these cells was confirmed with the expression of the late differentiation marker DNase1L2 that was expressed in all cell clones but at lower levels in keratinocytes overexpressing catalytic inactive HDAC1 (#H1). With the differentiation of the cells, the p21 expression levels for both HDAC1 WT clones (#A9 and #B5) stayed increased.

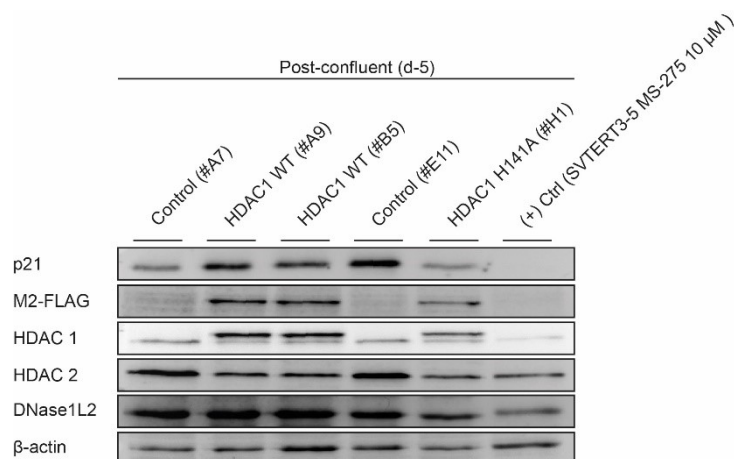


Figure 54: Immunoblot analysis of post-confluent keratinocytes expressing the respective transgene. The FLAG-tag detection confirmed the successful transgene insertion. The overexpression of the transgene upon the endogenous HDAC1 was determined with anti-HDAC1 antibodies. The upper band in HDAC1 panel represents the transgene and the lower the endogenous HDAC1. The cross-talk between HDAC1 and HDAC2 led to reduced HDAC2 protein expression levels in HDAC1 overexpressing cells. DNase1L2 served as a differentiation marker for used cells. -actin was used as a control.

These immunoblots gave us an insight of HDACs protein expression in growing and differentiated cells with knock-in. The expression patterns of all tested proteins were comparable among pre-confluent and post-confluent cells.

3.4.6. Impact of overexpression of HDAC1 H141A and HDAC1 WT on total cellular deacetylase activity and histone acetylation

The overexpression of either HDAC1 WT or HDAC1 H141A in positive cell clones could influence cellular HDAC activity. Therefore, the total HDAC activity in transgenic keratinocyte clones was measured with a radioactive HDAC activity assay. The results showed slightly increased deacetylase activity in the #A9 clone expressing HDAC1 WT compared to control clone #A7, and significantly lower total HDAC activity in HDAC1 H141A expressing clone #H1

(Fig. 55). The expression of catalytically inactive HDAC1 effectively decreased the total HDAC activity.

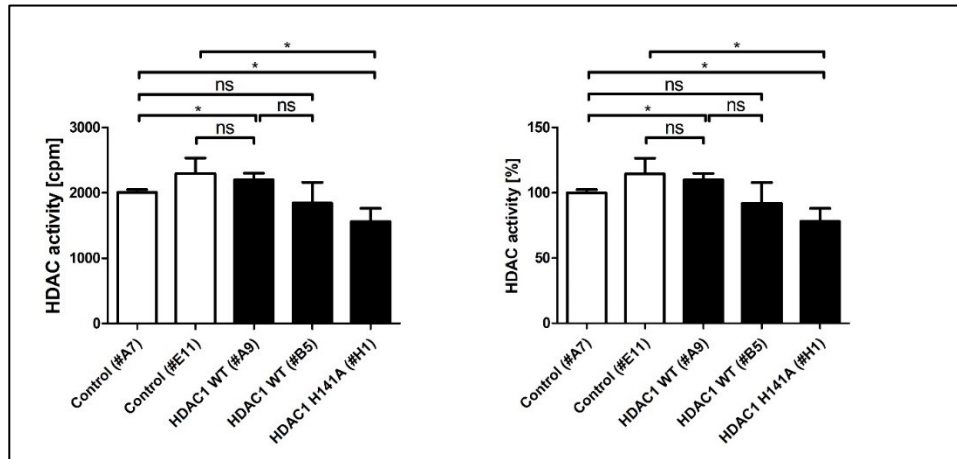


Figure 55: Total HDAC activity of clones expressing HDAC1 transgenes. HDAC1 WT-expressing clone #A7 showed insignificantly elevated HDAC activity, whereas the only clone expressing the catalytically inactive version of HDAC1 (#H1) displayed for 30 % reduced activity compared to control. cpm = counts per minute. $n = 3$.

To examine, whether various HDAC activities have an influence also on histone acetylation the Western blot analysis was conducted. Therefore, proliferating cell lines were harvested, and histones were purified using an acid extraction method as described in section 2.4.3. Histone acid extraction. Western blot analysis using H3K56ac and H4K8ac antibodies showed increased signals of these histone marks in the clone #H1, overexpressing the catalytically inactive HDAC1. Elevated acetylation levels were also seen in HDAC1 WT overexpressing #B5 clone. However, the loading control had not been loaded equally, hence the interpretation of the immunoblot (Fig. 56) is compounded.

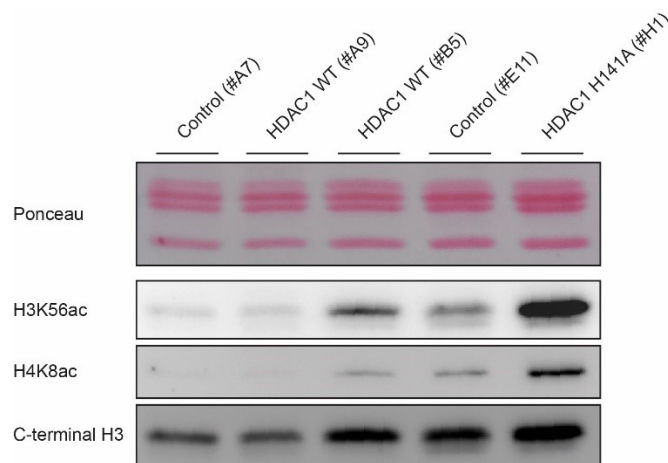


Figure 56: Immunoblot analysis of histone acetylation from transgene-containing cell clones. Increased acetylation is caused by an imbalance between HATs and HDACs or if the HDACs are hampered and cannot fulfil their function. The expression of the catalytically inactive HDAC1 version in clone #H1 showed increased acetylation

of histones H3 and H4. It seems that overexpression of the HDAC1 WT also poisons the HDAC deacetylation function (at least in #B5 clone), and results in higher acetylation levels. H3 c-terminal was used as a loading control.

3.4.7. Knockdown of HDAC1 in keratinocytes

To analyze the impact of reducing the level of endogenous HDAC1 in keratinocytes, and to compare it with the effects of overexpressing catalytic inactive HDAC1 H141A, an shRNA knockdown approach was conducted. Three different shRNA sequences specific for human HDAC1, and two unrelated control sequences were cloned into the pLKO-Tet-On vector that contains also a puromycin resistance sequence (knockdown performed by Oliver Pusch, CACB). After approval of the correct shRNA sequences by sequencing the plasmids, the constructs were transfected into 293T cells together with lentiviral packaging plasmids. Supernatants containing the lentiviruses were then used to transduce NHEK/SVTERT3-5 keratinocytes. Non-transduced cells were eliminated by puromycin selection. Cell lines were further propagated, and the knockdown of endogenous HDAC1 was validated.

The immunoblot analysis showed successful knockdown of HDAC1 in NHEK/SVTERT3-5 keratinocyte cell line (Fig. 57, red rectangle) since the HDAC1 band was strongly reduced. These cells do not contain the transgene; therefore, no FLAG tag bands were expected.

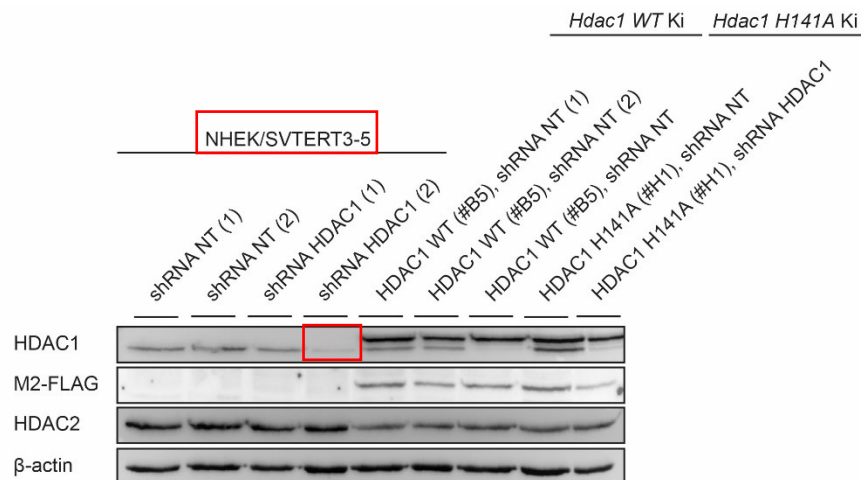


Figure 57: The successful knock-down of the endogenous HDAC1 in NHEK/SVTERT3-5 keratinocytes and in newly generated knock-in cell lines overexpressing either HDAC1 WT or catalytically inactive HDAC1 H141A. HDAC1 panel: the upper band represents the overexpressed transgene and the lower band the endogenous HDAC1. -actin was used as a loading control.

The effectiveness of the shRNA knock-down was also examined by measuring the total HDAC activity. The activity assay showed a significantly reduced total HDAC activity in NHEK knock-down cells compared to control.

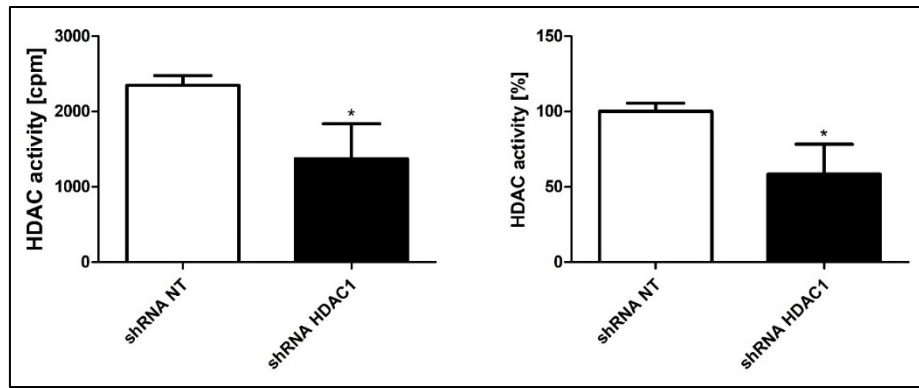


Figure 58: Total HDAC activity of NHEK/SV Tert3-5 keratinocytes. The NHEK/SV Tert3-5 knockdown cells exhibited 50 % reduced total HDAC activity compared to control. $n = 3$. $p = 0.0252$.

The analyzed qPCR data showed decreased HDAC1 mRNA expression and marginally affected mRNA expression of other tested genes.

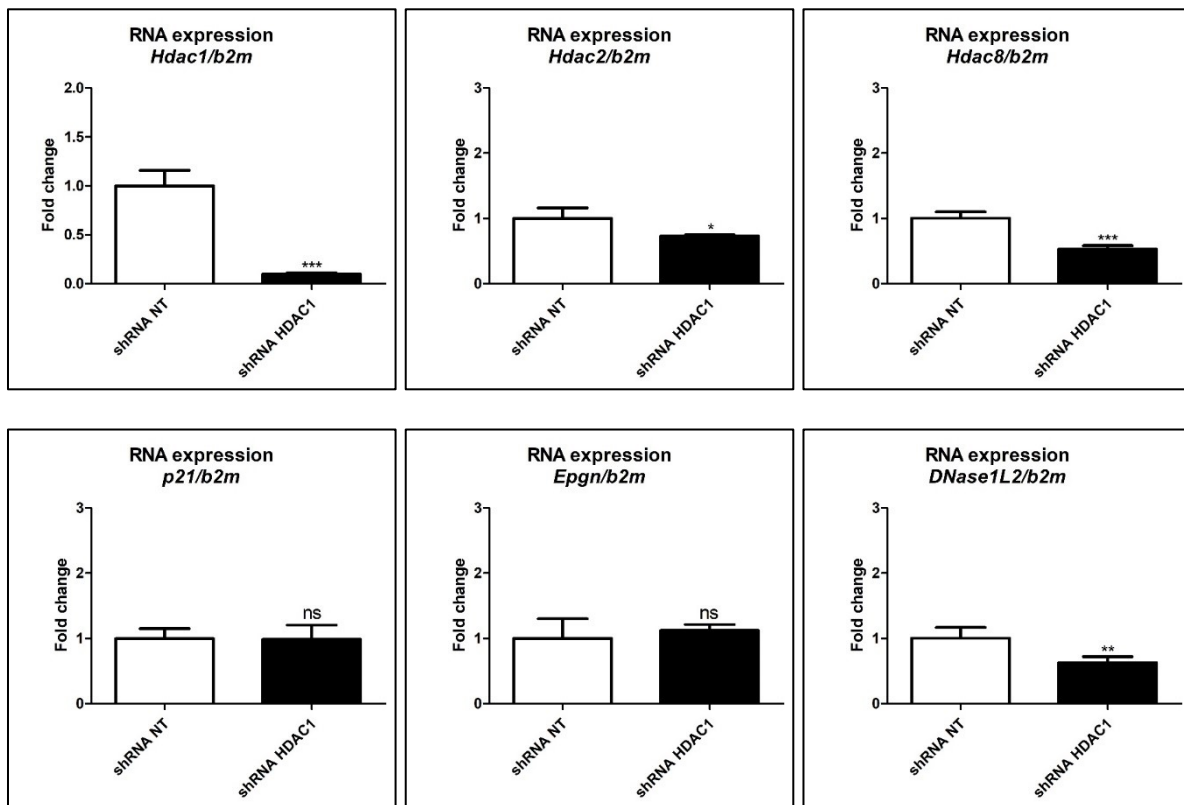


Figure 59: Relative mRNA expression levels of class I HDACs (except HDAC3), p21, EPGN and DNase1/L2 in NHEK/SV Tert3-5 cell line after knockdown of endogenous (human) HDAC1. The shRNA knockdown dramatically diminished the amount of HDAC1 mRNA. Furthermore, also the mRNA expression of HDAC2 and HDAC8 was decreased. In contrast, the knockdown did not affect the mRNA levels of p21 and EPGN. Unpaired *t*-test, two-tailed. $n = 4$. Error bars indicate SD. Housekeeping gene b2m (β -microglobulin) was used as a reference gene in comparative gene expression analysis. The data was copied from

3.4.7. Knockdown of HDAC1 in keratinocyte cell lines overexpressing HDAC1 wildtype and HDAC1 H141A

Additionally, we performed the *HDAC1* knockdown also in newly generated cell lines overexpressing either *HDAC1* WT or catalytically inactive *HDAC1* H141A. The shRNA for HDAC1 was designed in a way that it exclusively targets endogenous human *HDAC1* mRNA in NHEK/SVTERT3-5 cells. Indeed, no HDAC1 protein was detected by Western blot analysis (Fig. 60, green rectangle). In contrast, the used shRNA did not bind the murine *Hdac1* transgene mRNA. Accordingly, Western blot analysis showed that FLAG-tagged HDAC1 (either HDAC1 WT or HDAC1 H141A) proteins were not affected by the knockdown. The HDAC2 protein expression remained unchanged (Fig. 60) or slightly decreased (Fig. 57). The protein expression of the p21 and p53 did not change upon the HDAC1 knockdown.

In the case of the #H1 cell line, the expression of catalytically inactive HDAC1 instead of the endogenous wild-type protein, the knockdown of endogenous HDAC1 mimics the inhibition of HDAC1 inhibition by an isoform-specific HDAC inhibitor.

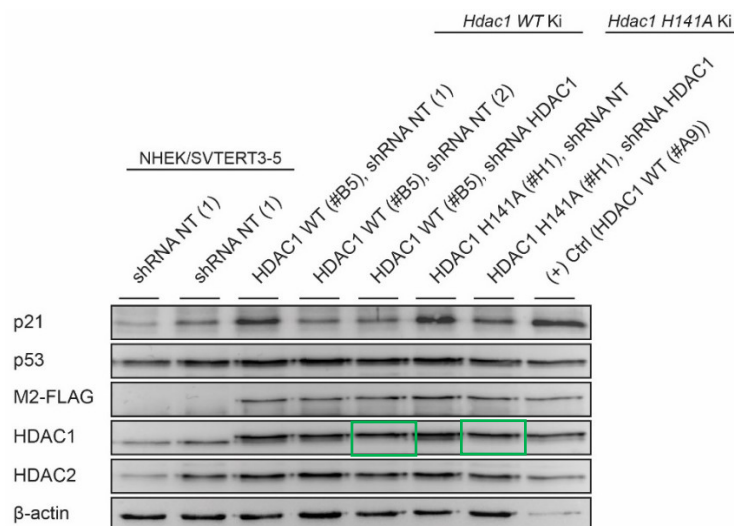


Figure 60: The successful knock-down of the endogenous *HDAC1* in newly generated knock-in cell lines overexpressing either *HDAC1* WT or catalytically inactive *HDAC1* H141A. *HDAC1* panel: the upper band represents the overexpressed transgene and the lower band the endogenous *HDAC1*. β -actin was used as a loading control.

3.4.8. Characterization of knock-in clones after shRNA knock-down

The impact of *Hdac1* knock-down on total HDAC activity was also measured in cell lines overexpressing HDAC1 WT and HDAC1 H141A. The HDAC activity stayed unchanged in cell line overexpressing the HDAC1 WT. Surprisingly, the HDAC activity of the cell line overexpressing catalytically inactive HDAC1 H141A was slightly but significantly increased.

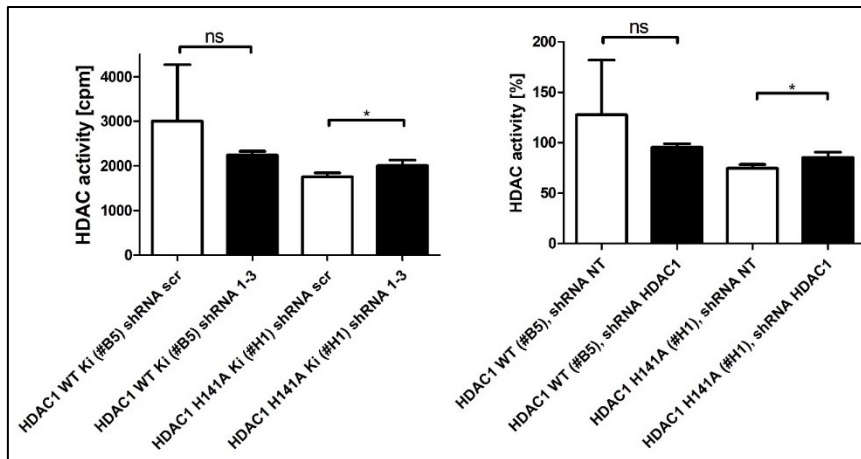
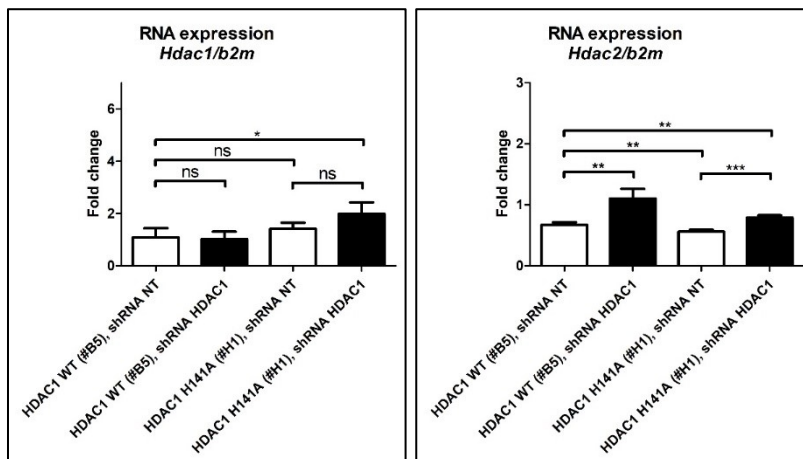


Figure 61: Total HDAC activity after knock-down of endogenous HDAC1 in cell lines overexpressing HDAC1 WT (#B5) or HDAC H141A (#H1). The knockdown experiment did not affect the HDAC activity in the cell line overexpressing HDAC1 WT, however, it increased the activity of HDAC1 H141A overexpressing cell line. $n = 3$, $p = 0.3584, 0.0464$.

The clones were also characterized by measuring mRNA expression of class I HDACs (except HDAC3), *p21*, *EPGN*, and differentiation marker *DNase1L2*. By qRT-PCR, no changes have been measured in *HDAC1*, *p21*, and *DNase1L2* RNA expression in cell lines overexpressing HDAC1 WT or HDAC1 H141A compared to their controls. The primer pair used could only bind to human (endogenous) *HDAC1* sequence, and not to murine overexpressed *Hdac1* variant. However, HDAC2, as well as HDAC8 and *EPGN* expression, was significantly upregulated.



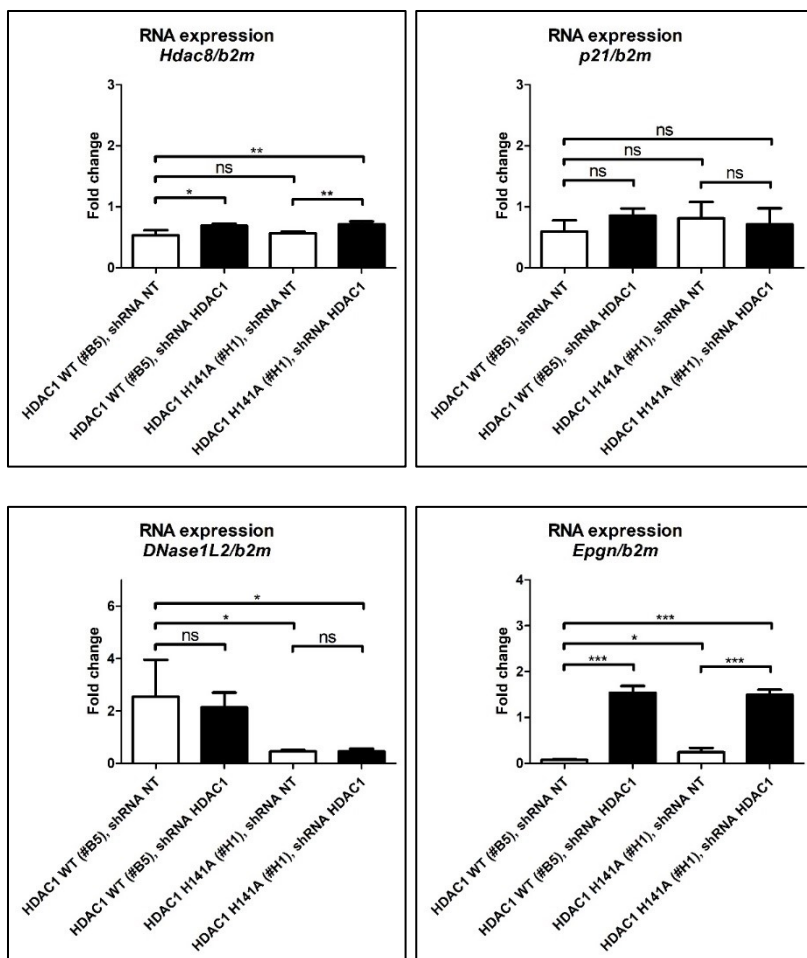


Figure 62: Relative mRNA expression levels of class I HDACs (except HDAC3), p21, Epgn and DNase1/L2 in HDAC1 WT (#B5) and HDAC1 H141A (#H1) overexpressing cell lines. Unpaired t-test, two-tailed. n = 4. Error bars indicate SD. Housekeeping gene b2m (β -microglobulin) was used as a reference gene in comparative gene

4. Discussion and Outlook

4.1. NHEK/SVTERT3-5 cell line can differentiate in 2D cell culture

The NHEK/SVTERT3-5 cell line used in our experiments had been previously used in 3D skin models, where it was shown that exhibits high similarity in differentiation pattern to primary keratinocytes (Weinmuellner et al., 2018). In our experiments with the NHEK/SVTERT3-5 cell line, we demonstrated the ability of these cells to differentiate in 2D cell culture upon increased Ca^{2+} concentration in the medium. The differentiated cells distinguished themselves visually from proliferating (pre-confluent) ones in their morphology and capability to form multilayering colonies. On the molecular level, mRNA and protein expression of differentiation markers, like KRT1 and DNase1L2, were assessed. The post-confluent d-5 and d-9 keratinocytes displayed significantly elevated mRNA and protein levels of these two differentiation markers. In summary, we could confirm that the NHEK/SVTERT3-5 cell line can also differentiate in the 2D cell culture.

4.1.2. Upregulation of the CDK inhibitor p21 correlated with the differentiation of NHEK/SVTERT3-5 cells

Additionally, we investigated the essential cell cycle regulator p21 and a proliferation marker KRT5. The cyclin-dependent kinase inhibitor p21 promotes G1 cell cycle arrest and DNA repair. In addition, the G1 arrest also enables cell differentiation. Steinman et al. described p21 upregulation during differentiation of hepatoma and hematopoietic cells. The post-confluent NHEK/SVTERT3-5 cells showed significantly increased *p21* mRNA levels which suggest that the induction of keratinocyte differentiation (genes) is also coupled to the regulation of the cell cycle. KRT14 the KRT5 proteins are abundantly expressed in mitotically active, proliferating, basal cells, though their expression is gradually decreased, and finally terminated as the cells differentiate (Alam et al., 2011). Our qPCR data, however, showed continued expression of KRT5 in post-confluent cells. These results could point to a potential regulation on the protein level, and to the fact that not all post-confluent cells are terminally differentiated.

4.1.3. Terminal differentiation of NHEK/SVTERT3-5 cells resulted in changed acetylation of H3K56 and H4K8 histone marks

Increased histone acetylation during cell differentiation is related to decreased levels of HDAC expression during transition from proliferation to differentiation, caused by induced expression of cell cycle inhibitor(s), like p21 and p27, that promote cell cycle arrest and differentiation (Coqueret, 2003). On the other hand, acetylation of *de novo* synthesized histones at H3K5, H4K8, H4K12 and H3K9 and H4K14 is linked to replication and is important for proper histone deposition (Benson et al). In accordance with these observations, H4K8 acetylation was

decreased in terminally differentiated NHEK/SVTERT3-5 keratinocytes which have exited the cell cycle. Acetylation of H3K56 is associated with DNA damage response in cells. Moreover, H3K56ac is abundantly expressed in human cells at all cell cycle stages (Das, Lucia, Hansen, & Tyler, 2009), and is a relevant target for HDAC1 and HDAC2 (Winter et al., 2013). This feature makes the H3K56ac convenient marker of HDAC1/HDAC2-regulated histone acetylation. Cell proliferation in pre-confluent cells is related to the higher expression of HDAC1 and HDAC2. The increased acetylation of H3K56 (Fig. 16) correlated well with down-regulation of HDAC1 and HDAC2 expression in post-confluent, differentiating (d-5, d-9) keratinocytes (Brunmeir et al., 2009; Tou et al., 2004).

Our data display increased acetylation of H3K56 and decreased acetylation of H4K8 during differentiation of NHEK/SVTERT3-5 keratinocytes.

4.1.4. HDAC8 expression is upregulated in post-confluent NHEK/SVTERT3-5 cells

HDAC1 is a crucial regulator of cellular proliferation (especially during development) that targets the cell cycle regulator p21. Zupkovitz et al. showed that HDAC1 down-regulates the p21 expression and furthermore, the p21 repression can be reversed using the HDACis (Gui, Ngo, Xu, Richon, & Marks, 2004). The protein expression of class I HDACs, apart from HDAC8 was slightly reduced upon the terminal differentiation of cells. However, these observations contrast with RNA expression levels, which indicates, that HDAC1 and 2 are downregulated at the posttranscriptional level. In contrast, the HDAC8 expression was significantly increased both on protein and mRNA level in post-confluent cells. The reason for this occurrence is still unknown but has also been described for human primary keratinocytes (Sanford et al., 2016). In this study the authors could show that depletion of HDAC8 increases TLR-mediated induction of inflammatory cytokine and chemokine expression, indicating an important role in repressing inflammatory gene expression.

4.1.5. H4K8 histone crotonylation is down-regulated during terminal differentiation of NHEK/SVTERT3-5 keratinocytes

HATs such as p300 have been identified as crotonylating enzymes (Sabari et al., 2015), whereas besides sirtuins class I HDACs have been shown to act as decrotonylases (Wei et al., 2017; Zhao, Zhang, & Li, 2018). Our results showed a decrease in histone crotonylation during ongoing terminal differentiation of keratinocytes. Lower levels of histone crotonylation (and acetylation), especially at the H4K8, indicate decreased activity of HATs as crotonylating enzymes or increasing activity of decrotonylases during keratinocyte differentiation. Further studies of this interesting finding are necessary to determine the identity of the responsible enzymes, and the biological relevance of the phenomenon. Cell growth and proliferation in pre-confluent cells relate to the higher expression of HDAC1 and HDAC2.

4.2. Treatment of NHEK/SVTERT3-5 keratinocytes with HDACi MS-275 differed

The experiments with the HDACi MS-275 on pre-confluent and post-confluent keratinocytes revealed distinct effects on proliferating and differentiated cells. Pre-confluent keratinocytes were, in general, less sensitive to changes in respect of morphology and showed a concentration-dependent increase in histone acetylation, and induced crotonylation of histones H3 and H4 in response to MS-275. Pre-confluent cells reacted upon the HDACi treatment with increased mRNA expression of *HDAC1* and *p21*. The mRNA levels of proliferation marker *EPGN* and early differentiation marker *KRT1* were significantly diminished upon MS-275 treatment. Post-confluent keratinocytes were more sensitive to MS-275 treatment. Keratinocytes from day 9 (d-9) reacted already to the lowest MS-275 concentration (0.5 μ M) with the creation of many apoptotic vacuoles inside the cytoplasm (Fig. 26). The analyzed q-RT-PCR data has shown a significant reduction in expression of HDAC class I genes (except *HDAC3*, not tested), *p21*, *EPGN* and terminal differentiation marker genes in both d-5 and d-9 keratinocytes.

4.2.1. Class I HDAC inhibition caused accumulation of histone acetylation and H4K8 crotonylation in NHEK/SVTERT3-5 cells

The accumulation of acetylated histones H3 and H4 upon MS-275 treatment has been described in several cell types such as human breast cancer cells and various colon cancer cell lines (Abu, Muhamad, Hassan, Zakaria, & Ali, 2016; B. I. Lee et al., 2001). In accordance with the keratinocytes of different differentiation stages, the MS-275 treatment showed a strong increase in acetylation of histone marks H3K56 and H4K8, that confirmed the efficient inhibition of HDACs by MS-275. Interestingly, the effect of MS-275 treatment was stronger for H4K8 than for H3K56, especially when differentiated keratinocytes were analyzed. This could be explained by the observation, that keratinocyte differentiation by itself results in an increase of the H3K56 acetylation, and thereby any further HDAC inactivation will cause only modest effect. By contrast, as keratinocyte differentiation by itself reduces H4K8 acetylation, the effect of HDAC inhibition may result in a relatively larger increase compared to H3K56 acetylation. Although acetylation and crotonylation share the same writers, the acetylation is 1000-times more abundant than crotonylation (Sabari et al., 2015). The crotonylation in keratinocytes appeared to be unregulated upon MS-275 treatment in pre-confluent cells. In the post-confluent cells, the crotonylation was merely observed on H4K8 histone mark. Taken together, MS-275 treatment of NHEK/SVTERT3-5 cells increased acetylation of histone 3 and 4 at lysines 56 and 8, whereas changes in crotonylation upon HDACi treatment could be notably observed only in d-5 post-confluent cells at H4K8.

4.2.2. Effects of class I HDAC inhibition on proliferating keratinocytes

The pre-confluent and post-confluent (d-5, d-9) cells were treated with rising MS-275 concentrations. The concentration range was chosen empirically, based on previous studies like Rosato, Almenara, & Grant, 2003. Proliferating, pre-confluent keratinocytes did not show any morphological changes due to the treatment at any MS-275 concentration. On the metabolically level, assessed by the MTS assay, only the highest MS-275 concentration (10 μ M) significantly impaired cell proliferation. MS-275 did not affect the mRNA levels of HDAC2, HDAC8, proliferation marker *KRT5*, and late differentiation marker *DNase1L2*. However, significant upregulation of HDAC1, p21 and *KRT1* on mRNA level was detected, whereas the proliferation-promoting gene *EPGN* remained down-regulated. These findings support the results from B. I. Lee et al., 2001 and Rosato et al., 2003, where MS-275 treatment induced transcription of *p21* and differentiation genes at already low inhibitor concentration (1.0 μ M). Only the highest (10 μ M) MS-275 concentration resulted in a two-fold increase of HDAC1 mRNA expression. Interestingly, on the protein level, no regulation of the HDAC1 or HDAC2 could be observed, however p21 expression was increased

4.2.3. Differentiated post-confluent cells reacted to MS-275 with increased sensitivity

The post-confluent cells grow differently than pre-confluent ones. The post-confluent cells built centrically multilayered colonies. This natural behavior of primary keratinocytes during the terminal differentiation can also be observed *in vitro*. Cell treatment with the highest MS-275 concentration (10 μ M) always resulted in cell death. It seemed that with progressing terminal differentiation, the sensitivity of the cells to the MS-275 increased. The d-9 cells reacted even to the lowest MS-275 concentration (0.5 μ M) with the creation of apoptotic vacuoles. The qPCR data analysis for post-confluent (d-5 and d-9) cells showed downregulation of *HDAC1*, *HDAC2*, *HDAC8*, proliferation (*KRT5*, *EPGN*) and differentiation markers (*KRT*, *DNase1L2*), and even of the differentiation-promoting gene *p21*. These observations signified the distinct behavior of post-confluent cells to MS-275, compared to the proliferating, pre-confluent cells. Differentiation-promoting HDACi MS-275 could not induce further differentiation of already differentiated cells, however, the increased sensitivity of the cells resulted in cell death at very low concentrations. MS-275 inhibited mRNA expression of HDAC1, HDAC2, and HDAC8 two- to three-fold.

4.3. Generation of transgenic keratinocyte-derived cell lines

With the attempt to generate cell clones expressing either HDAC1 WT or catalytically inactive variant, HDAC1 H141A, from the safe harbor locus AAVS, the NHEK/SVTER3-5 cells were transfected with several transfection agents. Out of several tested transfection reagents,

FuGENE® was found to be adequate to transfect the cells with sufficient efficiency (about 30%), and low cell toxicity (previous experiments).

To screen the single cell clones for the presence of the transgene, the transfected cells needed to get seeded in microtiter plates. In our first trial, the diluted cells were seeded into 384-well plates. Since the keratinocyte medium did not contain FBS or FCS which neutralize trypsin, required to detach the cells, small amounts of trypsin remained in the medium and caused cell death. This issue was solved by using the trypsin inhibitor, however, the keratinocytes in 384-well plate did not detach from the plate, and therefore the expansion of cell clones was virtually impossible. Accordingly, in the next transfection trial, we seeded the transfected cells into 96-well plates. These plates were better suited for visual screening, and the keratinocytes could be easier detached, and as a result, more transferred cells survived. In summary, the integration of the HDAC1 coding sequence into AAVS locus worked (positive nested PCR), and we subsequently identified approximately 44 single cell colonies. Some of them were seemingly transgene positive by PCR, however, none of them stably expressed transgenic HDAC1 protein. The reason for this low yield could have been the low transfection efficiency of human keratinocytes.

Since we could not obtain any positive clones containing the transgene of interest employing the chemical transfection method, we decided to use electroporation to transfect the keratinocytes.

As expected, many cells died after electroporation, and the surviving ones were used for clonal expansion in 96-well plates. The electroporation was performed once with Cas9 plasmid and once with Cas9 protein. The advantage of the Cas9 protein electroporation should be higher efficiency, since the functional protein is already present, and it does not need to be firstly transcribed and translated. The first attempt to electroporate the cells with Cas9 protein failed because all cells died. At the second attempt, Cas9 plasmid, as well as Cas9 protein, were used. From total 528 seeded wells with Cas9 plasmid electroporated cells and 1152 wells from Cas9 protein electroporation, we obtained 3 transgene-expressing clones from Cas9 plasmid electroporation, two of them contained HDAC1 WT and one HDAC1 H141A. There were no transgene-positive clones from Cas9 protein electroporation. Presumably, the keratinocyte cell line reacted too sensitive to Cas9 protein electroporation, and therefore all the cells died. Eventually, the conditions of this procedure might be optimized.

The transgene-expressing clones, either HDAC1 WT or HDAC1 H141A, were validated by PCRs, FLAG-tag detection using Western blot and immunofluorescent microscopy. HDAC1 overexpression was in all clones about 2.5-fold higher than in the control cell line (without transgene). For screening, we used various types of PCR: nested PCR (batch screen), indel PCR, screening and direct PCR. The nested PCR confirmed the presence of the transgene in

the AAVS gene locus immediately after electroporation. Indel PCR was done complementary to sequencing to verify the proper gRNA binding and Cas9 cut. The screening and direct PCR gave us more detailed hints which clone could contain the transgene, however, the results did not always match. Western Blotting and immunofluorescence screening (on the coverslip or in the 6-well plate) turned out to be the most accurate methods to confirm the presence of the transgene. Further development of FLAG-tag detection in 96-well plates by immunofluorescence microscopy would enable the accurate screen of thousands of clones at the same time and should be considered for the next experiments.

Previous gene editing experiment using the same HDAC1 constructs in the nearly haploid human tumor cell line HAP1 showed on average an efficiency of 2 positive clones out of 10 screened clones. In summary, human keratinocytes are much more difficult to edit by CRISPR-Cas9, due to their higher sensitivity to cell dilution and potential induction of differentiation during the screening process.

4.4. Overexpression of catalytically inactive HDAC1 variant significantly reduced cellular HDAC activity

Interestingly, HDAC2 expression had not been downregulated upon HDAC1 overexpression as observed in other cell models. As expected, HDAC1 overexpression notably repressed the expression of the cell cycle regulator p21 in both HDAC1 WT expressing cell lines (#A9 and #B5) but not in the HDAC1 H141A overexpressing #H1 cell line. This cell line displayed a lower cellular HDAC activity, and increased histone H3K56 and H4K8 acetylation. This indicates that point mutation of histidine at the position 141 to alanine significantly decreased the HDAC1 catalytic activity. Furthermore, it was demonstrated that HDAC1 greatly contributes to the total deacetylase activity of human keratinocytes.

4.5. Set-up of a specific shRNA-mediated knock-down of endogenous HDAC1 in human keratinocytes

With overexpression of the transgene, either HDAC1 WT or HDAC1 H141A, we could observe effects on HDAC1, HDAC2, HDAC8 and marker gene expression, as well as on total HDAC activity. The goal to create cell lines, mimicking complete inhibition by HDAC inhibitors, could be reached by suppressing the expression of the endogenous HDAC1 via knock-down approach. Cell lines overexpressing the catalytically inactive HDAC1 H141A, in the absence of endogenous wild-type HDAC1, would represent the model where the catalytical function of HDAC1 is absent, due to the point mutation, without affecting scaffolding properties for proper multisubunit complex functioning.

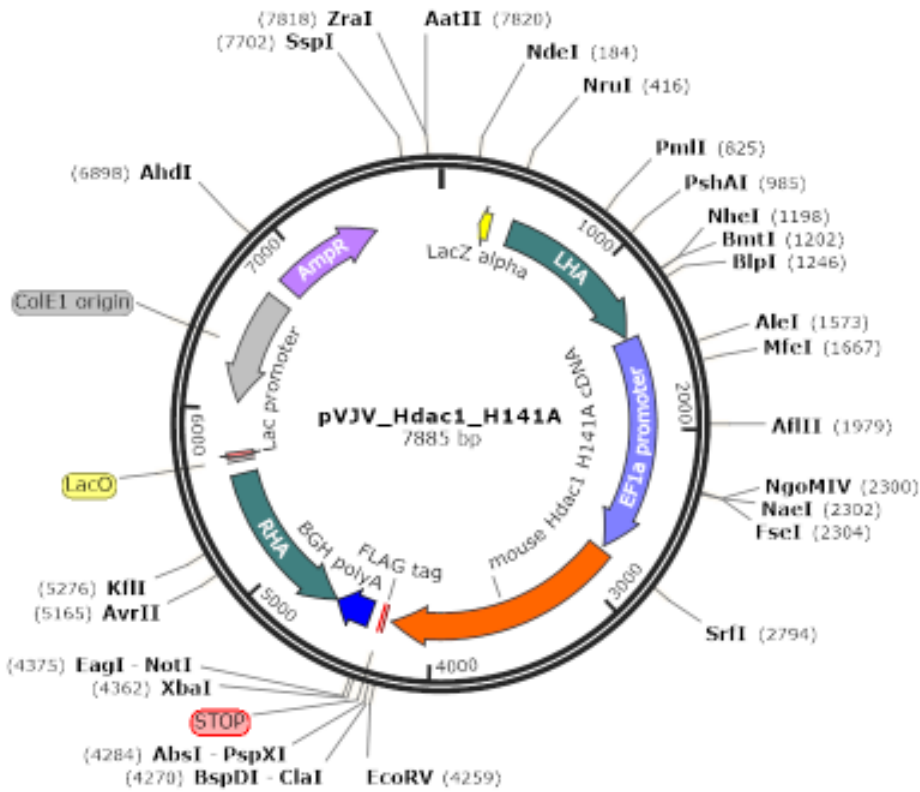
Therefore, our first aim was to perform an HDAC1 knock-down in NHEK/SVTER3-5 keratinocyte cell line and its comparison to cell line overexpressing catalytically inactive

HDAC1 H141A. The knock-down in original NHEK/SVTERT3-5 cell line resulted in almost complete repression of HDAC1 translation and its absence as a protein (Fig. 57). Total HDAC activity decreased by 50 % compared to the control (shRNA NT). In the next step, the knock-down was performed in the cell lines overexpressing the HDAC1 WT (#B5) and HDAC1 H141A (#H1) and the shRNA targeted human, endogenous HDAC1 instead of overexpressed mouse HDAC1 variants. The immunoblot showed a complete absence of the endogenous human HDAC1 and approved successful knock-down. Importantly, in both settings, the expression of the HDAC1 transgene was not affected by the shRNA.

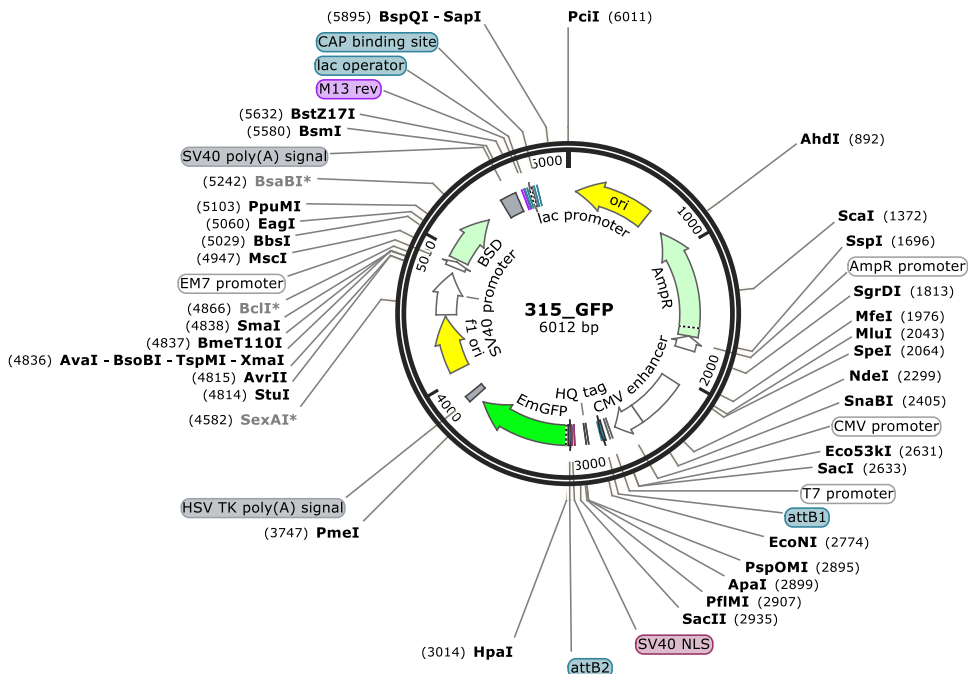
Outlook

Future experiments should elucidate the behavior of the newly created cell lines during terminal differentiation. The data of the pre-confluent wild-type and catalytically inactive HDAC1-overexpressing cell lines should also be compared to post-confluent cells, to see if catalytical inactivity alters the process of terminal differentiation and other cellular processes. To compare the data from genetically modified cell lines that mimic targeted and isolated HDAC inhibition, the data from MS-275 treatment of the original cell line NHEK/SVTERT3-5 needs to be repeated, especially the Western blot analysis, due to the inequality of loaded samples. Furthermore, the screening for single cell colonies would need to be tested by using the immunofluorescence labeling of FLAG-tag in 96-well plates. This procedure would allow for faster screening of countless clones without prior PCR screening. Eventually, with the use of these lately established procedures, cell lines expressing catalytical inactive isoforms could be generated for all the other class I HDACs.

5.3. Vector map HDAC1 H141A



5.4. Vector map GFP



References

- 5.1 Layers of the Skin – Anatomy and Physiology. (n.d.). Retrieved October 28, 2018, from <https://opentextbc.ca/anatomyandphysiology/chapter/5-1-layers-of-the-skin/>
- Abu, M., Muhamad, M., Hassan, H., Zakaria, Z., & Ali, S. A. M. (2016). Proximity coupled antenna with star geometry pattern amc ground plane. *ARPJ Journal of Engineering and Applied Sciences*, 11(14), 8822–8828. <https://doi.org/10.3892/ijo>
- Adams-Cioaba, M. a, & Min, J. (2009). Structure and function of histone methylation binding proteins. *Biochemistry and Cell Biology = Biochimie et Biologie Cellulaire*. <https://doi.org/10.1139/O08-129>
- Alam, H., Sehgal, L., Kundu, S. T., Dalal, S. N., & Vaidya, M. M. (2011). Novel function of keratins 5 and 14 in proliferation and differentiation of stratified epithelial cells. *Molecular Biology of the Cell*, 22(21), 4068–4078. <https://doi.org/10.1109/ICRMS.2016.8050059>
- ALLFREY, V. G., FAULKNER, R., & MIRSKY, A. E. (1964). Acetylation and Methylation of Histones and Their Possible Role in the Regulation of Rna Synthesis. *Proceedings of the National Academy of Sciences of the United States of America*, 51(1938), 786–94. <https://doi.org/10.1073/pnas.51.5.786>
- Alva, V., Ammelburg, M., Söding, J., & Lupas, A. N. (2007). On the origin of the histone fold. *BMC Structural Biology*, 7, 1–10. <https://doi.org/10.1186/1472-6807-7-17>
- Amini-nik, K. A. B. S., Alman, B. A., Brown, D. A., Gibran, N. S., Cha, J., Falanga, V., ... Kim, B. B. (2016). NIH Public Access. *Stem Cell Research & Therapy*, 27(1), 351–357. <https://doi.org/10.1055/s-0029-1237423.Epigenetics>
- Bannister, A. J., & Kouzarides, T. (2011). Regulation of chromatin by histone modifications. *Cell Research*, 21(3), 381–395. <https://doi.org/10.1038/cr.2011.22>
- Bikle, D. D., Xie, Z., & Tu, C.-L. (2013). Calcium regulation of keratinocyte differentiation. *Expert Rev Endocrinol Metab*, 7(4), 461–472. <https://doi.org/10.1586/eem.12.34.Calcium>
- Blixt, N. C., Faulkner, B. K., Astleford, K., Lelich, R., Schering, J., Spencer, E., ... Mansky, K. C. (2017). Class II and IV HDACs function as inhibitors of osteoclast differentiation. *PLoS ONE*, 12(9), 1–22. <https://doi.org/10.1371/journal.pone.0185441>
- Bolden, J. E., Shi, W., Jankowski, K., Kan, C.-Y., Cluse, L., Martin, B. P., ... Johnstone, R. W. (2013). HDAC inhibitors induce tumor-cell-selective pro-apoptotic transcriptional responses. *Cell Death & Disease*, 4(2), e519–e519. <https://doi.org/10.1038/cddis.2013.9>
- Botchkarev, V. A., Gdula, M. R., Mardaryev, A. N., Sharov, A. A., & Fessing, M. Y. (2012).

- Epigenetic regulation of gene expression in keratinocytes. *Journal of Investigative Dermatology*, 132(11), 2505–2521. <https://doi.org/10.1038/jid.2012.182>
- Brunmeir, R., Lagger, S., & Seiser, C. (2009). Histone deacetylase 1 and 2-controlled embryonic development and cell differentiation. *International Journal of Developmental Biology*, 53(2–3), 275–289. <https://doi.org/10.1387/ijdb.082649rb>
- Bygren, L. O., Tinghög, P., Carstensen, J., Edvinsson, S., Kaati, G., Pembrey, M. E., & Sjöström, M. (2014). Change in paternal grandmother's early food supply influenced cardiovascular mortality of the female grandchildren. *BMC Genetics*, 15, 2–7. <https://doi.org/10.1186/1471-2156-15-12>
- Candi, E., Schmidt, R., & Melino, G. (2005). The cornified envelope: A model of cell death in the skin. *Nature Reviews Molecular Cell Biology*, 6(4), 328–340. <https://doi.org/10.1038/nrm1619>
- Carette, J. E., Raaben, M., Wong, A. C., Herbert, A. S., Obernosterer, G., Mulherkar, N., ... Brummelkamp, T. R. (2011). Ebola virus entry requires the cholesterol transporter Niemann-Pick C1. *Nature*, 477(7364), 340–343. <https://doi.org/10.1038/nature10348>
- Cesar, S. A., Rajan, V., Prykhodzij, S. V., Berman, J. N., & Ignacimuthu, S. (2016). Insert, remove or replace: A highly advanced genome editing system using CRISPR/Cas9. *Biochimica et Biophysica Acta - Molecular Cell Research*, 1863(9), 2334–2344. <https://doi.org/10.1016/j.bbamcr.2016.06.009>
- Chaturvedi, V., Qin, J. Z., Denning, M. F., Choubey, D., Diaz, M. O., & Nickoloff, B. J. (1999). Apoptosis in proliferating, senescent, and immortalized keratinocytes. *Journal of Biological Chemistry*, 274(33), 23358–23367. <https://doi.org/10.1074/jbc.274.33.23358>
- Choi, B., Cui, Z., Kim, S., Fan, J., Wu, B. M., & Angeles, L. (2015). HHS Public Access, 3(31), 6448–6455. <https://doi.org/10.1039/x0xx00000x>
- Chu, D. H. (n.d.). Structure of Skin 1., (1), 1–24.
- Chun, P. (2015). Histone deacetylase inhibitors in hematological malignancies and solid tumors. *Archives of Pharmacal Research*, 38(6), 933–949. <https://doi.org/10.1007/s12272-015-0571-1>
- Ciccone, D. N., & Chen, T. (2009). Histone lysine methylation in genomic imprinting. *Epigenetics*, 4(4), 216–220. <https://doi.org/10.4161/epi.8974>
- Connelly, J. T., Mishra, A., Gautrot, J. E., & Watt, F. M. (2011). Shape-induced terminal differentiation of human epidermal stem cells requires p38 and is regulated by histone acetylation. *PLoS ONE*, 6(11), 1–10. <https://doi.org/10.1371/journal.pone.0027259>

- Coqueret, O. (2003). New roles for p21 and p27 cell-cycle inhibitors: a function for each cell compartment? *Trends in Cell Biology*, 13(2), 65–70. [https://doi.org/10.1016/S0962-8924\(02\)00043-0](https://doi.org/10.1016/S0962-8924(02)00043-0)
- CSHL. (2004). *Epigenetics. Cold Spring Harbor Symposia on Quantitative Biology. Volume 69*. <https://doi.org/10.1101/sqb.2007.72.069>
- Dali-Youcef, N., Lagouge, M., Froelich, S., Koehl, C., Schoonjans, K., & Auwerx, J. (2007). Sirtuins: The “magnificent seven”, function, metabolism and longevity. *Annals of Medicine*, 39(5), 335–345. <https://doi.org/10.1080/07853890701408194>
- Das, C., Lucia, M. S., Hansen, K. C., & Tyler, J. K. (2009). CBP/p300-mediated acetylation of histone H3 on lysine 56. *Nature*, 459(7243), 113–117. <https://doi.org/10.1038/nature07861>
- Dashwood, R. H., & Ho, E. (2008). Dietary agents as histone deacetylase inhibitors: sulforaphane and structurally related isothiocyanates. *Nutr Rev*, 66(1), 36–38. <https://doi.org/10.1111/j.1753-4887.2008.00065.x>
- Deans, C., & Maggert, K. A. (2015). What do you mean, “Epigenetic”? *Genetics*, 199(4), 887–896. <https://doi.org/10.1534/genetics.114.173492>
- Definition of entinostat - NCI Drug Dictionary - National Cancer Institute. (n.d.). Retrieved November 18, 2018, from <https://www.cancer.gov/publications/dictionaries/cancer-drug/def/entinostat>
- Deichmann, U. (2016). Epigenetics: The origins and evolution of a fashionable topic. *Developmental Biology*, 416(1), 249–254. <https://doi.org/10.1016/j.ydbio.2016.06.005>
- Devgan, V., Nguyen, B. C., Oh, H., & Dotto, G. P. (2006). p21WAF1/Cip1 suppresses keratinocyte differentiation independently of the cell cycle through transcriptional up-regulation of the IGF-I gene. *Journal of Biological Chemistry*, 281(41), 30463–30470. <https://doi.org/10.1074/jbc.M604684200>
- Dokmanovic, M., Clarke, C., & Marks, P. A. (2007). Histone Deacetylase Inhibitors: Overview and Perspectives. *Molecular Cancer Research*, 5(10), 981–989. <https://doi.org/10.1158/1541-7786.MCR-07-0324>
- Eckschlager, T., Plch, J., Stiborova, M., & Hrabeta, J. (2017). Histone deacetylase inhibitors as anticancer drugs. *International Journal of Molecular Sciences*, 18(7), 1–25. <https://doi.org/10.3390/ijms18071414>
- Eichner, R., Sun, T. T., & Aebi, U. (1986). The role of keratin subfamilies and keratin pairs in the formation of human epidermal intermediate filaments. *Journal of Cell Biology*, 102(5),

1767–1777. <https://doi.org/10.1083/jcb.102.5.1767>

Ellis, L., Hammers, H., & Pili, R. (2010). NIH Public Access. *Current Opinion in Genetics & Development*, 280(2), 1–15. <https://doi.org/10.1016/j.canlet.2008.11.012>. Targeting

Entinostat - Syndax Pharmaceuticals - AdisInsight. (n.d.). Retrieved November 18, 2018, from <https://adisinsight.springer.com/drugs/800012663>

Fellows, R., Denizot, J., Stellato, C., Cuomo, A., Jain, P., Stoyanova, E., ... Varga-Weisz, P. (2018). Microbiota derived short chain fatty acids promote histone crotonylation in the colon through histone deacetylases. *Nature Communications*, 9(1), 105. <https://doi.org/10.1038/s41467-017-02651-5>

Felsenfeld, G. (2007). A Brief History of Epigenetics - Chapter 2.pdf. *Epigenetics*, 15–22.

Fraga, M. F., Ballestar, E., Paz, M. F., Ropero, S., Setien, F., Ballestar, M. L., ... Esteller, M. (2005). From The Cover: Epigenetic differences arise during the lifetime of monozygotic twins. *Proceedings of the National Academy of Sciences*, 102(30), 10604–10609. <https://doi.org/10.1073/pnas.0500398102>

Fuchs, E. (1988). Keratins as biochemical markers of epithelial differentiation. *Trends in Genetics*, 4(10), 277–281. [https://doi.org/10.1016/0168-9525\(88\)90169-2](https://doi.org/10.1016/0168-9525(88)90169-2)

Fuchs, E. (1994). Epidermal differentiation and keratin gene expression. *Princess Takamatsu Symposia*, 24, 290–302. https://doi.org/10.1242/jcs.1993.Supplement_17.28

Fuchs, E. (1995). Keratins and the Skin. *Annual Review of Cell and Developmental Biology*, 11(1), 123–154. <https://doi.org/10.1146/annurev.cb.11.110195.001011>

Gammoh, N., Lam, D., Puente, C., Ganley, I., Marks, P. A., & Jiang, X. (2012). Role of autophagy in histone deacetylase inhibitor-induced apoptotic and nonapoptotic cell death. *Proceedings of the National Academy of Sciences*, 109(17), 6561–6565. <https://doi.org/10.1073/pnas.1204429109>

Gregory, P. D., Wagner, K., & Hörz, W. (2001). Histone acetylation and chromatin remodeling. *Experimental Cell Research*, 265(2), 195–202. <https://doi.org/10.1006/excr.2001.5187>

Gryder, B. E., Sodji, Q. H., & Oyelere, A. K. (2013). NIH Public Access, 4(4), 505–524. <https://doi.org/10.4155/fmc.12.3.Targeted>

Gui, C.-Y., Ngo, L., Xu, W. S., Richon, V. M., & Marks, P. A. (2004). *Histone deacetylase (HDAC) inhibitor activation of p21 WAF1 involves changes in promoter-associated proteins, including HDAC1.* Retrieved from www.pnas.org/cgi/doi/10.1073/pnas.0307708100

- Gupta, S., Kim, S. Y., Artis, S., Molfese, D. L., Schumacher, A., Sweatt, J. D., ... Lubin, F. D. (2010). Histone Methylation Regulates Memory Formation. *Journal of Neuroscience*, 30(10), 3589–3599. <https://doi.org/10.1523/JNEUROSCI.3732-09.2010>
- Haberland, M., Montgomery, R. L., & Olson, E. N. (2011). Physiology : Implications for Disease and Therapy. *Nature Reviews. Genetics*, 10(1), 32–42. <https://doi.org/10.1038/nrg2485>.The
- Hagelkruys, A., Mattes, K., Moos, V., Rennmayr, M., Ringbauer, M., Sawicka, A., & Seiser, C. (2016). Essential Nonredundant Function of the Catalytic Activity of Histone Deacetylase 2 in Mouse Development. *Molecular and Cellular Biology*, 36(3), 462–474. <https://doi.org/10.1128/MCB.00639-15>
- Hagelkruys Astrid, Sawicka Anna, Rennmayr Magdalena, S. C. (2011). The Biology of HDAC in Cancer: The Nuclear and Epigenetic Components. *Histone Deacetylases: The Biology and Clinical Implication*, 206.
- Hanahan, D., & Weinberg, R. A. (2011). Hallmarks of Cancer: The Next Generation. *Cell*, 144(5), 646–674. <https://doi.org/10.1016/J.CELL.2011.02.013>
- Handy, D., Castro, R., & Loscalzo, J. (2011). Epigenetic Modifications Basic Mechanisms and Role in Cardiovascular Disease. *Circulation*, 123(19), 2145–2156. <https://doi.org/10.1161/CIRCULATIONAHA.110.956839>.Epigenetic
- Harding, C. R. (2004). The stratum corneum: structure and function in health and disease. *Dermatologic Therapy*, 17(s1), 6–15. <https://doi.org/10.1111/j.1396-0296.2004.04S1001.x>
- Haumaitre, C., Lenoir, O., & Scharfmann, R. (2009). Cell Cycle Directing cell differentiation with small-molecule histone deacetylase inhibitors: The example of promoting pancreatic endocrine cells. <https://doi.org/10.4161/cc.8.4.7610>
- Holbrook, K. A. (1989). Biologic Structure and Function: Perspectives on Morphologic Approaches to the Study of the Granular Layer Keratinocyte. *Journal of Investigative Dermatology*. <https://doi.org/10.1038/jid.1989.36>
- Horvath, S. (2013). DNA methylation age of human tissues and cell types. *Genome Biology*, 14(10). <https://doi.org/10.1186/gb-2013-14-10-r115>
- Hyun-Chung, K., & Suk-Chul, B. (2011). HDAC inhibitors as anti-cancer drugs. *Am J Transl Res*, 3(2), 166–179. <https://doi.org/www.ajtr.org> /ISSN:1943-8141/AJTR1012002
- Illingworth, R. S., & Bird, A. P. (2009). CpG islands - "A rough guide." *FEBS Letters*, 583(11), 1713–1720. <https://doi.org/10.1016/j.febslet.2009.04.012>

- Inhibitor, K., Gene, C. I. P., Lagger, G., Doetzlhofer, A., Schuettengruber, B., Haidweger, E., ... Seiser, C. (2003). The Tumor Suppressor p53 and Histone Deacetylase 1 Are Antagonistic Regulators of the Cyclin-Dependent, 23(8), 2669–2679. <https://doi.org/10.1128/MCB.23.8.2669>
- Izzo, A., & Schneider, R. (2010). Chatting histone modifications in mammals. *Briefings in Functional Genomics*, 9(5–6), 429–443. <https://doi.org/10.1093/bfpg/elq024>
- Kabashima, K. (2016). Immunology of the skin: Basic and clinical sciences in skin immune responses. *Immunology of the Skin: Basic and Clinical Sciences in Skin Immune Responses*, 1–510. <https://doi.org/10.1007/978-4-431-55855-2>
- Kanitakis, J. (n.d.). Anatomy, histology and immunohistochemistry of normal human skin. *European Journal*, 12(4), 390-9; quiz 400–1. Retrieved from <http://www.ncbi.nlm.nih.gov/pubmed/12095893>
- Katoch, O., Dwarkanath, B., & K Agrawala, P. (2013). HDAC inhibitors: applications in oncology and beyond. *HOAJ Biology*, 2(1), 1. <https://doi.org/10.7243/2050-0874-2-2>
- Kelly, R. D. W., Chandru, A., Watson, P. J., Song, Y., Blades, M., Robertson, N. S., ... Cowley, S. M. (2018). Histone deacetylase (HDAC) 1 and 2 complexes regulate both histone acetylation and crotonylation in vivo. *Scientific Reports*, 8(1), 14690. <https://doi.org/10.1038/s41598-018-32927-9>
- Keratins, S. (2016). HHS Public Access, 18, 1–45. <https://doi.org/10.1016/bs.mie.2015.09.032.Skin>
- Kimura, A., Matsubara, K., & Horikoshi, M. (2005). A decade of histone acetylation: Marking eukaryotic chromosomes with specific codes. *Journal of Biochemistry*, 138(6), 647–662. <https://doi.org/10.1093/jb/mvi184>
- Kingston, R. E., Tamkun, J. W., Baulcombe, D. C., & Dean, C. (2014). Erasers of Histone Acetylation: The Histone Deacetylase Enzymes Erasers of Histone Acetylation: The Histone Deacetylase Enzymes, 1–26. <https://doi.org/10.1101/cshperspect.a018713>
- Kolarsick, P. A. J., Kolarsick, M. A., & Goodwin, C. (2011). Anatomy and Physiology of the Skin. , 3(4), 203–213. <https://doi.org/10.1097/JDN.0b013e3182274a98>
- Kopan, R., Traska, G., & Fuchs, E. (1987). Retinoids as important regulators of terminal differentiation: Examining keratin expression in individual epidermal cells at various stages of keratinization. *Journal of Cell Biology*, 105(1), 427–440. <https://doi.org/10.1083/jcb.105.1.427>

- Kroemer, G., Galluzzi, L., & Brenner, C. (2007). Mitochondrial Membrane Permeabilization in Cell Death. *Physiological Reviews*, 87(1), 99–163. <https://doi.org/10.1152/physrev.00013.2006>
- Kutil, Z., Novakova, Z., Meleshin, M., Mikesova, J., Schutkowski, M., & Barinka, C. (2018). Histone Deacetylase 11 Is a Fatty-Acid Deacylase. *ACS Chemical Biology*, 13(3), 685–693. <https://doi.org/10.1021/acscchembio.7b00942>
- Lagger, G., O'Carroll, D., Rembold, M., Khier, H., Tischler, J., Weitzer, G., ... Seiser, C. (2002). Essential function of histone deacetylase 1 in proliferation control and CDK inhibitor repression. *EMBO Journal*, 21(11), 2672–2681. <https://doi.org/10.1093/emboj/21.11.2672>
- LeBoeuf, M., Terrell, A., Trivedi, S., Sinha, S., Epstein, J. A., Olson, E. N., ... Millar, S. E. (2010). Hdac1 and Hdac2 Act Redundantly to Control p63 and p53 Functions in Epidermal Progenitor Cells. *Developmental Cell*, 19(6), 807–818. <https://doi.org/10.1016/j.devcel.2010.10.015>
- Lee, B. I., Park, S. H., Kim, J. W., Sausville, E. A., Kim, H. T., Nakanishi, O., ... Kim, S. J. (2001). MS-275, a histone deacetylase inhibitor, selectively induces transforming growth factor β type II receptor expression in human breast cancer cells. *Cancer Research*, 61(3), 931–934.
- Lee, S. H., Jeong, S. K., & Ahn, S. K. (2006). An update of the defensive barrier function of skin. *Yonsei Medical Journal*, 47(3), 293–306. <https://doi.org/10.3349/ymj.2006.47.3.293>
- Lin, C., McGough, R., Aswad, B., Block, J. A., & Terek, R. (2004). Hypoxia induces HIF-1 α and VEGF expression in chondrosarcoma cells and chondrocytes. *Journal of Orthopaedic Research*, 22(6), 1175–1181. <https://doi.org/10.1016/j.orthres.2004.03.002>
- Macleod, K. F., Sherry, N., Hannon, G., Beach, D., Tokino, T., Kinzler, K., ... Jacks, T. (1995). p53-Dependent and independent expression of p21 during cell growth, differentiation, and DNA damage. *Genes and Development*, 9(8), 935–944. <https://doi.org/10.1101/gad.9.8.935>
- Manuscript, A. (2009). Yeast To Mice and Men. *Molecular Cell*, 9(3), 206–218. <https://doi.org/10.1038/nrm2346>.The
- Mariadason, J. M. (2008). HDACs and HDAC inhibitors in colon cancer. *Epigenetics*, 3(1), 28–37. <https://doi.org/10.4161/epi.3.1.5736>
- Markova, N. G., Karaman-Jurukovska, N., Pinkas-Sarafova, A., Marekov, L. N., & Simon, M. (2007). Inhibition of histone deacetylation promotes abnormal epidermal differentiation

- and specifically suppresses the expression of the late differentiation marker profilaggrin. *Journal of Investigative Dermatology*, 127(5), 1126–1139. <https://doi.org/10.1038/sj.jid.5700684>
- Marks, P. A. (2010). The clinical development of histone deacetylase inhibitors as targeted anticancer drugs. *Expert Opinion on Investigational Drugs*, 19(9), 1049–66. <https://doi.org/10.1517/13543784.2010.510514>
- Martinsson, H., Yhr, M., & Enerbäck, C. (2005). Expression patterns of S100A7 (psoriasin) and S100A9 (calgranulin-B) in keratinocyte differentiation. *Experimental Dermatology*, 14(3), 161–168. <https://doi.org/10.1111/j.0906-6705.2005.00239.x>
- McLean, W. H. I. (2016). Filaggrin failure – from ichthyosis vulgaris to atopic eczema and beyond. *British Journal of Dermatology*, 175, 4–7. <https://doi.org/10.1111/bjd.14997>
- Menon, G. K., Lee, S. E., & Lee, S.-H. (2018). An overview of epidermal lamellar bodies: Novel roles in biological adaptations and secondary barriers. *Journal of Dermatological Science*, 92(1), 10–17. <https://doi.org/10.1016/J.JDERMSCI.2018.03.005>
- Moll, R., Divo, M., & Langbein, L. (2008). The human keratins: biology and pathology. *Histochem Cell Biol*, 129, 705–733. <https://doi.org/10.1007/s00418-008-0435-6>
- Moosavi, A., & Ardekani, A. M. (2016). Role of epigenetics in biology and human diseases. *Iranian Biomedical Journal*, 20(5), 246–258. <https://doi.org/10.22045/ibj.2016.01>
- Moreno-yruela, C., Galleano, I., Madsen, A. S., & Olsen, C. A. (2017). Histone Deacetylase 11 is an e - N -Myristoyllysine Hydrolase, 1–28. <https://doi.org/10.1016/j.chembiol.2018.04.007>
- Moser, M. A., Hagelkruys, A., & Seiser, C. (2014). Transcription and beyond: The role of mammalian class I lysine deacetylases. *Chromosoma*, 123(1–2), 67–78. <https://doi.org/10.1007/s00412-013-0441-x>
- Mrakovcic, M., Kleinheinz, J., & Fröhlich, L. F. (2017). Histone deacetylase inhibitor-induced autophagy in tumor cells: Implications for p53. *International Journal of Molecular Sciences*, 18(9). <https://doi.org/10.3390/ijms18091883>
- MS-275 A HDAC1 and HDAC3 inhibitor | Sigma-Aldrich. (n.d.). Retrieved November 18, 2018, from https://www.sigmaaldrich.com/catalog/product/sigma/eps002?lang=de®ion=AT&gclid=CjwKCAiA8rnfBRB3EiwAhrhBGpSYHNQDyxH47ztDqn1k45h92Rn37PXefBWKhJ-4JRNkXL_mIfT-ihoCYbUQAvD_BwE
- Newbold, A., Salmon, J. M., Martin, B. P., Stanley, K., & Johnstone, R. W. (2014). The role of

- p21waf1/cip1 and p27Kip1 in HDACi-mediated tumor cell death and cell cycle arrest in the Eμ-myc model of B-cell lymphoma. *Oncogene*, 33(47), 5415–5423. <https://doi.org/10.1038/onc.2013.482>
- ORLIKOVA, B., SCHNEKENBURGER, M., ZLOH, M., GOLAIS, F., DIEDERICH, M., & TASDEMIR, D. (2012). Natural chalcones as dual inhibitors of HDACs and NF-κB. *Oncology Reports*, 28(3), 797–805. <https://doi.org/10.3892/or.2012.1870>
- Painter, R. C., Osmond, C., Gluckman, P., Hanson, M., Phillips, D. I. W., & Roseboom, T. J. (2008). Transgenerational effects of prenatal exposure to the Dutch famine on neonatal adiposity and health in later life. *BJOG: An International Journal of Obstetrics and Gynaecology*, 115(10), 1243–1249. <https://doi.org/10.1111/j.1471-0528.2008.01822.x>
- Perri, F., Longo, F., Giuliano, M., Sabbatino, F., Favia, G., Ionna, F., ... Pisconti, S. (2017). Epigenetic control of gene expression: Potential implications for cancer treatment. *Critical Reviews in Oncology/Hematology*, 111, 166–172. <https://doi.org/10.1016/j.critrevonc.2017.01.020>
- Pfaffl, M. W. (2001). A new mathematical model for relative quantification in real-time RT-PCR. *Nucleic Acids Research*, 29(9), e45. <https://doi.org/10.1093/nar/29.9.e45>
- Ropero, S., & Esteller, M. (2007). The role of histone deacetylases (HDACs) in human cancer. *Molecular Oncology*, 1(1), 19–25. <https://doi.org/10.1016/j.molonc.2007.01.001>
- Rosato, R. R., Almenara, J. A., & Grant, S. (2003). The histone deacetylase inhibitor MS-275 promotes differentiation or apoptosis in human leukemia cells through a process regulated by generation of reactive oxygen species and induction of p21CIP1/WAF1. *Cancer Research*, 63(13), 3637–3645. <https://doi.org/10.1097/00001813-200201000-00001>
- RUIJTER, A. J. M. de, GENNIP, A. H. van, CARON, H. N., KEMP, S., & KUILENBURG, A. B. P. van. (2003). Histone deacetylases (HDACs): characterization of the classical HDAC family. *Biochemical Journal*, 370(3), 737–749. <https://doi.org/10.1042/bj20021321>
- Ryan, D. P., Henzel, K. S., Pearson, B. L., Siwek, M. E., Papazoglou, A., Guo, L., ... Ehninger, D. (2017). A paternal methyl donor-rich diet altered cognitive and neural functions in offspring mice. *Molecular Psychiatry*, (February), 1–11. <https://doi.org/10.1038/mp.2017.53>
- Sabari, B. R., Tang, Z., Huang, H., Yong-Gonzalez, V., Molina, H., Kong, H. E., ... Allis, C. D. (2015). Intracellular Crotonyl-CoA Stimulates Transcription through p300-Catalyzed Histone Crotonylation. *Molecular Cell*, 58(2), 203–215.

<https://doi.org/10.1016/j.molcel.2015.02.029>

- Sanford, J. A., Zhang, L.-J., Williams, M. R., Gangoiti, J. A., Huang, C.-M., & Gallo, R. L. (2016). Inhibition of HDAC8 and HDAC9 by microbial short-chain fatty acids breaks immune tolerance of the epidermis to TLR ligands. *Science Immunology*, *1*(4), eaah4609. <https://doi.org/10.1126/sciimmunol.aah4609>
- Schotterl, S., Brennenstuhl, H., & Naumann, U. (2015). Modulation of immune responses by histone deacetylase inhibitors. *Critical Reviews in Oncogenesis*, *20*(1–2), 139–54. Retrieved from <http://www.ncbi.nlm.nih.gov/pubmed/25746108>
- Schübeler, D. (2015). Function and information content of DNA methylation. *Nature*, *517*(7534), 321–326. <https://doi.org/10.1038/nature14192>
- Shen, L., Farid, H., & Mcpeek, M. A. (2008). Clinical Dermatology. *Evolution*, 1–14.
- Shi, Y., Lan, F., Matson, C., Mulligan, P., Whetstine, J. R., Cole, P. A., ... Shi, Y. (2004). Histone demethylation mediated by the nuclear amine oxidase homolog LSD1. *Cell*, *119*(7), 941–953. <https://doi.org/10.1016/j.cell.2004.12.012>
- Shulak, L., Beljanski, V., Chiang, C., Dutta, S. M., Van Grevenynghe, J., Belgnaoui, S. M., ... Lyles, D. S. (2014). Histone Deacetylase Inhibitors Potentiate Vesicular Stomatitis Virus Oncolysis in Prostate Cancer Cells by Modulating NF- B-Dependent Autophagy. *Journal of Virology*, *88*(5), 2927–2940. <https://doi.org/10.1128/JVI.03406-13>
- Singh, A. K., Bishayee, A., & Pandey, A. K. (2018). *Targeting histone deacetylases with natural and synthetic agents: An emerging anticancer strategy*. *Nutrients* (Vol. 10). <https://doi.org/10.3390/nu10060731>
- Sites, J. B. C. A. (2012). Vincent Allfrey's Work on Histone Acetylation. *Journal of Biological Chemistry*, *287*(3), 2270–2271. <https://doi.org/10.1074/jbc.O112.000248>
- Slingerland, M., Guchelaar, H.-J., & Gelderblom, H. (2014). Histone deacetylase inhibitors. *Anti-Cancer Drugs*, *25*(2), 140–149. <https://doi.org/10.1097/CAD.0000000000000040>
- Speed, U. (n.d.). *Smarter , Faster Search for Better Patient Care*. <https://doi.org/10.1016/B978-1-4557-0296-1.09985-1>
- Steinman, R. A., Hoffman, B., Iro, A., Guillouf, C., Liebermann, D. A., & el-Houseini, M. E. (1994). Induction of p21 (WAF-1/CIP1) during differentiation. *Oncogene*, *9*(11), 3389–96. Retrieved from <http://www.ncbi.nlm.nih.gov/pubmed/7936667>
- Sterner, D. E., & Berger, S. L. (2000). Acetylation of Histones and Transcription-Related Factors. *Microbiology and Molecular Biology Reviews*, *64*(2), 435–459.

<https://doi.org/10.1128/MMBR.64.2.435-459.2000>

- Subramanian, S., Bates, S. E., Wright, J. J., Espinoza-Delgado, I., & Piekarczyk, R. L. (2010). Clinical toxicities of histone deacetylase inhibitors. *Pharmaceuticals*, *3*(9), 2751–2767. <https://doi.org/10.3390/ph3092751>
- Sun, T. T., & Green, H. (1976). Differentiation of the epidermal keratinocyte in cell culture: Formation of the cornified envelope. *Cell*, *9*(4 PART 1), 511–521. [https://doi.org/10.1016/0092-8674\(76\)90033-7](https://doi.org/10.1016/0092-8674(76)90033-7)
- Suroliya, I., & Bates, S. E. (2018). Entinostat finds a path: A new study elucidates effects of the histone deacetylase inhibitor on the immune system. *Cancer*, (July), 1–4. <https://doi.org/10.1002/cncr.31766>
- Tan, M., Luo, H., Lee, S., Jin, F., Yang, J. S., Montellier, E., ... Zhao, Y. (2011). Resource Identification of 67 Histone Marks and Histone Lysine Crotonylation as a New Type of Histone Modification. *Cell*, *146*(6), 1016–1028. <https://doi.org/10.1016/j.cell.2011.08.008>
- Telser, A. (2002). *Molecular Biology of the Cell*, 4th Edition. *Shock*. <https://doi.org/10.1097/00024382-200209000-00015>
- Tou, L., Liu, Q., & Shivdasani, R. A. (2004). CC -view D, *24*(8), 9. <https://doi.org/10.1128/MCB.24.8.3132>
- Tsankova, N., & Nestler, E. J. (2010). Epigenetic Regulation in, *VIII*(3), 435–448. <https://doi.org/10.1101/cshperspect.a019315>
- Venturelli, S., Berger, A., Böcker, A., Busch, C., Weiland, T., Noor, S., ... Bitzer, M. (2013). Resveratrol as a Pan-HDAC Inhibitor Alters the Acetylation Status of Histone Proteins in Human-Derived Hepatoblastoma Cells. *PLoS ONE*, *8*(8), e73097. <https://doi.org/10.1371/journal.pone.0073097>
- Verdone, L., Caserta, M., & Mauro, E. Di. (2005). Role of histone acetylation in the control of gene expression. *Biochemistry and Cell Biology*, *83*(3), 344–353. <https://doi.org/10.1139/o05-041>
- Wagner, T., Gschwandtner, M., Strajeriu, A., Elbe-Bürger, A., Grillari, J., Grillari-Voglauer, R., ... Mildner, M. (2018). Establishment of keratinocyte cell lines from human hair follicles. *Scientific Reports*, *8*(1), 1–12. <https://doi.org/10.1038/s41598-018-31829-0>
- Watt, F. M. (1989). Terminal differentiation of epidermal keratinocytes. *Current Opinion in Cell Biology*, *1*, 1107–1115. [https://doi.org/10.1016/S0955-0674\(89\)80058-4](https://doi.org/10.1016/S0955-0674(89)80058-4)
- Wei, W., Liu, X., Chen, J., Gao, S., Lu, L., Zhang, H., ... Wong, J. (2017). Class I histone

deacetylases are major histone deacetylases : evidence for critical and broad function of histone crotonylation in transcription, 1–17. <https://doi.org/10.1038/cr.2017.68>

Weinmuellner, R., Kryeziu, K., Zbiral, B., Tav, K., Schoenhacker-Alte, B., Groza, D., ... Heffeter, P. (2018). Long-term exposure of immortalized keratinocytes to arsenic induces EMT, impairs differentiation in organotypic skin models and mimics aspects of human skin derangements. *Archives of Toxicology*, 92(1), 181–194. <https://doi.org/10.1007/s00204-017-2034-6>

Wickett, R. R., & Visscher, M. O. (2006). Structure and function of the epidermal barrier. *American Journal of Infection Control*, 34(10 SUPPL.), 98–110. <https://doi.org/10.1016/j.ajic.2006.05.295>

Wiederschain, D., & Ph, D. (n.d.). Addgene: Tet-pLKO-puro, 1–7. Retrieved from <https://www.addgene.org/21915/%5Cnhttps://www.addgene.org/static/data/32/66/1658e8f8-af64-11e0-90fe-003048dd6500.pdf>

Winter, M., Moser, M. A., Meunier, D., Fischer, C., Machat, G., Mattes, K., ... Seiser, C. (2013). Divergent roles of HDAC1 and HDAC2 in the regulation of epidermal development and tumorigenesis. *EMBO Journal*, 32(24), 3176–3191. <https://doi.org/10.1038/emboj.2013.243>

Xiong, Y., Hannon, G. J., Zhang, H., Casso, D., Kobayashi, R., & Beach, D. (1993). P21 Inhibitor of Cyclin Kinase. *Nature*, 366(6456), 701–704.

Yamaguchi, T., Cubizolles, F., Zhang, Y., Reichert, N., Kohler, H., Seiser, C., & Matthias, P. (2010). Histone deacetylases 1 and 2 act in concert to promote the G1-to-S progression, 455–469. <https://doi.org/10.1101/gad.552310.proposed>

Yanginlar, C., & Logie, C. (2018). HDAC11 is a regulator of diverse immune functions. *Biochimica et Biophysica Acta - Gene Regulatory Mechanisms*, 1861(1), 54–59. <https://doi.org/10.1016/j.bbagr.2017.12.002>

Yousef, H., & Sharma, S. (2018). *Anatomy, Skin (Integument), Epidermis. StatPearls*. StatPearls Publishing. Retrieved from <http://www.ncbi.nlm.nih.gov/pubmed/29262154>

Zhang, Y., & Reinberg, D. (2001). Transcription regulation by histone methylation: Interplay between different covalent modifications of the core histone tails. *Genes and Development*, 15(18), 2343–2360. <https://doi.org/10.1101/gad.927301>

Zhao, S., Zhang, X., & Li, H. (2018). ScienceDirect Beyond histone acetylation — writing and erasing histone acylations. *Current Opinion in Structural Biology*, 53, 169–177. <https://doi.org/10.1016/j.sbi.2018.10.001>

Zupkovitz, G., Grausenburger, R., Brunmeir, R., Senese, S., Tischler, J., Jurkin, J., ... Seiser, C. (2010). The Cyclin-Dependent Kinase Inhibitor p21 Is a Crucial Target for Histone Deacetylase 1 as a Regulator of Cellular Proliferation. *Molecular and Cellular Biology*, 30(5), 1171–1181. <https://doi.org/10.1128/MCB.01500-09>